Structure and Electrical Properties of Assemblies of Polyaniline: From Blends to Self-Assembled Multilayers

William B. Stockton

B.S. Chemical Engineering, Rice University (1985)
M.S. Chemical Engineering, Princeton University (1987)

Submitted to the Department of Materials Science and Engineering and the Program in Polymer Science and Technology in partial fulfillment of the requirements for the degree of

Doctor of Philosophy

at the

Massachusetts Institute of Technology

June 1995

© 1995 Massachusetts Institute of Technology

Signature of Author_____
Department of Materials Science and Engineering
May 5, 1995

Certified by_____
Professor Michael F. Rubner
TDK Professor of Polymer Science
Thesis Supervisor

Accepted by_____
Professor Carl V. Thompson II
Professor of Electronic Materials
Chair, Departmental Committee on Graduate Students

and by_____
Professor Edwin L. Thomas
Morris Cohen Professor of Polymer Science
Director, Program in Polymer Science and Technology

STRUCTURE AND ELECTRICAL PROPERTIES OF ASSEMBLIES OF POLYANILINE: FROM BLENDS TO SELF-ASSEMBLED MULTILAYERS

William B. Stockton

ABSTRACT

Assemblies of polyaniline (PAn) have been manipulated on two levels, 1) preliminary investigations into solution-cast blends and 2) a more detailed study of self-assembled multilayer thin films formed via polymer adsorption.

Relatively stable, electrically conducting compatible blends of PAn with poly(vinyl pyrrolidone) (PVP) have been cast from both N-methyl pyrrolidone (NMP) and N,N-dimethyl acetamide (DMAc). The two polymers were miscible to the extent probed by thermal analysis (DSC and DMA), light microscopy, and SAXS. Blended films with a conductivity on the order of pure PAn (~1 S/cm) require ≥ ~25 wt% PAn; conductivities two orders of magnitude lower can be obtained with less than 5 wt% PAn. TGA results revealed high solvent retention, particularly NMP, even after considerable drying of the films. This residual solvent hinders conductivity. Conducting blends of PVP with *pre-doped* PAn can also be cast directly from solution, but display lower conductivities.

The formation of thin polymer films through molecular layer-by-layer adsorption on a variety of substrates has been demonstrated for PAn alternating with non-ionic water soluble polymers. The adsorption is enabled by the strong interchain interactions with PAn, such as hydrogen bonding. Multilayer build-up has been demonstrated with four distinctly different non-ionic water soluble polymers: PVP, poly(vinyl alcohol) (PVA), poly(acrylamide) (PAAm), and poly(ethylene oxide) (PEO). Thus, non-ionic water soluble polymers containing a wide variety of functional groups such as amide, hydroxyl or ether groups can be used to successfully fabricate multilayer thin films with polyaniline. FTIR spectroscopy measurements show the PAn to be hydrogen bonded in these multilayer films. The technique uniformly deposits multiple molecular layers, with each layer completely covering the preceding one, as revealed by contact angle measurements. Conductivities for acid-doped multilayer films are on the order of 1-4 S/cm. Conductivities on the order of 0.1 S/cm can be achieved for a *single* mixed layer self-assembled from a mixed solution of PAn/PVP or PAn/PAAm. Effects of molecular weight, solution pH, and concentration on the adsorption mechanism and resulting film structure are investigated.

ACKNOWLEDGMENTS

3

TABLE OF CONTENTS

I. Introduction

II. Structure and Electrical Properties of Blends of Polyaniline with Poly (vinyl pyrrolidone)

III. Self-Assembled Multilayer Films of Polyaniline

IV. Conclusions, Summary, and Future Work

LIST OF FIGURES

LIST OF TABLES

STRUCTURE AND ELECTRICAL PROPERTIES OF ASSEMBLIES OF POLYANILINE: FROM BLENDS TO SELF-ASSEMBLED MULTILAYERS

CHAPTER I. INTRODUCTION

I.A. Conducting Polymers

I.A.1. Introductory Remarks

The field of electrically conducting polymers continues to grow rapidly, with the range of applications, both speculated and realized, ever expanding. The driving force behind much of this work is the potential for a variety of electroactive properties combined with some of the advantages of polymers, such as the relative ease in processing, certain mechanical properties, chemical resistance, and light weight. Conducting polymers are well suited for many applications, including semiconductor devices [1], energy storage and distribution [2], conductive composites and coatings, a wide variety of sensors, rechargeable batteries, nonlinear optical materials [3], and even electromechanical actuators [4]. Polyaniline alone has been investigated for uses as rechargeable battery electrodes [5-7], conductive fibers and textiles [8, 9], EMI shielding [10], transparent thin film electrodes [11-13], electrochromic windows and devices [5, 14-17], infrared polarizers [18], electrostatic discharge [19, 20] and non-conducting applications such as a patternable photoresist [20, 21], fluid separation membranes [22], and corrosion resistant coatings [23]. These examples constitute only a small fraction of the many proposed and investigated applications of what can be considered a rather novel material.

There are, of course, significant hurdles to overcome in achieving more wide-spread use of conducting polymers and to tap into the specific electrical

properties, such as the reversible switching from insulator to conductor. The achievable levels of conductivity range from highly insulating (generally $< 10^{-8}$ S/cm for conjugated polymers [24]) up to about 10^5 S/cm (for highly oriented iodine-doped polyacetylene in inert atmospheres) [25]. More typical values for air stable systems are between 10^{-1} and 10^2 S/cm, which are generally quite adequate for a wide variety of applications calling for limited electronic conduction. To put these values into perspective, conventional metal conductors such as silver, copper, and gold have conductivities on the order of 10^5 - 10^6 S/cm.

Also, it is well known that conducting polymers are relatively unstable conductors, being susceptible to environmental (extrinsic) and/or thermodynamic (intrinsic) forces that can act to "dedope" the polymer, or revert the material back to insulating. This dedoping can occur extrinsically, such as thermal or externally-driven chemical reversal of an oxidized (doped) backbone, or intrinsically, where there is little energy barrier for the doped state to return to its more stable insulating form by reversing the doping process.

Several classes of conducting polymers are known for their relative stability within the class of conducting polymers, namely polyanilines, polypyrroles, and polythiophenes. These three are intrinsically conducting in their doped form, susceptible primarily to external dedoping processes. It is these three types that show the most promise in terms of the above mentioned applications, primarily for stability reasons.

Processing and manipulating these polymers into desired shapes, be it films, fibers, or thin coatings, presents an additional challenge. Generally speaking, the processing of conducting polymers is tremendously less energy intensive than for conventional electronic materials, but is still somewhat problematic relative to conventional polymers. It is this challenge, that of manipulating conducting polymers into useful blends, coatings, or films, that is the basis of this thesis. The goal of this work is to develop and characterize the structure and resulting electrical properties of assemblies of conducting polymers.

I.A.2. Conducting Polymers - Background

Conducting polymers generally refers to a class of organic conjugated polymers that demonstrate, under certain conditions, electrical conductivity. This is distinguished from ionic conductivity in that the charge carriers are more akin to those in metals (electrons and holes), rather than ionic species (electrolytes). What enables electrical conduction in an organic polymer is its conjugation, or overlapping of p_z orbitals along the backbone, that can lead to mobile charge carriers. Electrons can be delocalized over a series of π molecular orbitals, as opposed to the tightly bound, highly localized electrons in saturated σ bonding orbitals. The existence of a conjugated chain is not sufficient to render a polymer conductive, however, as the lowest energy state of these polymers generally does not consist of completely delocalized π-electrons. The model example of this is polyacetylene, one of the first discovered conducting polymers [26]. Every carbon along its backbone has a p_z orbital overlapping with its neighbor. But rather than having uniformly distributed π-electrons (completely delocalized), the ground state of polyacetylene consists of alternating single and double bonds, with only very limited delocalization. The result is a band gap (between the bonding π-valence band and the antibonding π^*-conduction band) of about 1.5 eV [27], close to that of semiconductors. Similarly for other conjugated polymers, the ground state limits electron delocalization, and their band gaps typically range from 1-4 eV [24].

What was observed by Shirakawa, et al., was that charge carriers could be created in polyacetylene by chemically oxidizing the backbone (removing electrons), thus creating charge defects [26]. A single charge defect is called a polaron, which is a positive charge coupled with an unpaired electron, as a result of the electron transfer to the oxidant (called the dopant). The dopant (now ionized) remains associated with the polaron as a counterion. This process is called doping, but is only loosely analogous to doping in the semiconductor industry [28]. Traditional semiconductor dopant concentrations are in the parts per million range. For conducting polymers, dopant concentrations necessarily exceed 1 mol%, as high as 50 mol% in some cases, thus can add significant mass to the final system. The presence of dopant ions can also cause structural changes. It is likely that for many dopants, these changes cause structural

disorder, although efforts have been made to use dopant counterions that will enhance order [29].

Due to the conjugation, this new charge defect (the polaron) can be delocalized to some extent along the polymer backbone, but not completely. It is still confined by the energetics of bond configurations, as well as counterion mobility. Thus these charge carriers are also not free to move like partially-filled valence band electrons, as in metallic conduction.

The formation of a polaron creates a new energy state in the middle of the band gap. Further oxidation on the same chain generally creates dications, (by removal of the unpaired electron) as it is energetically more favorable than the creation of a second polaron along a single polymer chain. For polyacetylene, which has a degenerate ground state, this dication is called a soliton. Additional doping forms more solitons. These cationic charge defects all show approximately the same energy state, thus their energy falls within one band, called the soliton band. For non-degenerate ground state polymers (most all others), the subsequent oxidation of a polaron forms two non-equivalent energy states. The two cations become delocalized over several repeat units, coupled in a state that has two possible configurations (one with a higher energy that the other), called a bipolaron. Thus, two mid-gap bands are formed, one of higher energy than the other, called bipolaron bands [28].

Continued doping in either case acts to widen the mid-gap bands (either soliton or bipolaron) due to intrachain interactions as additional bipolarons or solitons are formed. Eventually, these bands become close enough to the valence and conduction bands to enable metal-like conductivity along a single polymer chain.

Of course, macroscopic conductivity must involve charge transfer from chain to chain, and for polymers this can present a substantial barrier. The relative importance of inter- to intra- chain charge mobility depends on the polymer's microstructure, but both mechanisms contribute to an overall bulk conductivity. Certainly, ordered structures (crystals, drawn fibers) have better conductivities, although this enhanced conductivity is generally anisotropic. Chain elongation leads to both longer conjugation lengths, thus smaller band gaps, and enhanced packing, thus easing interchain charge transfer.

Charge carriers must hop or tunnel through structural barriers such as chain ends, disordered domains, and weakly doped regions. Many models have been proposed describing the conduction mechanism, which can vary from

polymer to polymer. Determining the temperature dependence of conductivity can reveal a general type of mechanism. If the conductivity is thermally enhanced, it suggests charge mobility is enhanced by hopping activation, which is a non-metallic-like conduction mechanism. Thermally hindered conductivity suggests that increased "lattice" vibrations act to scatter electrons (phonon scattering), thus more metallic-like conduction [28, and references therein]. Both of these types of behavior have been seen in conducting polymers, depending on the polymer type and more importantly, its structure.

Of course, many other conjugated structures exist beyond polyacetylene, primarily aromatic and heterocyclic polymers. Several examples are listed in Figure I.1, plus many derivatives of these also exist. Doping is most commonly oxidative, called p-type due to the positive charge created on the polymer backbone. Chemical reduction is also possible (adding an electron to the polymer), called n-type doping, but is less common. One additional type of doping occurs with polyaniline. The imine nitrogen atoms in the emeraldine form of polyaniline (see Section I.B.1.) can act as proton acceptors, which creates positive charges on the polymer chain. The chain conjugation allows electronic rearrangement that makes these charges mobile. Thus polyaniline can be doped with protonic acids such as hydrochloric or sulfuric acid. This implies that the extent of polyaniline doping, and thus its conductivity, are pH sensitive. Exposing polyaniline to aqueous solutions with pH $\geq$ ~ 5 will completely "dedope" the polymer, with a corresponding conductivity of about 10^{-10} S/cm [30]. Lowering the pH gives rise to an increasing conductivity, down to about pH $\approx$ 1, below which no increased conductivity occurs, about 1-10 S/cm [30]. Thus polyaniline can span 10-12 orders of magnitude of conductivity simply by changing its pH conditions.

I.B. Polyaniline

I.B.1. Background

The focus of this work will be on polyaniline (PAn), for several reasons. Polyaniline is a relatively well-investigated conducting polymer, having been the subject of extensive research for over nine years. PAn presents itself as well suited for a variety of applications due to its relative ease in synthesis, low cost

Polyacetylene
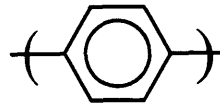
Poly (p-phenylene)
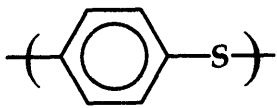
Poly (p-phenylene sulfide)
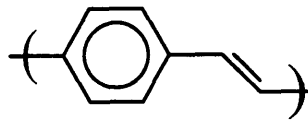
Poly (p-phenylene vinylene)
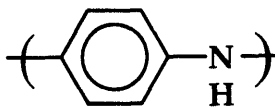
Polyaniline
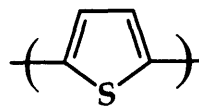
Polythiophene
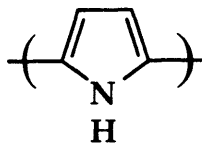
Polypyrrole
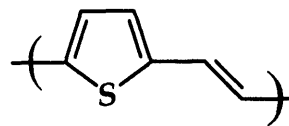
Poly (thienylene vinylene)
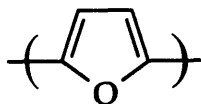
Polyfuran

Figure I.1. Chemical structure of several conducting organic polymers.

and stable electronic conduction. PAn does have a somewhat limited processability due to its very high glass transition temperature (T_g) and even higher melting temperature, and very limited solubility, particularly in its doped state. Its T_g ranges from about 220-250°C [31], with a melting temperature likely well in excess of this (although there is low crystallinity in dedoped PAn base). Relative to most conducting polymers, however, PAn is significantly more processable.

PAn exists in several different oxidation states, as shown in Figure I.2a. It is generally processed in its partially oxidized state, the emeraldine base, which is the state best suited for obtaining maximum conductivity. The emeraldine base form is rendered conductive by "doping" with a protonic acid, shown in Figure I.2b. The doping essentially acts to put stable charge defects (in this case protons) along the polymer backbone, creating charge carrier sites. The more of these sites created, the higher the conductivity. This type of doping is quite different from the standard oxidative or reductive doping used with the majority of conducting polymers, which involve electron transfer to or from the polymer. Although PAn can be doped oxidatively, better conductivity results from protonic doping. Thus for PAn, its conductivity depends on its pH conditions, and is reversibly doped and dedoped by adjusting the pH. Once doped, the newly formed emeraldine salt generally becomes more rigid due to an increased conjugation length, often accompanied by enhanced crystallinity. Thus the doped form is even less soluble.

PAn is usually synthesized chemically by the oxidative coupling of aniline using an appropriately strong oxidant such as ammonium persulfate or ammonium dichromate. The synthesis is done under acidic conditions, thus forms doped polyaniline, the emeraldine salt form. From there, it can be dedoped in a basic aqueous solution such as ammonium hydroxide. This forms the emeraldine base, which is the soluble form of polyaniline.

PAn can also be readily synthesized electrochemically, through the electrolysis of aniline monomer in acidic aqueous conditions. The conducting form, emeraldine salt, is grown directly onto the working electrode under an applied potential (or potential sweep). After synthesis, any oxidation state of PAn is obtainable by varying the applied voltage. These states are reversibly interconverted between the fully reduced leucoemeraldine (clear), the emeraldine salt (green) or base (blue), and the fully oxidized pernigraniline
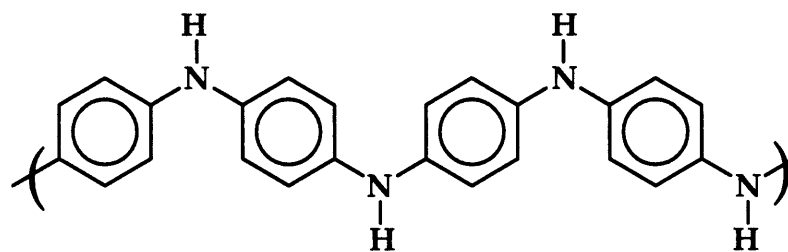
Leucoemeraldine
(fully reduced, clear)
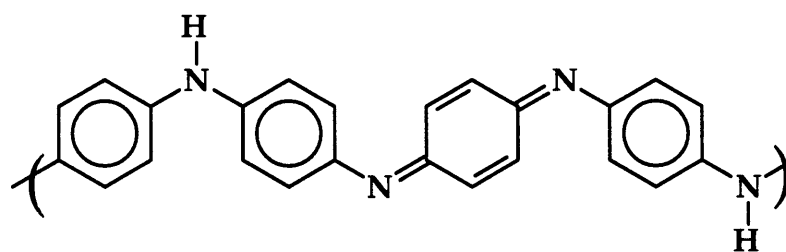
Emeraldine Base
(partially oxidized, blue)
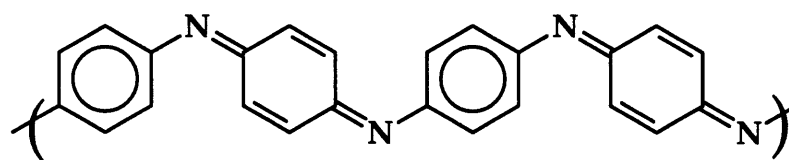
Pernigraniline
(fully oxidized, violet)

Figure I.2a. Chemical structures of the three oxidation states of polyaniline (all insulating). The color of each state is indicated.

17

Emeraldine Base (insulating)

Dope with Protonic Acid
H+A-

Dedope with Strong Base
R+OH-

intermediate

electronic rearrangement

Emeraldine Salt (conducting)
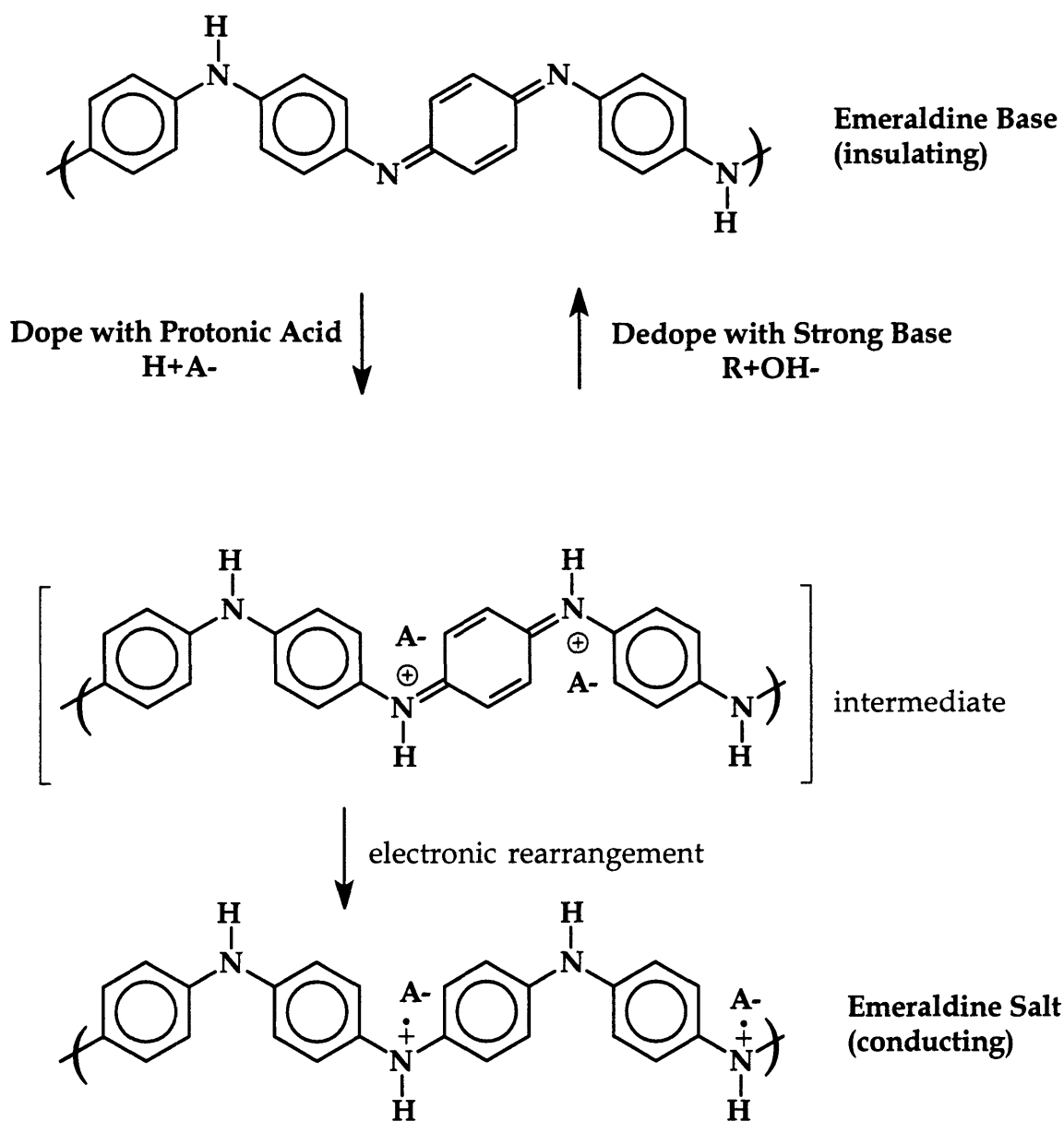
Figure I.2b. Chemical structures of the emeraldine base, its acid-doped intermediate, and final doped form, emeraldine salt.

(violet) [32]. The ease and reversibility of these conversions leads to polyaniline's use in electrochromic devices.

MacDiarmid and Epstein have identified three forms of the emeraldine base distinguished by their x-ray diffraction spectra and their solubility behavior [33]. They label them EB I, EB II, and EB II'. EB I is the most common, amorphous form, soluble in NMP, DMAc, and the like. EB II is a partially crystalline form insoluble in these solvents. EB II' is formed by acid-doping EB II, then dedoping. The resulting form is amorphous and soluble, but differs from EB I. There are two doped forms of PAn (emeraldine salt), also distinguishable by their crystal structure, labeled ES I and ES II [33]. Acid-doping EB I gives ES I, a partially crystalline material, while acid-doping EB II gives ES II, also partially crystalline, but a different crystal structure than ES I. Most work involved with PAn solutions therefore uses the EB I form, as the EB II crystals are generally filtered out.

Two recent stability studies on PAn have shown its conductivity stability to depend on the dopant [34] as well as the synthesis route [35]. In all cases, conductivity levels for bulk PAn show little, if any, decline *in air* at temperatures up to about 130°C for over 24 hour exposure. Above 130°C, conductivity starts to decrease relatively rapidly, depending on the dopant. Generally speaking, sulfonic acid dopants (like methane sulfonic acid and toluene sulfonic acid) show the highest stability, relative to other common dopants like hydrochloric and sulfuric acid. Of course, sample geometry is an important factor, as diffusion kinetics generally limit conductivity degradation. Thinner samples degrade faster by the diffusion in of oxygen and moisture, plus the diffusion out of dopants. Although the presence of moisture actually enhances the conductivity of PAn, too much for too long can lower the pH or otherwise cause sample degradation. A wide range of "half-lives" and "$t_{1/10}$" (time for conductivity to drop one order of magnitude) values at room temperature have been estimated for PAn, again varying due to differences in synthesis, dopant, and film thickness. A rough estimate is that bulk PAn will maintain its conductivity within an order of magnitude for a period of several years.

It should also be noted that a water soluble derivative of PAn has been synthesized by sulfonating the emeraldine base [36-38], with its chemical structure shown in Figure I.3. This form also has the added property of "self-doping." With a sulfonic acid group attached to approximately every other ring,

Sulfonated Polyaniline

Conducting

Aqueous Protonic Acid
(pH < 7)

Aqueous NaOH
(pH > 7)

Water Soluble, Insulating
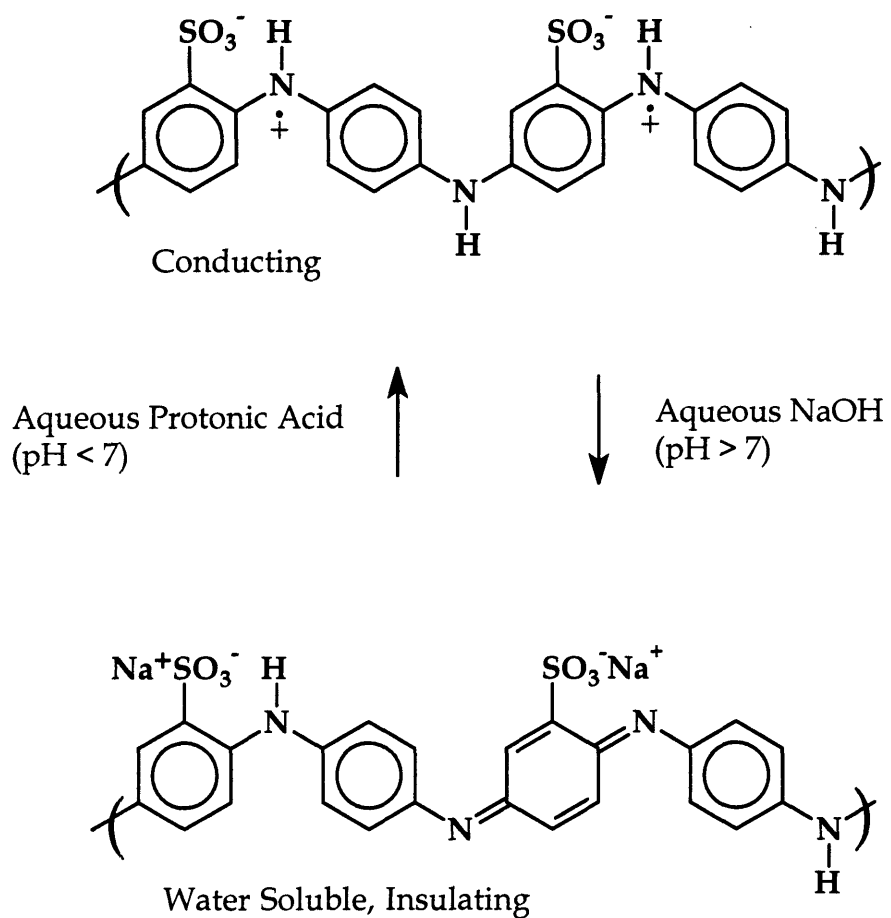
Figure I.3. Chemical structure of sulfonated polyaniline in its (self) doped conductive form and its insulating sodium salt, which is water soluble.

the sulfonated polyaniline (SPAn) effectively dopes itself over a broad pH range, up to as high as pH=7. As depicted in Figure I.3, for pH values above about 7, the salt form of the sulfonic acid is formed, which dedopes the backbone, but renders the polymer soluble in water. The compromise for this water solubility and the increased pH range of the conducting form is a drop in conductivity. The reported value is around 0.1 S/cm [36]. This reduced conductivity is due to the sulfonic acid side groups that act to reduce the planarity of the neighboring rings, which reduces p_z-orbital overlap, thus a shorter effective conjugation length.

I.B.2. Processing of Polyaniline Blends

The only solvents reported as useful for PAn are either concentrated acids, such as sulfuric acid, or amide-type polar solvents such as N-methyl pyrrolidone (NMP), dimethyl acetamide (DMAc), dimethyl formamide (DMF), and dimethyl propylene urea (DMPU). Only the base forms of PAn (non-conducting) were considered soluble in these solvents. Once doped by either protonation or by oxidation, the resulting conducting form generally became intractable and brittle. Thus, processing of PAn is somewhat limited, and pure PAn has little mechanical integrity.

It may be that this is related to molecular weight, as the most common synthesis route generally yields molecular weights (M_n) in the 20-25,000 range, which may be below the entanglement molecular weight. Polyaniline is a rigid polymer with a relatively long persistence length, which suggests that its entanglement molecular weight is higher than more flexible polymers (for polystyrene, for example, the entanglement molecular weight is about 35,000, for poly(ethylene terephthalate, however, it is only about 6000) [39]. Tensile strengths of stretch-oriented films of plasticized PAn have been reported for several molecular weight regimes [40], showing significant increase in tensile strength with molecular weight increase from about M_n = 26,000 to M_n = 125,000.

Blending PAn with a host polymer has the advantage of enhancing the overall mechanical properties, versatility, and processability. Blends also reduce the amount of polyaniline necessary for conductivity and increase the stability of this conduction by providing environmental protection. PAn blends

have generally been observed to be immiscible, however, reducing many of the above mentioned advantages.

Attempts to blend PAn with a host polymeric matrix have resulted in a variety of approaches, most of which require subsequent doping to render the composite conductive. Little morphological characterization has been done; the blends are generally phase separated in both the doped and undoped states due to the low inherent miscibility of rigid conjugated polymers. Recently, several research groups have reported approaches to process PAn in its doped, conducting form. Both pure PAn films, as well as conducting blends, have been reported, as noted below.

The use of "functionalized" protonic acids to dope PAn base renders the doped polymer soluble in several organic solvents [41-44]. The protonic acid is usually a large sulfonic acid, primarily DBSA (dodecylbenzene sulfonic acid) and CSA (camphor sulfonic acid); many other sulfonic acids have shown varying degrees of success. PAn-CSA has been blended with PMMA in m-cresol, showing high conductivity and a percolation threshold as low as 1-2 wt% PAn. The blends were shown by TEM to be phase separated on the submicron level, with fibril-like continuous paths of PAn formed in the host matrix. Blends with several other host polymers have been reported, including nylon, PVC, PS, PVA, PP, PE, ABS, and polycarbonate [43, 44].

It has also been shown that certain residual solvents, such as m-cresol, can act to significantly enhance the conductivity through solvent-induced ordering of the doped PAn [45, 46]. MacDiarmid, et al, have shown significant increases in structural order and resulting conductivities in the above mentioned "functionalized" sulfonic acid-doped PAn that has been cast from, or exposed to, m-cresol.

Conducting PAn/poly (alkyl methacrylate) blends have been prepared by emulsion polymerization in the presence of HCl [47, 48]. A percolation threshold of about 3-4% PAn in PEMA is observed, while for PAn/PBMA, the threshold is closer to 10%.

Conducting PAn films have been cast from a ferric chloride solution in nitromethane, starting with either PAn base or already-doped PAn [49]. The ferric chloride acts to oxidize the PAn, and a conducting film can be cast. A blend with cellulose acetate butyrate resulted in a conducting composite, but with relatively low conductivity (10^{-3} S/cm).

Doped PAn can be rendered soluble by the addition of a Lewis base, such as a tertiary amine [50]. The Lewis base acts to complex the dopant, effectively reverting the PAn to its soluble base form. The Lewis base can be later driven off by heating, reverting the PAn back to it doped state.

PAn doped with 5-sulfosalicylic acid (SSA) is soluble in DMSO, DMF, and NMP up to 11 mg/ml [51]. The aniline is polymerized in the presence of SSA; resulting conductivities are around 0.2 S/cm.

Several groups have reported doping PAn with polymeric dopants, both sulfonated polystyrene and poly(acrylic acid) [52-55]. Both solid state (mechanical mixing and compression molding) and solution doping resulted in low conductivities, due to steric hindrance of the dopant, and to low mobility of the dopant [52, 53]. Electrochemical polymerization of aniline in the presence of sulfonated polystyrene resulted in a film that was 66.5 mol% PAn with a conductivity of 2-3 S/cm [54]. Chemical polymerization of aniline in the presence of either sulfonated polystyrene or poly(acrylic acid) resulted in a water soluble complex with conductivity of cast films about 0.1-1 S/cm [55].

Water soluble complexes of PAn and PAn derivatives with a polyacid have been reported [56, 21]. These complexes can form solutions that are concentrated enough to spin coat, and have been proposed to have applications in the microelectronics industry, among other areas.

Chapter II of this thesis addresses the issue of manipulating PAn in its bulk state, such as in blends of both its doped and dedoped states. In an attempt to prepare miscible systems, we have examined blends of PAn base with poly(vinyl pyrrolidone) (PVP). PVP was chosen because of its ability to form strong secondary bonds, such as hydrogen bonds, with PAn. PVP is the polymer analog of NMP, a known good solvent for PAn base. The strong interactions between these two polymers leads to enhanced solubility of PAn in NMP and to the creation of miscible blends. We have found PAn base to be compatible with PVP under certain processing conditions [57]. This compatibility is assessed in terms of the mechanical, thermal, and electrical properties of the blend.

It was also found that, depending on the processing conditions, *doped* PAn can show a large extent of compatibility with PVP [58]. The presence of PVP enhances the solubility of doped PAn in NMP. As a result, doped PAn blends with PVP were also prepared, in the form of spin coated and static cast

23

films, and self-assembled into multilayer coatings. Three sulfonic acid dopants were evaluated; methane sulfonic acid (MeSA), camphor sulfonic acid (CSA), and dodecylbenzene sulfonic acid (DBSA). The resulting solution cast films show some phase segregation of PAn, but also show significant compatibility of the doped PAn with PVP.

I.C. Self-Assembled Multilayer Films

The manipulation of PAn on the molecular level is discussed in Chapter III. Assemblies of PAn are formed by means of polymer adsorption in a layer-by-layer fashion onto substrates, referred to as self-assembly. The general idea of self-assembly is to simply deposit conjugated polymer monolayers onto a variety of substrates by adsorption from solution. From there, a tremendous range of possible molecular level structures becomes possible, primarily in the form of electroactive thin films and coatings.

There has been extensive work in our group manipulating conjugated polymers by means of self-assembly onto a variety of substrates [58-65]. Thin film assemblies are grown on a molecular level, layer by layer, by means of polymer adsorption from solution, a technique adapted in our research group for conjugated polymers. This technique is well suited for depositing controlled multilayer coatings of polymers, and in particular interest to our group, conducting, or more generally, conjugated polymers. The advantages include the relative ease of the technique combined with the quality of deposited films. Adsorption is done primarily from aqueous solutions, thus limiting or eliminating the use of organic solvents. Therefore, the formation of stable aqueous solutions in the concentration range of interest is quite important. Most all polyelectrolytes are water soluble, thus layer by layer build up by electrostatic assembly is well suited for this technique. There are many varieties of water-soluble polymers, both ionic and non-ionic, that are useful for not only adsorption studies, but are of significant interest in terms of a wide variety of potential applications. These include all types of surface modifications, adhesion-promoters, biocompatiblizers, as well as electroactive coatings, like transparent electrodes, sensors, and semiconductor devices.

Understanding the structure of such systems is important for determining the extent of monolayer coverage, the film uniformity, and

interfacial diffuseness. The effects of pH conditions, molecular weight, and concentration (among others) on polyaniline adsorption are addressed as well. This will shed light on the nature of self-assembly deposition and the extent of polymer/polymer interactions in molecular level assemblies.

I.C.1. Polymer Adsorption Background

There are several forces that must be considered that are involved in the adsorption of a polymer chain onto a solid surface. Competing enthalpic and entropic energies determine the extent of adsorption and subsequent desorption. In terms of enthalpic energies, the strongest adsorptive forces are chemisorption processes, where molecules become chemically bonded to the surface. This implies an exothermic reaction is the driving force for the adsorption, with energies on the order of 100-700 kJ/mol (depending on the types of bonds involved) [66]. The next strongest bonding is electrostatic attraction, in the case of charged polymers with oppositely charged surfaces. Coulombic interactions are on the order of 50-200 kJ/mol. Hydrogen bonding interactions are important for systems capable of forming such bonds, which will be a significant portion of the systems investigated in this work. These interaction energies are in the range of 20-40 kJ/mol, depending on the proximity of the species involved. Hydrogen bonds thus are more easily reversed thermally. Important for organic polymer systems in aqueous solutions are hydrophobic interactions. Hydrocarbon chains can be driven enthalpically to a surface to minimize their interactions with water. The weakest forces that lead to polymer adsorption are van der Waals forces (such as dispersive forces and dipole-dipole interactions) between the surface and polymer chains in immediate proximity. These cohesive forces are estimated to be in the range of 1-5 kJ/mol [66].

All of the above mentioned enthalpic forces act to enhance adsorption. There are entropic energies primarily related to chain configuration that generally act to inhibit adsorption. A polymer chain must undergo some extent of configurational changes (primarily elongation) along with confinement to remain adsorbed. These are entropic penalties, more so in good solvents. There can be, however, a slight entropy gain as surface solvent is desorbed in place of adsorbed polymer chains, gaining degrees of freedom.

It is also important to consider the surface upon which adsorption takes place. Aside from the interaction energies depending on the chemical make-up of the surface, geometrical factors such as surface roughness also act to affect adsorption. By presenting more interaction sites in a confined space, a roughened surface allows polymer chain adsorption without as large of an entropic penalty as a smooth surface [67]. As depicted below in Figure I.4, the polymer chain can remain in a more coiled configuration while still participating in many surface interactions on the rougher film.
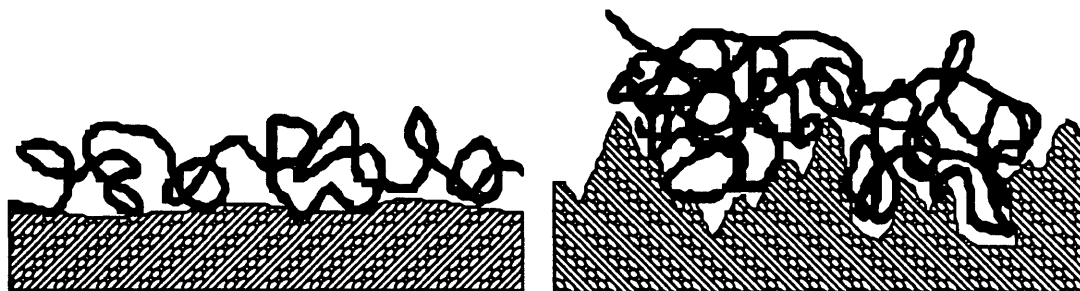
Figure I.4. Polymer chain adsorbed to a smooth vs. rough surface [67].

This effect will be seen to be important in the case of adsorbed polyaniline, which forms relatively rough surfaces (see Section III.J.2), thus enhancing additional adsorption on top of it. Thermodynamically, polymer adsorption is thus governed by the balance of these interactions under the given conditions of concentration, ionic strength, pH, temperature, solvent, etc. These are all addressed in Chapter III for the specific case of adsorption of polyaniline with the series of previous mentioned polymers.

I.C.2. Multilayer Adsorption of Conjugated Polymers

Multilayer assemblies of doped conjugated polymers can be fabricated quite simply from aqueous solutions. The doping renders the conjugated polymer charged (by means of delocalized charges), thus it behaves as a polyion. In the case of PAn, doping by protonation puts on a positive charge, thus is called p-type doping. Alternating layers of polycations and polyanions can then be built up, adsorbing by means of electrostatic forces. Multilayer build-up has previously been demonstrated with flexible polyions such as poly(vinyl sulfate) and sulfonated polystyrene (anionic) with poly(allyl amine)

26

(cationic) [68, 69]. Researchers in our lab have demonstrated electrostatic self-assembly with quite a variety of conjugated polymers, including poly(p-phenylene vinylene) [61, 63], polypyrrole [64], poly(thiophene acetic acid) [59], and both polyaniline and sulfonated polyaniline (SPAn) [60]. Many non-conjugated polyions and molecules have been incorporated as well, including sulfonated buckminster fullerene [63] and a wide variety of dye molecules [70]. These systems have applications ranging from simple anti-static coatings to electroactive devices such as light-emitting diodes and capacitors.

Recent work in other research groups include attaching ionic biological molecules such as DNA [71], and monitoring adsorption kinetics as a function of polyelectrolyte molecular weight distribution [72]. Multilayer coatings of cationic polyelectrolytes alternating with individual sheets of anionic hectorite (a layered silicate) have also been demonstrated [73]. It is clear that this technique is rapidly becoming a quite useful and versatile approach to forming thin film assemblies with molecular level control.

In the work presented in this thesis, molecular level manipulation of a conjugated polymer, PAn, is demonstrated with strongly interacting polymers, both ionic and non-ionic, through the use of polymer adsorption. This adsorption is from aqueous solutions, with the exception of 5-10% organic solvent necessary for the PAn solution. Depending on the conditions, PAn can be maintained in a metastable solution that is 90-95% water, thus well suited for self-assembly. The details will be outlined in the experimental section. SPAn forms more stable aqueous solutions than PAn, and proves to be quite interesting for electrostatic self-assembly since it contains both positive and negative sites at pH < 7, but was not investigated in this thesis work, primarily because of its lower conductivity.

These above mentioned polyions all rely on electrostatic forces for polymer chain adhesion. Electrostatic forces are certainly not the only means of molecular adsorption, as it is also well known that surface adsorption can be driven by molecular forces like hydrogen-bonding. The strong chain interactions between PAn and PVP, for example, due primarily to hydrogen bonding, enable molecular layer-by-layer build-up of doped PAn alternating with PVP. There is some extent of molecular level blending between the layers due to the large extent of interpenetration expected for strongly interacting polymers. We believe that this is the first demonstration of polymer-polymer multilayer build-up of a rigid conjugated polymer (PAn) through hydrogen

bonding to a flexible, electrostatically neutral polymer (such as PVP). The layer thickness can be controlled by the processing conditions such as solution concentration, pH, and ionic strength, as well as the adsorption time. The structure can also vary considerably with molecular weight. It is this ability to controllably form thin electroactive films capable of adhering to a variety of surfaces that renders this technique so useful. This is a new approach to polymer multilayer self-assembly, extending the range of types of heterostructures possible by self-assembly.

In the work of this thesis, four distinctly different non-ionic water soluble polymers were used to fabricate multilayer thin films with PAn; poly(vinyl pyrrolidone) (PVP), poly(vinyl alcohol) (PVA), poly(acrylamide) (PAAm), and poly(ethylene oxide) (PEO), along with an ionic polymer for comparison, sulfonated polystyrene (SPS), shown in Figure I.5. Multilayer build-up with PAn was also demonstrated with poly(acrylic acid) (PAA), an ionic water soluble polymer, while poly(ethylene imine) (PEI), also water soluble, was sometimes used as the first layer in multilayer systems (both also shown in Figure I.5). Thus, both ionic and nonionic water soluble polymers containing a wide variety of functional groups such as amide, alcohol, or ether groups can be used to successfully fabricate multilayer thin films with p-type doped polyaniline. Each of these groups is capable of forming hydrogen bonds with polyaniline. Again, the results and discussion are in Chapter III.
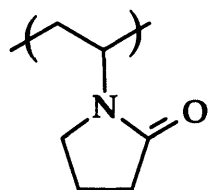
Poly (vinyl pyrrolidone), PVP
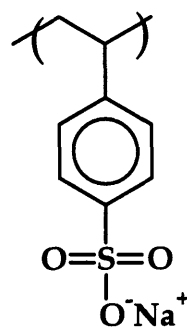
Sulfonated Polystyrene, SPS
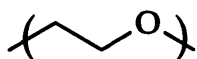
Poly (ethylene oxide), PEO
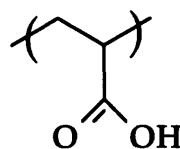
Poly (acrylic acid), PAA
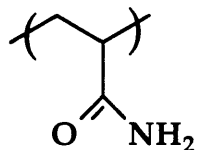
Polyacrylamide, PAAm
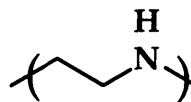
Poly (ethylene imine), PEI
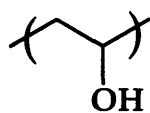
Poly (vinyl alcohol), PVA

Figure I.5. Chemical structure of water soluble polymers used in this work.

29

CHAPTER II. STRUCTURE AND ELECTRICAL PROPERTIES OF BLENDS OF POLYANILINE WITH POLY(VINYL PYRROLIDONE)

As outlined in the Introduction, conducting composites of PAn blended primarily with PVP have been explored. These composites were blended in solution and cast from either NMP or DMAc in the form of films. The films were characterized in terms of their morphology and electrical properties.

II.A. Experimental

II.A.1. Synthesis and Preparation of Blends

PAn was synthesized chemically by the direct oxidation of freshly distilled aniline by slowly adding an equimolar amount of ammonium persulfate (dissolved in 1 M HCl) to freshly distilled aniline, also dissolved in 1 M HCl (similar to the method described in [74]). Both solutions were pre-cooled to 4°C, and the mixture was stirred for 3 hours at 4°C, as polyaniline precipitated. The precipitate was then filtered, washed with methanol and water, then de-doped in a 0.1 M solution of ammonium hydroxide. Based on results from many similar syntheses [75, 40], the molecular weight (M_n) is estimated to be 20-25K g/mole with a polydispersity of about 2.5. PAn was dissolved in either N-methyl pyrrolidone (NMP) or dimethyl acetamide (DMAc) at 20 mg/ml by first stirring overnight, then sonicating the solution for about 8-10 hours. The solution had some fine particulates which were removed by filtering through a 2 μm paper filter, followed by a 0.45 μm solvent-resistant filter, or by filtering through a 0.7 μm glass filter.

PVP of three different molecular weights was used. High molecular weight (M_w = 1,000,000 g/mole), designated PVP-M, and low molecular weight

(M_w =10,000 g/mole - PVP-10K) were used as received from Polysciences. Low molecular weight PVP (approx. 8000 g/mole - PVP-8K) synthesized in our lab by free radical polymerization of N-vinyl pyrrolidone was also used. PVP was also dissolved in either DMAc or NMP, then filtered through a 0.22 μm filter. Various concentrations of PVP were used for comparisons. Appropriate ratios of the two solutions were mixed to give desired compositions. The blended solutions were generally about 2 wt% polymer in solvent, and were stirred overnight before use. Films consisting of the entire composition range (0-100 wt% PAn) were explored.

Doped blends were formed by mixing in excess molar amounts of either methane sulfonic acid (MeSA), camphor sulfonic acid (CSA), or dodecylbenzene sulfonic acid (DBSA), previously dissolved in NMP. The doped solutions instantly turned from a deep blue to a dark green, characteristic of doped PAn. In some cases the doped solutions were filtered through a 0.45 μm filter for comparison to unfiltered films.

Several series of blends were cast, including spin-coated films and static-cast films, from all three PVP types, and with both solvents. Thinner films (60 μm and less), used for light microscopy and conductivity measurements, were dried in a vacuum oven at 70-100°C for at least one day. Vigorous drying is necessary to remove as much NMP as possible, but care was taken to minimize thermal dedoping of the doped samples. Thicker films (0.3 mm), used in the thermal analysis (DMA, DSC, and TGA) and SAXS, were dried for several days under vacuum at 70-100°C.

II.A.2. Characterization Techniques

Microscopy was performed on a Zeiss light microscope with a maximum magnification of 1000x. The thickness of the static cast films ranges from 4-8 μm; the spin coated films ranged in thickness from 0.3-0.6 μm. Color photographs were taken with an attached 35 mm camera.

Thermogravimetric analysis, TGA, was run on 10 mg samples in a Seiko TG/DTA-320. The samples were run from 30-510°C, 20°C/min. under a nitrogen purge. Differential scanning calorimetry, DSC, was done using a Perkin-Elmer DSC-7. Samples were either cast directly into the DSC pans, or cast into films, then cut into small pieces to be placed in the pans. Sample sizes were typically 5-12 mg. In all cases, the DSC pans had lids, but were not sealed air-tight. To further dry the samples, and erase any thermal history, the samples were first

run up to 220°C in the DSC, and held for one minute under a nitrogen purge. The samples were then cooled to 10°C, and scanned from 10-220°C at 20°C/min (collecting data). Dynamic mechanical analysis, DMA, was run on a Seiko DMS-200 using small strips cut from solution-cast films, 25 mm long, 5 mm wide, and 0.3 mm thick. The samples were run in tension mode from 20-220°C, 2°C/min., and five frequencies were scanned, 1, 2, 5, 10, and 20 Hz.

Pieces cut from these same films used for DMA were used for small angle x-ray scattering (SAXS) measurements. The films were mounted in the x-ray beam with transmission through the film thickness. A sample-to-detector distance of 272 cm enabled a scattering angle (2θ) collection range of approx. 0.16° to 1.05°. This corresponds to a d-spacing range of 540-84Å. The SAXS was calibrated using duck tendon, with scattering collected by a two-dimensional detector for 30 minute exposure times. This time was sufficient for a test sample of a phase separated block copolymer with lamellar morphology to show the first two orders of d-spacing peaks.

All conductivities were measured in air by the van der Pauw four corner probe method [76]. Relative humidity ranged from 20-75 over the course of several months in which the measurements were made. Samples measured at both ends of this range showed only a slight increase in conductivity with increasing humidity. Conductivities were remeasured for some of the samples after one year of storage in atmospheric conditions, and showed about an order of magnitude drop. This depended on the sample thickness, as thinner samples dedope more quickly.

II.B. Solvent Effects

It is worth noting some interesting solution behavior observations made during the course of preparing the blends. Several series of PAn/PVP compositions were blended, varying both the solvent and the PVP molecular weight. Due to the relatively low solubility of PAn, the solutions were all low concentration, about 2 wt% polymer in all cases. With PVP-10K, the two-polymer mixture was soluble in both solvents for all PAn:PVP-10K ratios prepared (up to 30/70 PAn/PVP). PAn and PVP-M were soluble in NMP for all ratios of PAn:PVP-M (0/100 to 100/0 PAn/PVP). PVP-M and PAn mixed together were not soluble in DMAc, however, even though both polymers individually are

DMAc-soluble. Mixing the two in DMAc resulted in the immediate formation of a thick PVP-M/PAn "gel", regardless of the fraction of PAn. It is possible to use a DMAc/NMP solvent mixture, but at least 80% NMP is necessary for the blend to remain in solution. Heating the gelled solution reduced the amount of gel (possibly reversing some hydrogen bonding), but did not completely dissolve it. This solution behavior reflects the significant effect both solvent and molecular weight have on polymer-polymer interactions. Apparently, NMP and its polymer analog PVP interact more strongly with PAn than does DMAc. In a DMAc solution, the PAn interacts more strongly with PVP, creating a gel. The gel is a result of tightly associated PAn and PVP molecules that behave as a non-soluble complex. In NMP, the interactions are similar between PAn and both NMP and PVP, thus it remains in solution. Low molecular weight PVP blended with PAn remains in solution in DMAc, however, thus the PVP-10K must be a low enough molecular weight to prevent enough interchain physical crosslinking that would form a gel. Thus, for some cases, only NMP can be used as a solvent to solution cast PAn/PVP blends.

It is possible that these interactions can be thermally weakened, such as the thermal dissociation of hydrogen bonding. Thus heating the solutions might act to initially dissociate complexed PAn and PVP chains, increasing their solubility. Of course, raising the temperature could also weaken the solvent strength. These temperature effects were not explored, however, as all solutions and films were prepared at room temperature.

II.C. Thermal Analysis Results

II.C.1. Thermal Gravimetric Analysis (TGA)

TGA was run on the thick cast films to monitor the presence of solvents. All samples had been under dynamic vacuum right up until they were loaded into the instrument to minimize adsorbed moisture. The loading time is about one minute, which is enough air-exposure time to absorb 2-3% by weight moisture from the humid air (Relative humidity = 70-75). Three distinct regions of weight loss are evident in the TGA thermograms represented graphically in Figure II.1.
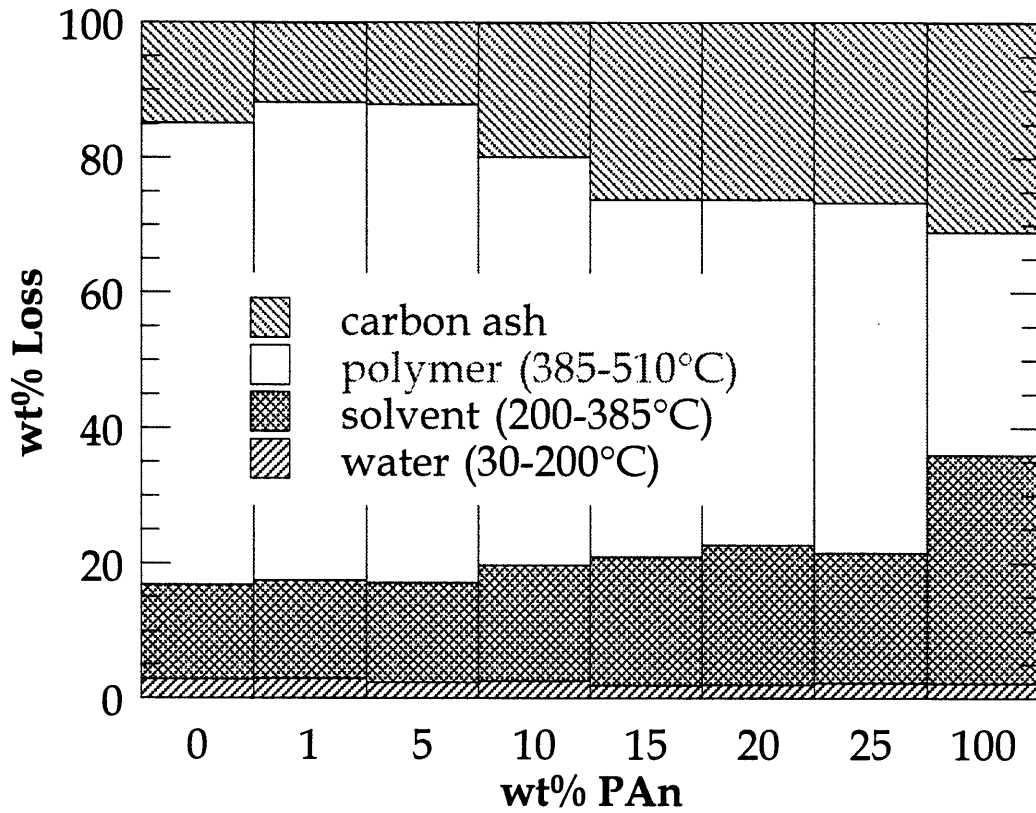
Figure II.1. Histogram of TGA wt% loss from PAn/PVP-1M blend films (cast from NMP) showing three weight loss regions.

In the first region, there is a steady weight loss of about 2-3% from 30-200°C, corresponding to the above-mentioned adsorbed water. From 200-385°C there is a steeper drop, with a corresponding weight loss of 14-20%, depending on the amount of PAn in the blend. This loss is due to trapped NMP being driven off. Although the boiling point of NMP is 202°C, it is physically bound to both the PVP and PAn, thus difficult to drive off. Similar results were seen with samples cast from DMAc, which has a boiling point of 165°C, except that less DMAc was retained than was NMP. The NMP is bound more tightly to PAn than to PVP, as is evident by the increasing amount of retained NMP as the percentage of PAn increases. All but about 10-25% carbon ash is burned off from 385-510°C, during the steepest drop in the TGA curve. The amount of remaining ash also increases with increasing amounts of PAn.

TGA on pure PAn and pure PVP were run for comparison, on three different samples each (dry powder, films cast from NMP, and films cast from DMAc). These results are shown schematically in Figure II.2. All three sample types showed a small amount of moisture retention up to about 200°C. Beyond this, the PVP powder showed minimal weight loss from 200-385°C (about 2%), the PVP film cast from DMAc had a small dip from 200-385°C (about 4-5%), while the PVP film cast from NMP showed about 18% weight loss from 200-385°C. The PAn film cast from NMP was about 33% NMP by weight, compared to only 12% DMAc for the PAn film cast from DMAc.

The TGA thus revealed both the hygroscopic and high solvent binding nature of PAn and PVP. Despite efforts to remove the solvent by vacuum drying at elevated temperatures (about 100°C), both PAn and PVP tenaciously retained significant fractions of solvent. Several other research groups have reported this behavior for PAn [31, 77, 78], but rarely is this condition mentioned in the vast majority of work done with NMP solution cast films of PAn. Thus all samples characterized by thermal analysis (as well as otherwise) had some extent of residual solvent and moisture present, which must be considered in interpreting the results. Complete removal of these solvents requires high temperatures which were not used throughout this study in order to avoid sample degradation. Wei, et al., have suggested repeatedly HCl solution-doping followed by NH_4OH solution-dedoping of the pure PAn for extended periods of time to remove residual NMP [31]. This was not an option in the case of PAn/PVP blends, since PVP is water soluble.
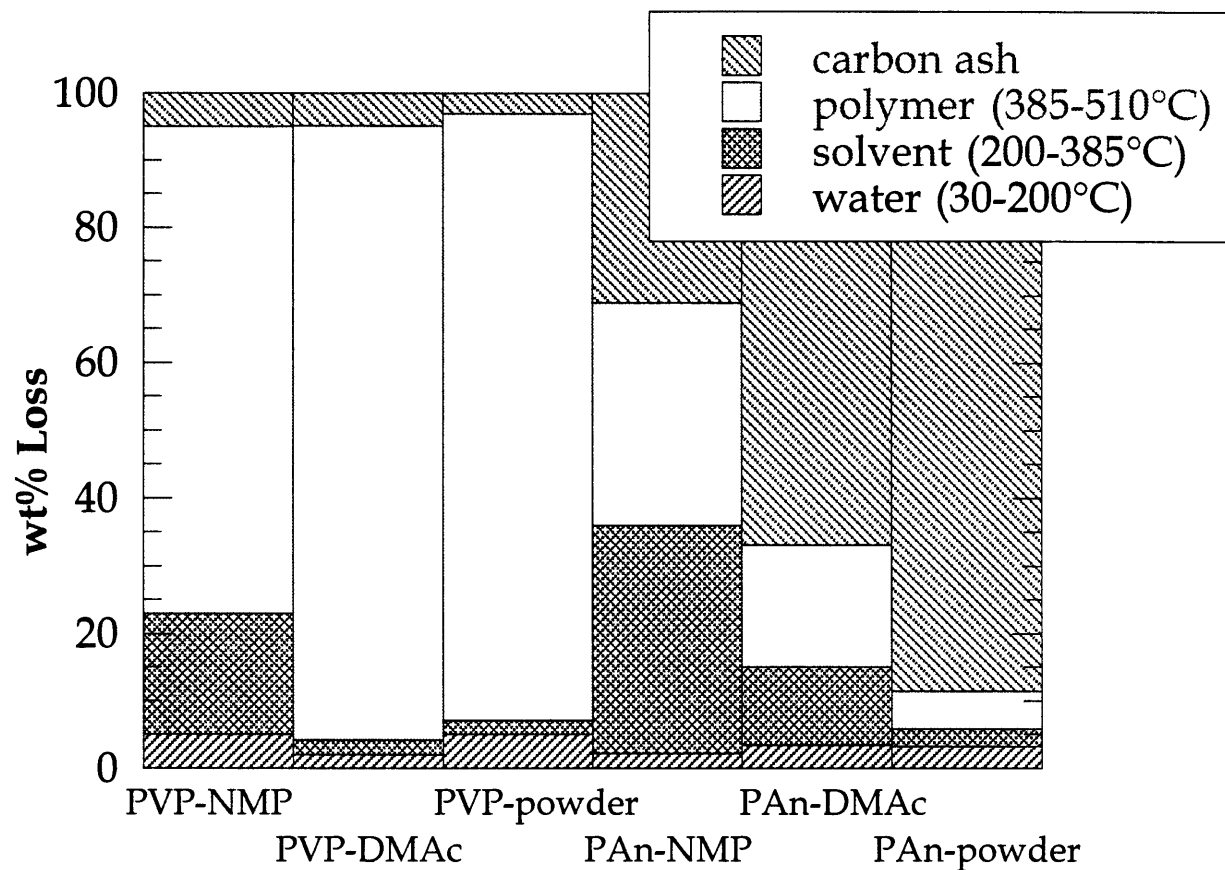
Figure II.2. TGA wt% loss for PAn and PVP homopolymers cast from DMAc, NMP, or "dry" powder.

II.C.2. Differential Scanning Calorimetry (DSC)

Figure II.3 shows the glass transition (T_g) and the change in heat capacity at T_g (ΔCp) vs. wt% PAn (measured by DSC) for two series of blends cast from NMP, one with PVP-M, the other with PVP-10K. The samples were cast directly into DSC pans (again, from about 2 wt% polymer solution), then vacuum oven dried overnight at 100°C before running in the DSC (thermal cycle given in experimental section). In all cases, a single T_g was observed, and no other transitions. If the blends were truly homogeneous, the blend T_g would appear between that of the two homopolymers. Here, the T_g generally rises with the addition of PAn, suggesting that the two polymers are phase mixed. Pure polyaniline, however, shows no thermal transitions in the DSC up to about 280°C, due to its high melting temperature and rigid structure (although it has low crystallinity). Its T_g has been reported as between 220-250°C [31]. Thus, a phase separated system would still show a single T_g, but always near the same temperature. There are some fluctuations seen in Figure II.3, likely due to varying amounts of residual solvent. Since the wt% of solvent can actually be higher than that of PAn, its T_g-lowering effect can act to oppose the T_g-raising effect of added PAn.

For a homogeneous blend, the ΔC_p would similarly be the sum of the two homopolymer ΔC_ps, weighted by their respective fractions. If they were phase separated, the T_g of the PVP phase would not vary much and the ΔC_p would be proportional to the amount of PVP, thus would decrease with added PAn. It can be seen in Figure II.3 that the ΔC_p values do not change much over this composition range, with the exception of one data point. This is also evidence for a phase mixed blend.

One might be tempted to verify if this system follows a Gordon-Taylor relation for T_gs of miscible blends, and to estimate the T_g of PAn by using a relation such as:

$$A_1(T_g-T_{g1})w_1 = A_2(T_{g2}-T_g)w_2,$$

where A_1 and A_2 are constants; w_1 and w_2 are the weight fractions. Plotting T_g vs. $(T_{g2}-T_g)w_2/(1-w_2)$ gives intercept T_{g1}. For the 10K series, this gave a T_g of PAn ≈ 179°C. The 1M series predicts the T_g of PAn ≈ 229°C. Simply extrapolating the T_g values in Figure II.3 to 100% PAn gives T_g of PAn closer to 260°C. This
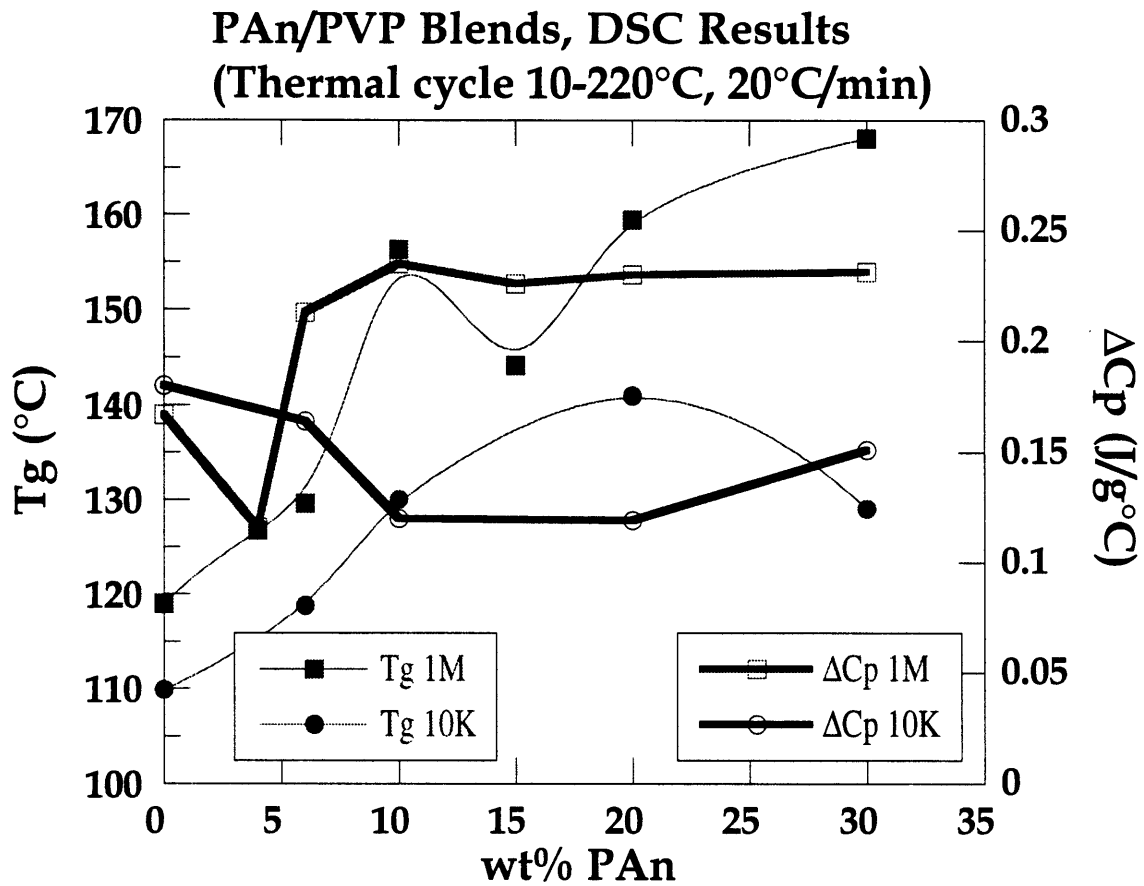
Figure II.3. DSC results (Tg and ΔCp) for PAn blends with PVP-1M and PVP-10K.

broad range of predicted T_gs exemplifies the complications encountered in characterizing this three-component system of PAn, PVP, and solvent. Even though the samples were heated to 220°C for one minute in the DSC (in covered but unsealed pans to allow vapor to escape), apparently this was not sufficient to uniformly remove all residual NMP. As seen in the previously mentioned TGA results, the NMP does not begin to come off during a heating scan until about 200°C, and is not completely removed until about 380°C, which takes 9 minutes at 20°C/min. Therefore, in retrospect, is it clear that some residual NMP remains, likely acting to plasticize the samples used in DSC runs. This effect will also be seen in the DMA results. None-the-less, the DSC results suggest, at least for this three-component system, that there is significant PAn/PVP compatibility.

II.C.3. Differential Mechanical Analysis (DMA)

T_gs were measured for two other series, cast from a NMP/DMAc mixture (the amount of DMAc was proportional to the amount of PAn; the wt% of DMAc equaled 0.8 times the wt% of PAn). One series was cast directly in the DSC pans, the other was the thick film (0.3 mm) series. Although all of these samples displayed a single T_g, they had less definite trends. The T_g generally increased with increasing wt% PAn, but not uniformly. These results are seen in Figure II.4, along with DMA results. DMA was run on the 0.3 mm thick films of PAn/ PVP-M cast from the above mentioned NMP/DMAc mixture. Again, a single loss peak (tan δ) was seen, and the loss peak at 1 Hz is shown to represent T_g. The storage modulus, E', ranged from 2 to 3 GPa, generally increasing with increasing wt% PAn. These films are therefore relatively stiff materials, but embrittle with increasing percentage of PAn.

It is difficult to draw conclusions from the thermal analysis due to the variable amounts of bound solvent in the films and to the varying effects of DMAc vs. NMP. There is competition between the plasticizing effect of residual solvent, and the stiffening effect of added PAn. Added PAn acts to increase the T_g and modulus, but also retains more solvent (as seen in Figure II.1), which acts to plasticize. The result is the wavy trend seen in Figure II.4 - a T_g that fluctuates as the relative amount of the three components varies. For the thick films run in TGA, DSC, and DMA, there does appear to be a correlation between the amount of retained solvent and both the measured T_g and the modulus. As seen in Figure II.4, the T_g displayed by DMA (open circles) and DSC (open triangles) follow a

39

Tg vs. wt% PAn in PAn/PVP-1M Blend
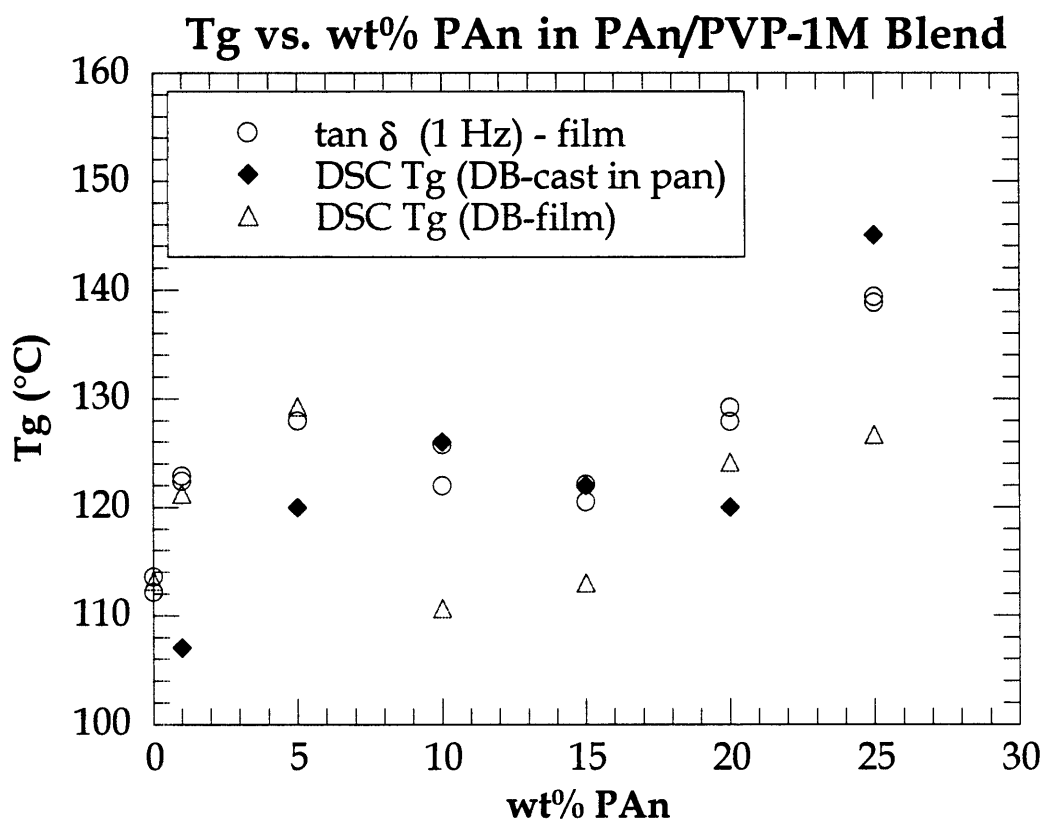
Figure II.4. Tg of PAn/PVP-1M blend (DB series) as measured by both DSC and DMA (loss tangent peak).

similar trend, as these samples were cut from the same film. There is an initial rise up to about 5 wt% PAn, followed by a region of decreasing T_g up to about 15% PAn, then an increasing T_g above that. Again, if there was macroscopic phase separation, the loss tangent would show little trend with added PAn. A similar trend was seen with the modulus. This behavior is likely due to competing effects, that of an increasing amount of NMP with increasing wt% PAn that acts to counter the stiffening effect of added PAn. It is apparent that PAn can be compatiblized with PVP in an NMP solution, but the resultant blend is a three component system containing variable amounts of solvent.

II.D. Light Microscopy

Microscopy samples were prepared by spin-coating PAn/PVP-M blends ranging from 0-100% PAn in the aforementioned NMP/DMAc solution onto silicon wafers, then drying in a vacuum oven overnight at about 100°C. These films are approximately 0.5 μm thick. Since the solvent is a high-boiling/low vapor pressure solvent, the spin coating does not rapidly remove the solvent as in conventional spin coating. The cast films therefore are not "quenched-in" kinetically restricted structures, but still maintain some chain mobility until drying is complete. The overnight drying at 100°C, although below T_g, also allows some additional chain mobility, such that the final structure is likely closer to an "equilibrium" structure than to a quenched phase-mixed one.

The undoped blends all appear miscible, as evident by uniform color of the films, at the resolution limit of light microscopy. This limit is estimated to be about 1000Å for good contrast at 1000x magnification. Since PAn is dark blue and PVP is transparent, contrast is indeed reasonably good (for films of appropriate thickness). There were some micro-particulates in many of the samples, but these were mostly due to undissolved PAn, not due to phase segregation in the presence of PVP. This is evident by the fact that pure undoped PAn (no PVP) contained a few small (submicron) undissolved aggregates in the solution cast films. Most all of the aggregates disappeared after filtering the PAn solution (using a 0.45 μm filter), and the filtered solutions did not become lighter in color. Also, in the case of the blends, the amount of visible particulates was too low to account for the amount of PAn present. These particulates appeared primarily in samples that were prepared with unfiltered PAn.

41

Figure II.5 shows light micrographs of three PAn/PVP-1M solution-cast films (from NMP), containing 5, 15, and 50 wt% PAn. For comparison to a highly incompatible system, a 50 wt% PAn/PMMA blended film, also cast from NMP, is shown. These are all taken at 200x magnification. All three of the PAn/PVP samples appear uniform, even up to 50% PAn. The vertical striations in the 5% and 15% photographs are due to the light filament image, not sample features. The PAn/PMMA sample is clearly phase separated. The two 50% PAn samples are shown in Figure II.6 at higher magnification, 1000x. Again, the uniformity of the PAn/PVP sample is evident, with the possibility of some light spottiness, whereas the phase-separated PAn/PMMA structure is evident. Thus while PVP and PAn are compatible, PMMA and PAn are clearly not, despite having the ability to form hydrogen bonds with each other. Apparently, PVP interacts much more strongly with PAn than does PMMA. This issue of polymer-polymer interactions is addressed in more detail in Chapter III.

These solution-cast films all remain uniform upon doping with HCl vapor, showing little or no signs of phase separation. Also, all blended samples were dark under crossed polarizers, indicating that there were no crystallites (at least not larger than about 1000Å, the estimated resolution limit of the microscope).

These blends can also be doped while still in solution (NMP) with a number of protonic acids, including methane sulfonic acid, camphor sulfonic acid, and dodecylbenzene sulfonic acid. Excess acid is simply added directly to the NMP solution such that the PAn becomes fully doped. In most cases, the doped blends remain soluble. In pure NMP, PAn/PVP mixtures were soluble in all ratios, and the resulting films also remained miscible. Upon doping with MeSA, the solutions remained visibly soluble for all ratios. There were likely some microaggregates at this point, however, as indicated by their presence in the cast films. For samples doped with DBSA and CSA, the blended solution was not soluble at all ratios. The highest fraction of doped PAn soluble with PVP was about 30/70 PAn/PVP (2 wt% total polymer in NMP) for both CSA and DBSA, above this precipitation occurred. The solution doped films showed extensive crystallinity for all ratios greater than 50/50 PAn/PVP, as observed under crossed polarizers. For PAn ratios less than 50/50, the amount of crystallites quickly diminished. This is not what was observed for the films cast in the dedoped state, as mentioned above. No crystalline regions were observed at any PAn/PVP ratio in the films that were cast dedoped, then subsequently doped. It could be that there are very small crystallites in this case, or that the degree of
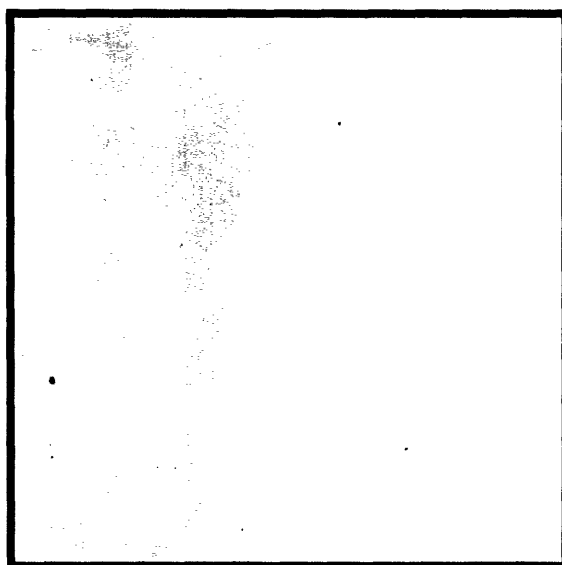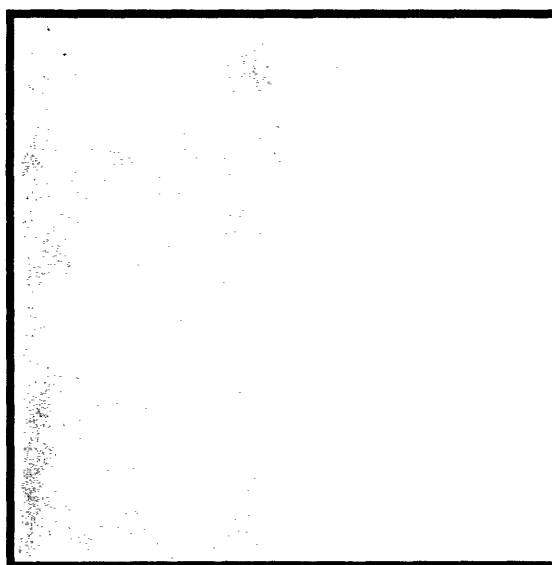
5% PAn in PVP   15% PAn in PVP
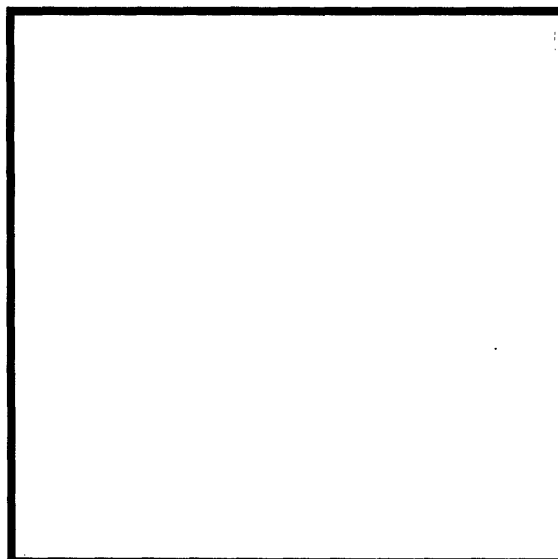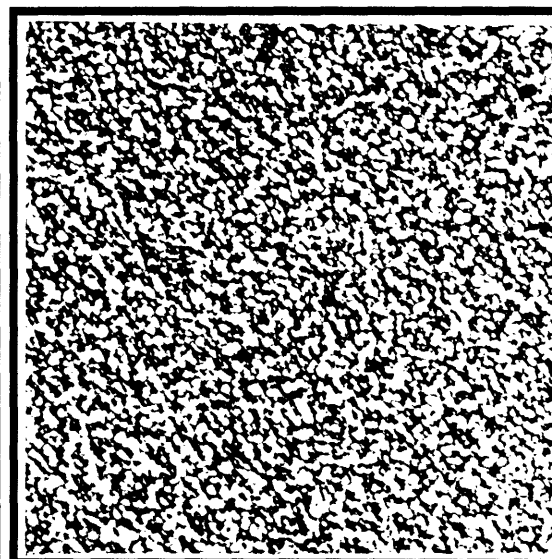
50% PAn in PVP   50% PAn in PMMA

Figure II.5. Light micrographs of PAn blends with PVP and PMMA, films cast from NMP (200x magnification).
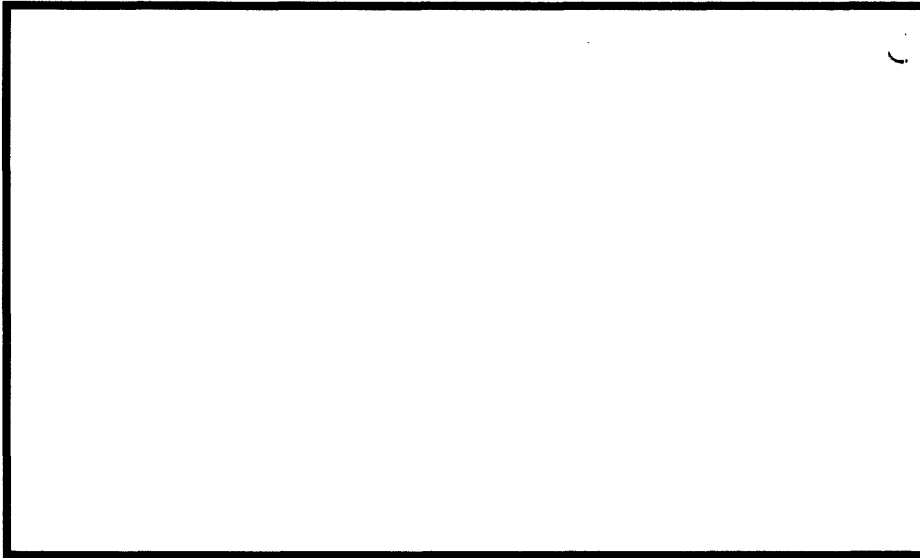
50% PAn in PVP
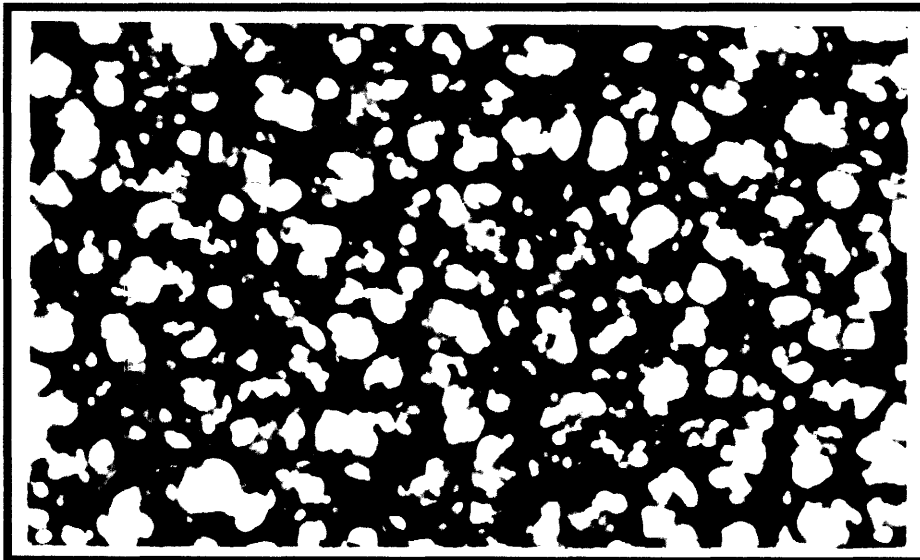
50% PAn in PMMA

Figure II.6. Light micrographs of PAn blends with PVP and PMMA, films cast from NMP (1000x magnification).

mixing with PVP has hindered PAn crystallite formation. In summary, it appears that at higher PAn ratios (greater than 50/50), doping while in solution leads to a higher fraction of crystallinity, while for lower fractions of PAn and for non-doped solutions, the presence of PVP hinders the crystallinity, indicative of some extent of phase mixing.

Light micrographs of samples with these three dopants are shown in Figure II.7. All samples are 10 wt% PAn, three in PVP, one in PMMA for comparison, doped in solution in NMP, then cast into films. The PAn/PVP films appear mostly uniform, especially compared to the PAn/PMMA film. The doped-PAn/PMMA blend is grossly phase separated, even in solution. Doping the PAn in DMAc with any of the three above mentioned sulfonic acids (in the presence of PMMA) resulted in the immediate precipitation of the PAn.

In the films cast from these pre-doped solutions of PAn/PVP there was some level of phase segregation, as evidenced by the increasing appearance of microaggregates in the cast films with increasing wt% PAn. The aggregate sizes were difficult to determine due to resolution limits, but they appear to range in size from 0.1 - 1.0 μm. The smallest domain sizes were observed with MeSA as the dopant. The largest particulates appeared in the PAn-DBSA films. Presumably, these aggregates are doped PAn crystallites. Under crossed polarizers, however, both MeSA and CSA doped samples appeared dark, while the DBSA doped samples showed some faint scattered light, indicating the presence of PAn crystallites. As mentioned above, the frequency of crystallites increased with increasing fraction of PAn.

It should be noted that in all of the microscopy results presented here, the PVP molecular weight used was 1M. Similar compatibility results were observed with PVP-10K. Since compatibility was observed for both a high molecular weight (thus very limited mobility) and low molecular weight (very mobile) PVP, this suggests that phase separation kinetics were not a limiting factor in the morphologies observed. Although it is possible to quench in a phase mixed morphology in an incompatible blend, the rapid formation of two phases in PAn/PMMA blends observed, and the lack of phase separation for low molecular weight PVP suggest that this is not the case here.
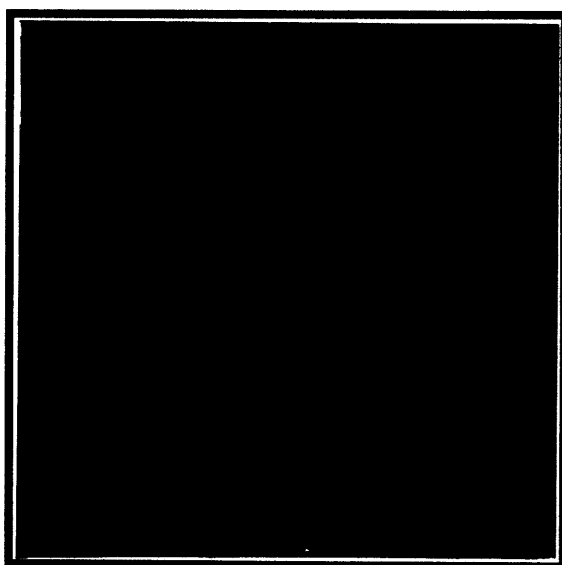
10% PAn-MeSA in PVP
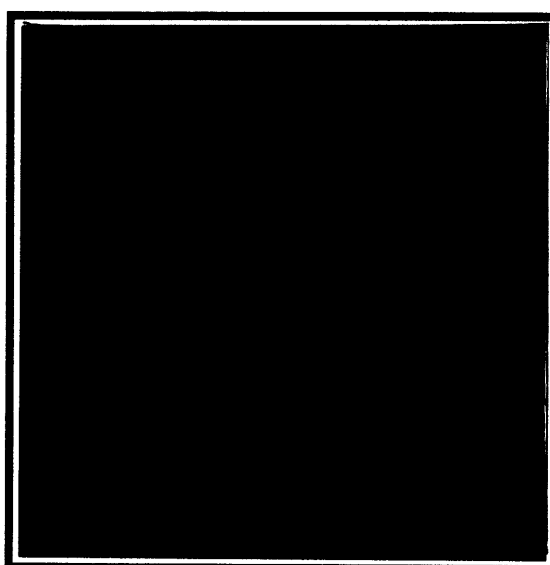
10% PAn-DBSA in PVP
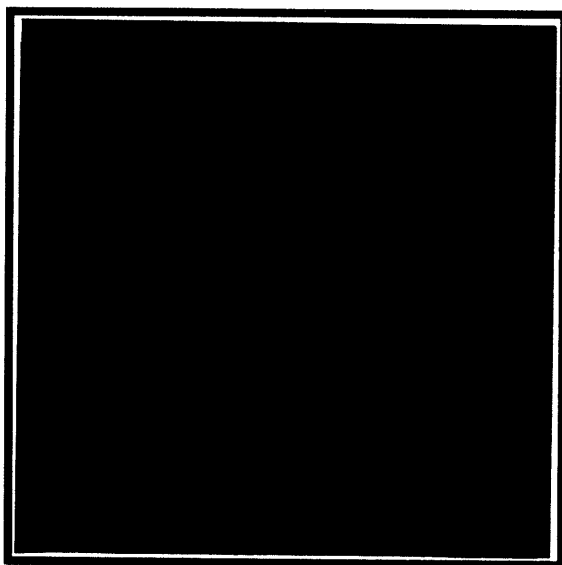
10% PAn-CSA in PVP
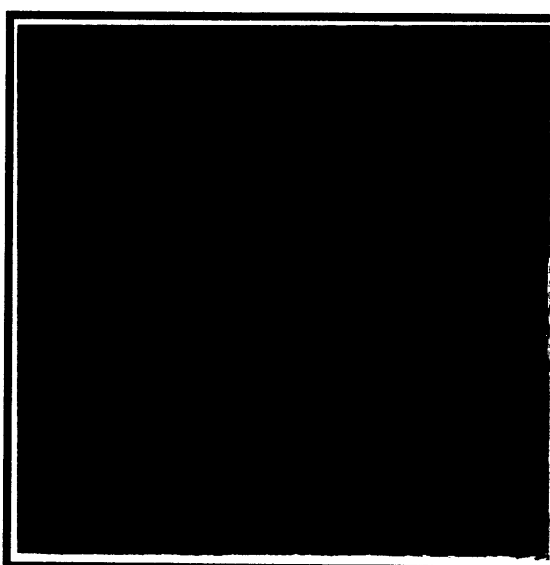
10% PAn-CSA in PMMA

Figure II.7. Light micrographs of pre-doped PAn blends with PVP and PMMA, films cast from NMP (1000x magnification).

II.E. Small-Angle X-Ray Scattering (SAXS)

Transmission SAXS was run on solution cast films ranging from 5-30% PAn (same samples as used for DMA). There were no detectable scattering peaks from any of them, suggesting a lack of any periodic domain spacings on the order of 540-84Å. Since the highest wt% PAn was only 30%, it is possible that the domain spacing, if it existed, was greater than about 540Å, the limit of the detector. The less PAn present, the larger the spacing, for a phase separated sample. Therefore, the only conclusion that can be drawn from the SAXS results is that either the samples are not phase separated, or that there are domains spaced greater than 540Å apart. Light microscopy suggested that there are not domains larger than about 1000Å, thus it is possible that phase separation has occurred in the 500-1000Å size range. The thermal behavior suggests that this is not the case, however. No SAXS measurements were taken on doped samples, but this would certainly be valuable information.

II.F. Electrical Conductivity

It might be expected that a macrophase separated blend with an insulating polymer matrix would insulate the conducting domains until a percolation threshold was achieved. This value is typically predicted to be near 16 vol% for the conducting phase, using a small-spheres packing model for a 3D system. A more compatible blend would act to disperse the conducting component, giving rise to non-sharp percolation type behavior. In addressing this issue, conductivity was measured as a function of PAn wt% in several series of blends. Six series of PAn/PVP blends were cast into films, dried under vacuum, doped with HCl vapor, and measured for conductivity. They are :

1. **D8KS**. - PAn blended with PVP-8K in DMAc, spin-coated to 0.6-1.2 µm thick.
2. **D10KS**. - PAn blended with PVP-10K in DMAc, spin-coated to 0.4-0.6 µm thick.
3. **N10KS**. - PAn blended with PVP-10K in NMP, spin coated to 0.3-0.5 µm thick.
4. **N10K**. - PAn/PVP-10K in NMP, static cast to 24-60 µm thick.
5. **N1MS**. - PAn with PVP-M in NMP, spin-coated to 0.5-0.7 µm thick.
6. **N1M**. - PAn/PVP-M in NMP, static cast to 24-60 µm thick.

The results are plotted in Figure II.8, and show the conductivity to range from 10^{-3} to 2 S/cm for PVP-M blends ranging from 3-30 wt% PAn. There is not a sharp percolation threshold, but rather a gradual decrease in conductivity as the % PAn is decreased, with a sharper drop around 5-8 wt% PAn (depending on the series). The drop-off is gradual, indicating a gradual insulating dilution of PAn rather than a sharp break in conducting domains. For films with less than about 4% PAn, the conductivity was below the range of our instrument (about 10^{-5} S/cm), and this may be where percolation occurs. It is possible that the extent of miscibility of these two polymers results in the gradual dilution of PAn chains, rather than the formation of discrete domains, to the point where they are no longer near enough for effective charge transport.

The conductivity may also be limited by the presence of NMP, which can weakly complex the proton involved in doping PAn, hindering the doping process. Several authors have reported similar results [50, 78]. The two series cast from DMAc rather than NMP, the D8KS and D10KS series, showed a large increase in conductivity compared to the equivalent series cast from NMP (N10K series), as seen in Figure II.8. As seen earlier, it is easier to remove residual DMAc than NMP. For the two 1M series, thicker films (static cast) showed about double the conductivity of the thinner spin-coated samples. This thickness effect is attributed to the increased chances of forming percolation pathways that traverse the entire film in thicker films. The PVP-M blends showed a conductivity about an order of magnitude higher than the PVP-10K blends. It is not clear why this is the case, although the PVP-1M films tended to be thicker than the PVP-10K films, thus there can be a thickness effect. In terms of stability, the conductivity dropped about one order of magnitude over the course of one year for the thicker solution-cast films (stored in air).

A much different trend was seen for the pre-doped films, cast from doped solutions. The conductivity was relatively low, however, and did not increase much with increasing amounts of PAn. For a pre-doped blend of only 1 wt% PAn in PVP (doped with MeSA), the conductivity was already 5×10^{-3} S/cm, but increased to only about 3×10^{-2} S/cm for pure PAn. Conductivities for CSA and DBSA doped PAn were even lower, on the order of 10^{-3} S/cm, and also showed little increase with increasing wt% PAn. These low values, again, are likely due to interactions with NMP, both in-solution and in the cast films. As mentioned above, the NMP acts to weakly complex the proton involved in doping PAn. It is also very likely that there is considerable residual NMP (approx. 10-20 wt%) in

Conductivity vs. wt% PAn in PAn/PVP Blends
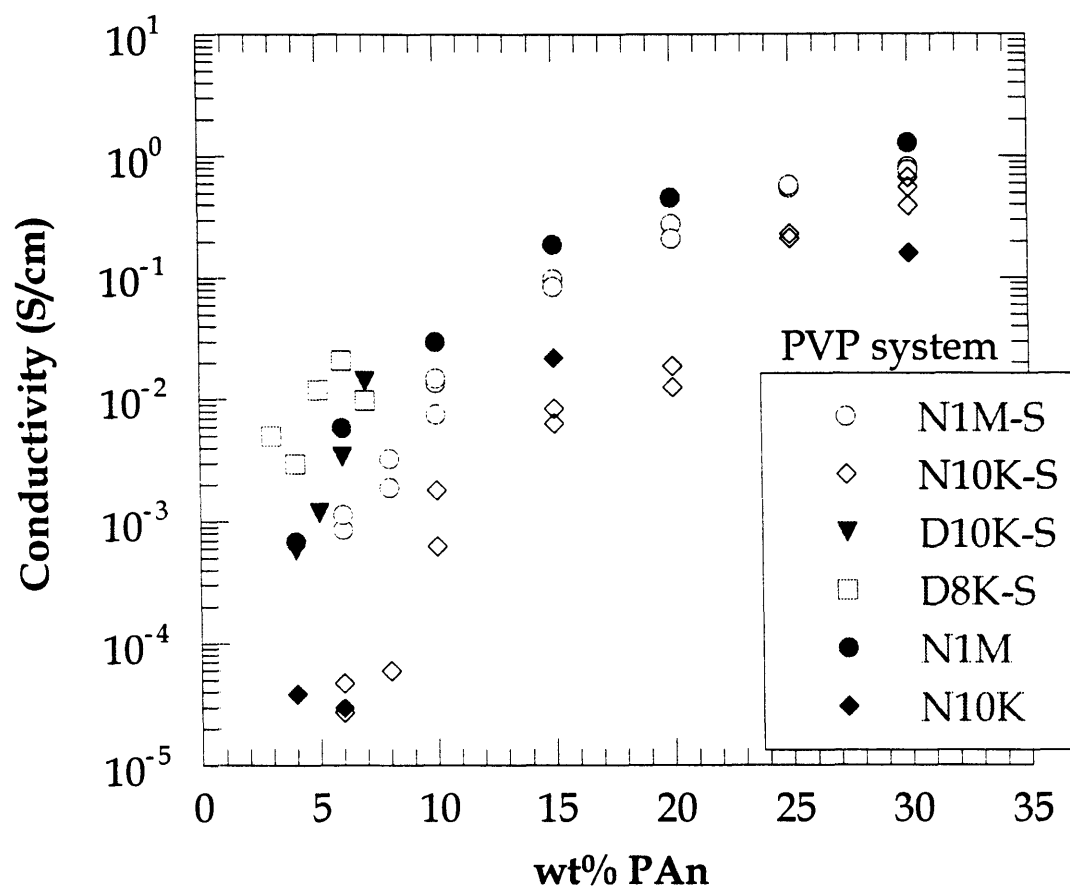
Figure II.8. Conductivity of HCl-doped PAn/PVP Blends.

these pre-doped cast films, again as evident of the earlier mentioned TGA results. Since PAn binds NMP more tightly than does PVP, there is more NMP in the higher wt% PAn samples. Also, since the solution doped blends appear to have a higher extent of phase separation relative to the undoped blends, they are less likely to have a continuous conducting path of PAn. The undoped blends can remain more phase-mixed upon doping, since chain mobility is restricted in the solid state.

It is also possible that PVP, which, like NMP, can weakly complex the dopant proton, reduces the effective extent of doping. The strong interactions between these two polymers that enables the formation of a compatible system might simultaneously act to hinder the formation of ordered or high conjugation length regions of PAn, thus restricting conductivity.

It has been shown that PAn forms compatible blends with PVP, the first such system reported for PAn. Even upon subsequent doping, the blend remains miscible. If pre-doped PAn is solution mixed with PVP (in NMP), there is still considerable compatibility, although PAn crystallites can form, which are not present in "post-doped" PAn/PVP blends.

The PAn/PVP blend can be doped to reasonable conductivity levels, but since PVP is water soluble, its structural usefulness has obvious limitations. However, one can exploit the strong polymer-polymer interactions that drive the miscibility in the formation of adsorbed multilayer films. It was the recognition of the strong interaction strength, primarily through hydrogen bonding. between PAn and PVP that led to the idea of using these two polymers, and others capable of such interactions, in the formation of self-assembled multilayer films. This is the subject of the next chapter.

CHAPTER III. SELF-ASSEMBLED MULTILAYER FILMS OF POLYANILINE

III.A. Introductory Remarks

As mentioned in the introduction, multilayer assemblies of conjugated polymers deposited by means of self-assembly have been demonstrated and investigated for quite a number of systems. The idea is to fabricate molecular coatings onto a variety of substrates by simply allowing the polymers to adsorb onto the surface. Adhesion is maintained by a variety of forces, including electrostatic attraction, and secondary molecular forces, such a hydrogen bonding or hydrophobic interactions. Previous work in our group has been exclusively with charged polymers (doped conjugated polymers and polyelectrolytes), including some structural characterization. In the work presented in this chapter, we exploit the strong interchain interactions between PAn and several non-ionic water soluble polymers that enable multilayer build-up. As described in the introduction (Section I.C), the films consist of alternating layers of PAn with one of several other strongly interacting polymers.

There remain, however, some questions concerning the extent of coverage, the nature of the interfaces, and the polymer configuration once adsorbed onto the surface. These questions, as well as the effects of the various processing parameters on both film structure and adsorption mechanisms, will be addressed.

III.B. Experimental

III.B.1. Solution Preparations

The self-assembly technique for PAn is described in detail in [79], and outlined with some variations here. The basis for the technique involves coating substrates with layers of polymers by means of spontaneous adsorption from aqueous solutions. Multilayers are built up by dipping the substrate alternately from one solution to the next, using solutions of suitable concentrations, pH conditions, and for sufficient lengths of time.

PAn was synthesized chemically as described in Section II.A.1, and dissolved in either NMP or DMAc (at 18 mg/ml), as before. The PAn dipping solution was prepared by slowly adding one part (by volume) of the filtered PAn solution (in DMAc or NMP) in with 9 parts water with the pH adjusted to about 3.0-3.5 with methane sulfonic acid (MeSA). The pH was then quickly lowered to 2.5-2.6 by adding drops of concentrated MeSA. Care must be taken to not go below pH=2.5 or above pH=3.5 to avoid precipitating the doped PAn. The solution was filtered through a 0.45 μm filter just before use. The PAn concentration can be varied by adjusting either the amount of PAn in DMAc, or by adjusting the amount of water added. We believe that at least 5% DMAc is necessary to form a metastable solution, although it may be possible to use less. There is a range of concentrations and pH conditions that are suitable for self-assembly; this range has been mapped out by Cheung [79]. The PAn concentration primarily used throughout this paper is 0.01 M (Molar in terms of two aniline structural units), and pH as mentioned above, 2.5-2.6.

In forming the other dipping solutions, all polymers were used as-received, and dissolved in water to form 0.01 M solutions, molar in terms of one monomer repeat unit. For the pH study, the pH was adjusted by using either MeSA or ammonium hydroxide. The solutions were all filtered through a 0.2 μm filter.

Solutions of different molecular weights of poly(vinyl pyrrolidone) (PVP, Mw=1,000,000 g/mole and Mw=10,000, Polysciences, narrow molecular weights from American Polymer Standards) were prepared by dissolving the polymers in water at 1.11 mg/ml. These solutions have a pH of about 4.5. Poly(vinyl alcohol) (PVA, Mw=86,000, Scientific Polymer Products) was dissolved in water at 0.44 mg/ml. The resulting solution has a pH of 6.25.

Poly(acrylamide) (PAAm, Mw=5,500,000, Polysciences) was dissolved in water at 0.71 mg/ml, with a resulting pH of 6.2. Poly(ethylene oxide) (PEO, Mw=5,000,000, Aldrich) was dissolved in water at 0.44 mg/ml and has a pH of 6.3. Poly(acrylic acid) (PAA, Mw=1,000,000, Polysciences) was dissolved in water at 0.72 mg/ml, with a resulting pH of 3.44. Solutions of sulfonated polystyrene (SPS, Mw=70,000 and Mw=500,000, plus a monodisperse molecular weight series, Polysciences) were prepared by dissolving in water at 2.06 mg/ml, and the pH was adjusted to 2.5-2.6 with MeSA. Poly(ethylene imine) (PEI, Mw=70,000, Polysciences) comes dissolved in water, and was further diluted to form a 0.02 M solution, then adjusted to pH = 2.6 with MeSA. All chemical structures of these polymers were shown in Figure I.4.

III.B.2. Film Deposition

The films were deposited on a variety of substrates, including glass, plastics, metal, and silicon. Adhesion could be enhanced by surface treatment of the substrate. Glass slides and silicon wafers were rendered charged by one of two types of surface treatments. Briefly, there were four main steps in the treatments, as follows. First the slides were acid cleaned in a sulfuric acid/hydrogen peroxide bath (piranha), then second they were hydroxylated in an ammonium hydroxide/hydrogen peroxide bath. Third, the glass or silicon was rendered positively charged by one of two approaches. The surface was either silanized with an amine-terminated trifunctional silane in toluene, or coated by adsorption with a monolayer of PEI. In either case, this enabled rendering the surface positively charged through the protonation of the amine ends. The final step was to coat the surface with a protective monolayer of SPS by immersion into a SPS solution at pH=2.5, which gave the surface a negative charge. Doped PAn is effectively a polycation, thus adsorbs quite readily to a negative surface (such as SPS), which improves the adhesion of the first layer.

The dipping procedure using these treated substrates was as follows. The treated slides were first immersed into the PAn bath for 15 minutes, followed by rinsing with water at pH=2.5 (MeSA), then drying with a compressed air jet. A 15 minute dip time was used because adsorption vs. time experiments in our lab have shown that almost 100% of the equilibrium thickness deposits in the first 15 minutes (for concentrations of PAn ≥ 0.0005 M). A plot of absorbance at 880 nm vs. time in Figure III.1 shows the self limiting "high affinity" adsorption

PAn Monolayer Adsorption
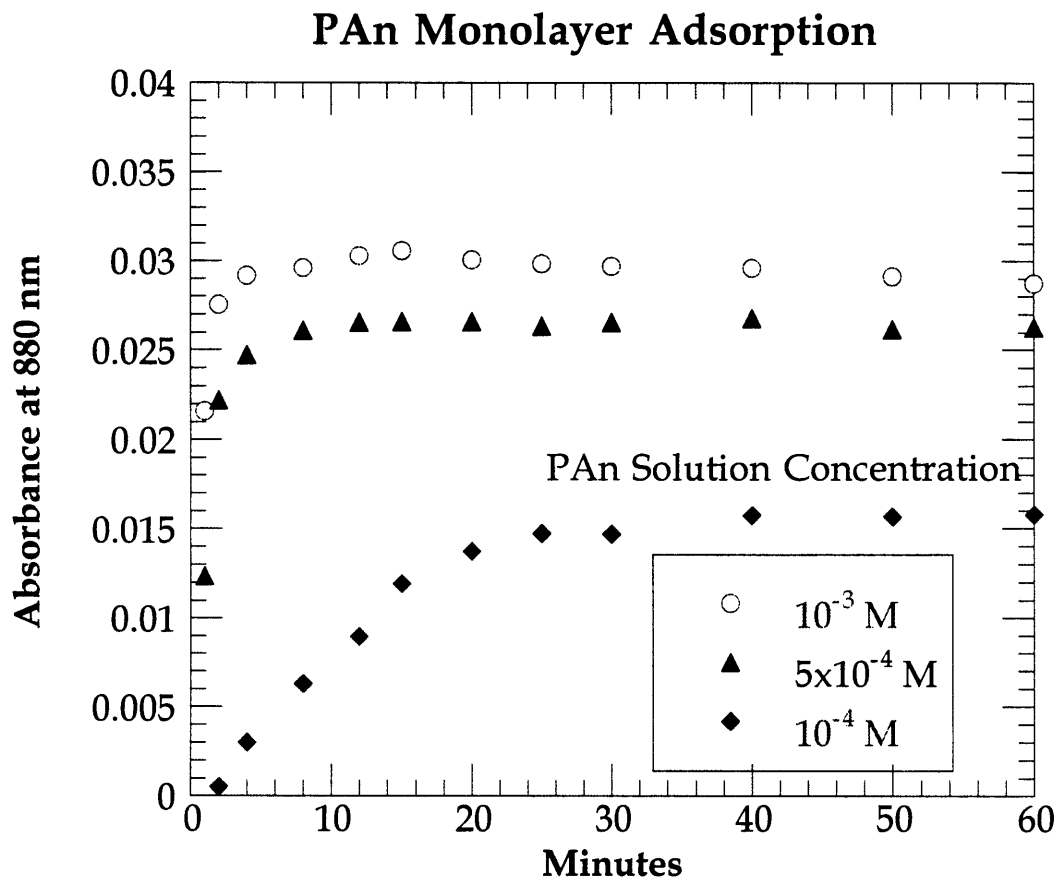
Figure III.1. Light absorbance vs. adsorption time for PAn adsorption (from three concentrations) onto SPS treated glass.

of PAn, onto SPS in this case. Three lower concentrations are shown, 0.0001, 0.0005, and 0.001 M. It can be expected that the 0.01 M concentration would behave similarly to 0.001 M solution, or deposit faster, as it is well known that increases in concentration generally accelerate the kinetics of adsorption.

The films were then immersed in the non-ionic polymer bath for 15 minutes, followed by rinsing with neutral water, and compressed air drying. From there, layers were simply alternated between PAn and the non-ionic polymer. The resulting films were only lightly doped; they were immersed in a 1 M MeSA solution to fully dope, followed by a quick rinse in a 1 M HCl solution to remove residual surface MeSA.

III.B.3. Characterization Techniques

Layer-by-layer build-up was monitored by visible and infrared spectroscopy. UV-Visible light absorption spectra were taken directly from coated glass slides using an Oriel Multispec spectrophotometer. Dichroic ratios of PAn (S-polarized/P-polarized absorbance) were measured at a 45° angle of incidence using polarized light. IR spectra were taken on films built up on ZnSe plates, using a Nicolet 510P FTIR. Both UV-vis and IR spectra were taken between each bilayer after dedoping the films by rinsing with 0.1 M ammonium hydroxide. This was to ensure a uniform electronic state in all films for direct comparison of absorption spectra. Contact angle measurements were made using a VCA 2000 video image system by the sessile drop technique, measuring advancing angle. Atomic force microscopy (AFM) was performed using a Digital Instruments Nanoscope III operating in tapping mode. The film thicknesses were measured by both profilometry (using a Sloan Dektak 8000) and by ellipsometry (for films on reflective surfaces, using a Gaertner three wavelength ellipsometer). A Zeiss light microscope with a maximum magnification of 1000x was used for light microscopy. All conductivities of fully doped films were measured in air by the van der Pauw four corner probe method. As with the blends of Chapter II, measurements were made in relative humidity ranging from 20-75. Samples measured at both ends of this range showed only a slight increase in conductivity with increasing humidity.

III.C. Multilayer Film Deposition

An example of a typical starting point for a multilayer system, as described in Section III.B.2, is shown schematically in Figure III.2. The steps of treating a glass slide, then dipping into the various polymer solutions are depicted.

Deposition is typically on a glass or silicon substrate that has been treated with an amino silane, which is positively charged at low pH values. The substrate is then dipped in a SPS solution. SPS chains adhere primarily due to electrostatic attraction, which renders the surface negatively charged. From there, a layer of partially doped PAn is deposited, also adhering primarily due to electrostatic attraction. PAn can also be deposited directly onto non-charged surfaces, such as plastics, metal, and untreated glass or silicon. The surface negative charge does act to improve adhesion, however. The next layer, PVP in this case, adsorbs through secondary molecular forces, primarily hydrogen bonding. Subsequent alternating layers of PAn and PVP are built up similarly.

The multilayer deposition can be monitored by either UV-visible or infrared spectroscopy, where absorbance per bilayer is measured. For visible light, the absorbance at 630 nm is monitored, which corresponds to an exitonic absorption for the dedoped form of PAn, the emeraldine base. In the case of doped PAn, there is a strong absorbance near 880 nm (corresponding to free charge carrier absorption), which can also be monitored. None of the other polymers absorbs in this wavelength range, thus the monitored build-up corresponds only to that of PAn. By plotting the absorbance as a function of number of bilayers, the extent of growth is determined.

Figure III.3 shows such results for six different systems, all of the same concentration (0.01 M). The PAn concentration was also held constant at 0.01 M. The linearity of the absorbance at 630 nm indicates uniform multilayer build-up for all of these systems. Each bilayer is delivering approximately the same amount of PAn, with the exception of the first bilayer. Since all of these films were deposited on SPS-treated glass, as depicted in Figure III.2, the first bilayer is effectively a PAn/SPS bilayer. Thus, the thickness of the first bilayer should be closer to that of the PAn/SPS system. There is also some uncertainty as to the extent of coverage of the first bilayer. Properties such as conductivity and surface hydrophillicity (as determined by contact angle) indicate that the first

1. Clean Substrate (glass or Si)

2. Silane in toluene (overnight)

3. SPS Solution (15 minutes)

4. PAn Solution (15 minutes)

5. PVP Solution (15 minutes)

Figure III.2. Schematic of the self-assembly process, showing treating a glass slide, coating with SPS, then a PAn/PVP bilayer.

bilayer behaves differently than the subsequent layers, suggesting non-uniform coverage.

As evident in Figure III.3, there is quite a range of absorbances, depending on the particular system. The most polyaniline is deposited with PAAm, while the ionic system, SPS, delivers the least. All of the non-ionic polymers of this study deposited more PAn per bilayer than did the ionic polymer, SPS. The implication is that there are strong interactions between PAn and these ionic polymers that lead to considerable bilayer thicknesses, relative to that formed with polyanions (additional work in our group has demonstrated similar PAn deposition levels with other polyanions such as poly(methacrylic acid) and poly (vinyl sulfonate)).

There are many factors that influence polymer adsorption, however, and these must all be considered in comparing the various systems. Solution concentrations are important, as it is known that generally thicker films are deposited from more concentrated solutions. This results from the fact that polymer chains adsorbing from very dilute solutions have opportunity to reconfigure with time on a surface, spreading out to maximize surface interactions. In more concentrated solutions, adsorption happens faster, and all surface sites can become quickly occupied, preventing the subsequent elongation of a chain. Depending on the solvent strength, the polymer adsorbed from the more concentrated solution is therefore more coiled, forming a thicker layer.

The molecular weight, and thus the size, of the adsorbed polymer can certainly influence film thickness, depending on the chain conformation. The interaction strength between the surface polymer and the adsorbing polymer is also important. The strength of the interactions can depend on pH conditions, charge densities and ionic strength, and solvent conditions. In the case of polyelectrolyte adsorption, the primary interaction energy is electrostatic attraction (for oppositely charged polymers), which is on the order of 50-200 kJ/mol. For the non-ionic polymers of this study, there are little, if any, Coulombic interactions. Thus, there must be other secondary interactions that lead to this enhanced deposition. These water soluble polymers are all capable of forming hydrogen bonds with PAn, with interaction energies in the range of 20-40 kJ/mol. Certainly these must be important, but it is possible that there are other specific interactions with PAn that are also involved.
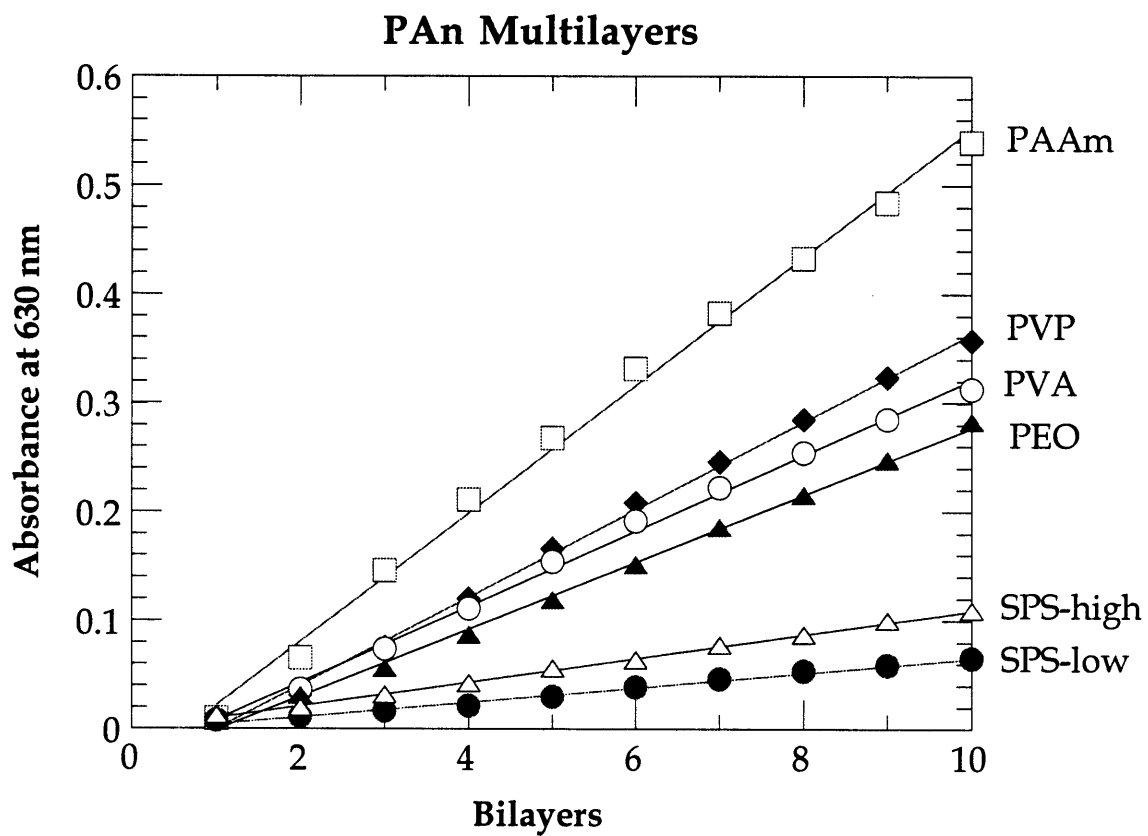
Figure III.3. Absorbance at 630 nm vs. number of bilayers for PAn multilayer films deposited with six different polymers.

The solvent strength also affects polymer adsorption by dictating the chain configuration. The energetics of adsorption must be sufficient to outweigh both the solvent-polymer interaction energies as well as the entropic penalty of confining and reconfiguring a polymer chain at a surface. For PAn, the 90% water/10% DMAc solution is a very poor solvent, thus adsorption happens quite readily. For the water-soluble polymers, surface interactions (such a hydrogen bonding) become more important, as will be discussed.

III.D. FTIR Determination of Hydrogen Bonding.

The possiblity of hydrogen bonding interactions as a mechanism driving the adsorption of non-ionic polymers was investigated. If a primary means of adhesion from layer to layer for the non-ionic multilayer systems is by hydrogen bonding, the actual extent of interaction between any two layers can be monitored to some extent by the presence of H-bonds, as measured by FTIR. Coleman and Painter have used such an approach for determining the extent of hydrogen bonding in polyurethanes [80] and for determining the extent of phase separation in H-bonding polymer blends [81, 82]. They have shown distinct absorption bands for free and H-bonded carbonyl groups and N-H stretches. The energy of the N-H stretch (of PAn), and the carbonyl C=O stretch (in PVP) both depend on whether they are H-bonded or not, thus these two absorption peaks can be monitored as a function of their environment. Because PAAm and PVA both H-bond with themselves, it is more difficult to determine whether the H-bonds are inter- or intra- molecular. PEO is also more difficult since there is not a strong energy shift for a free ether linkage compared to a H-bonded one [82].

To prepare the films, the self-assembled films were grown onto ZnSe plates, which do not absorb in the middle IR region. A PAn layer is deposited first, as it readily adsorbs onto ZnSe. Two multilayer systems were evaluated, PAn/PVP and PAn/PEO (10 bilayers each). In looking at the IR spectra shown in Figures III.4 and III.5, the presence of hydrogen bonding is evident in the N-H stretch region in Figure III.4 for PAn/PVP and in Figure III.5 for PAn/PEO. The N-H stretch of pure PAn in its dedoped state (not charged) appears at 3382 cm^{-1}. This corresponds to the free (not hydrogen bonded) N-H. PAn can hydrogen bond to itself, and there is evidence of a small fraction of H-bonded
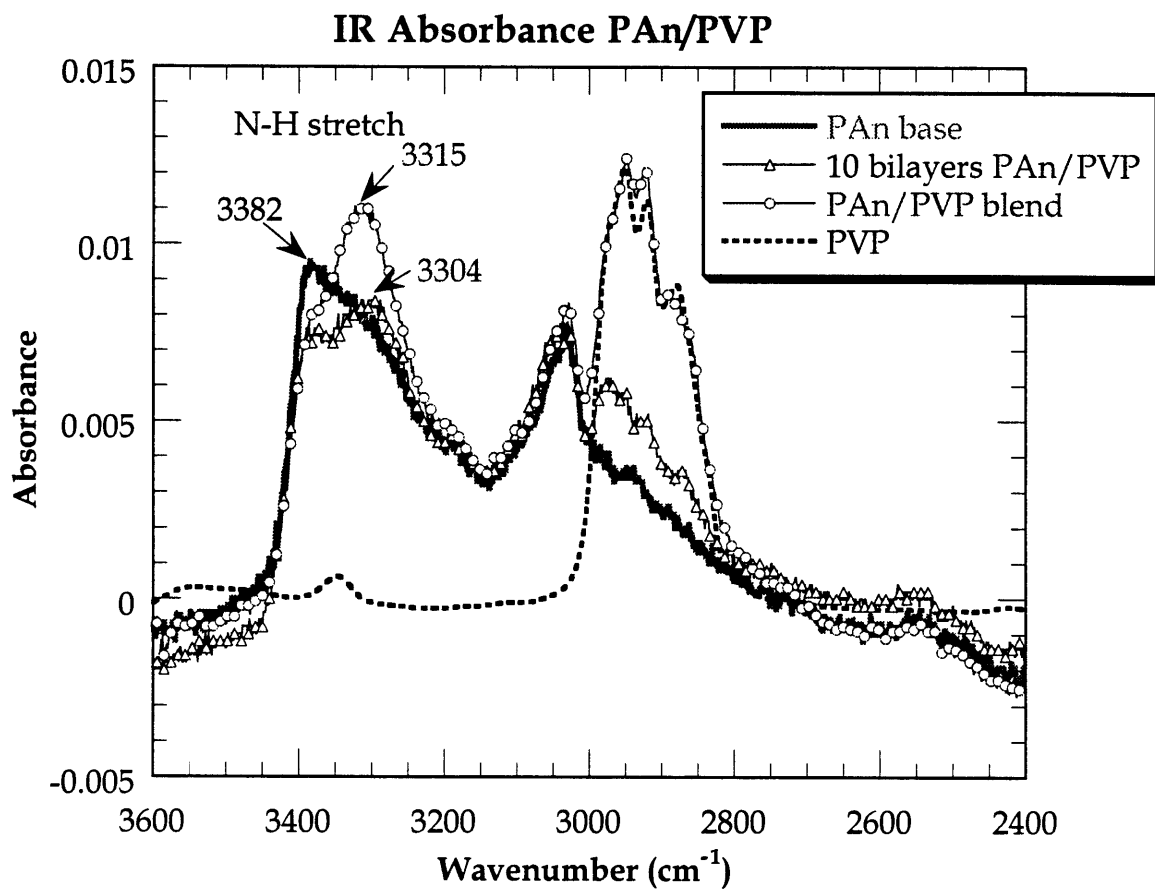
Figure III.4. IR spectra showing the N-H stretch region for PAn base, a 10 bilayer film of PAn/PVP, a 50/50 PAn/PVP blend, and PVP.
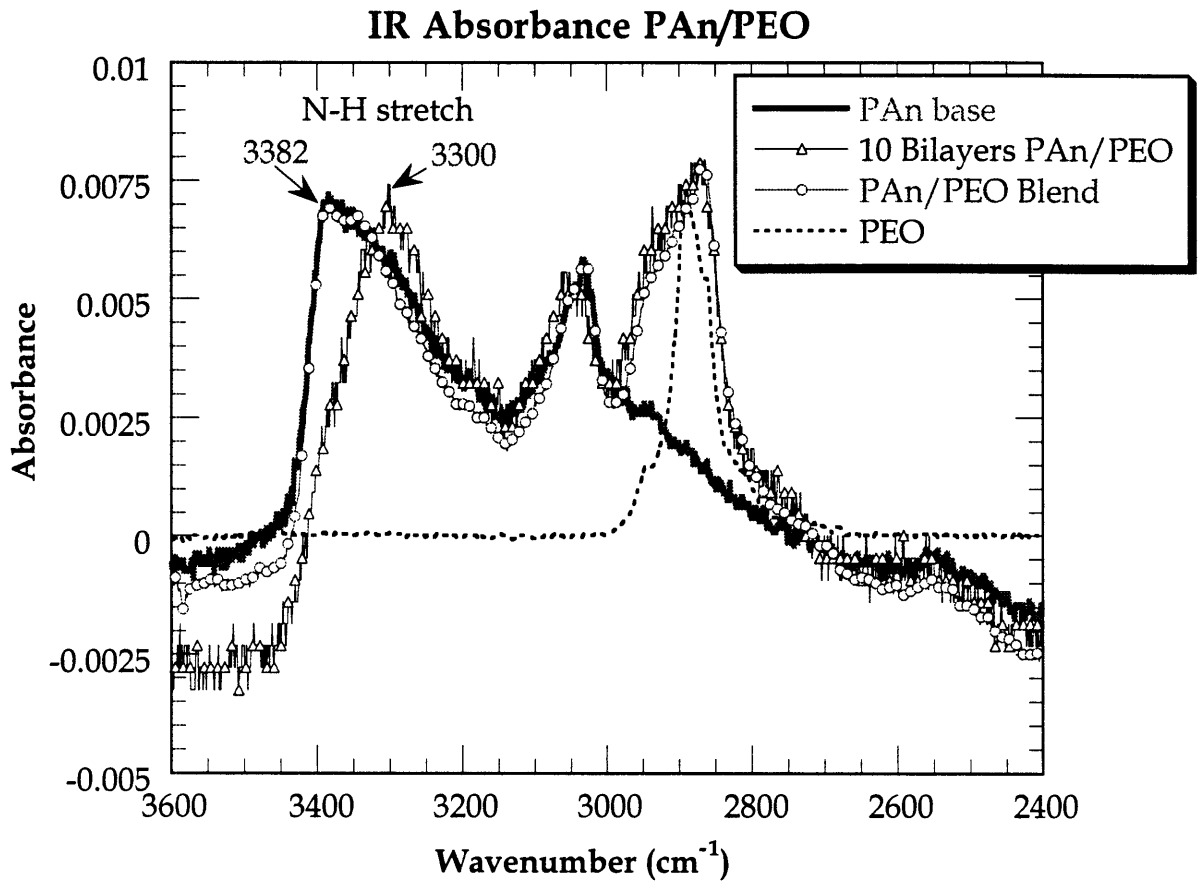
Figure III.5. IR spectra showing the N-H stretch region for PAn base, a 10 bilayer film of PAn/PEO, a 50/50 PAn/PEO blend, and PEO.

N-H groups, seen by the shoulder on the right side of the N-H peak for pure PAn.

In a multilayer system with either PVP or PEO, there is a new peak at 3300 cm^{-1} (with PVP) or at 3330 cm^{-1} (with PEO). This shift to lower energy corresponds to a hydrogen bonded N-H. There is a fraction of these hydrogens that remain free, as evident by the presence of the original peak at 3382 cm^{-1}. Thus both systems have a fraction of N-H bonds that are involved in hydrogen bonds. It is difficult to determine what this fraction is from just the IR data, since the hydrogen bonded N-H stretch absorbs more strongly than the free N-H, thus the peak areas are not directly related.

Also shown for comparison are blended systems; films of approximately 50/50 PAn/PVP or PAn/PEO cast from a mixed solution in NMP. The PAn/PVP blend also shows the peak shift to about 3317 cm^{-1}, thus there is some extent of H-bonded N-H. This indicates that PAn and PVP are compatible, forming highly interacting blends, which agrees with results seen in Chapter II. The PAn/PEO blend shows no shift, suggesting a phase separated system, thus few hydrogen bonding interactions. Observing these blends under a light microscope at 1000x confirms the phase separated structure of the PEO blend, and the phase mixed structure of the PVP blend.

Looking at the carbonyl peak around 1685 cm^{-1} for the PVP was less informative. It turns out that a hydrogen-bonded carbonyl in PVP only acts to widen the absorption band, and it was difficult to determine the extent of peak widening for the PAn/PVP vs. pure PVP spectra.

It is interesting to note that PAn will hydrogen bond with both PVP and PEO, but shows much stronger interactions with PVP, as evident by the blend behavior of these pairs. Pearce has shown that miscibility between normally immiscible pairs can be enhanced by the modification of one component to incorporate a certain percentage of hydrogen bonding functional groups [83, 84]. For example, he has shown that polystyrene becomes miscible with PMMA by copolymerizing styrene with only about 5% vinyl phenol. The added hydroxyl groups are capable of forming hydrogen bonds with the acrylate carbonyl in PMMA. This miscibility is thermally reversible, thus the blend behaves as a LCST blend (phase separates at elevated temperatures), typical of many hydrogen bonded blends.

Apparently, for PAn/PEO, the presence of hydrogen bonding is sufficient to drive the adsorption of PEO from water onto PAn (even though

water is a good solvent for PEO), but not sufficient to form a miscible blend. As seen in Chapter II, PAn with PVP does form a miscible system, but PAn with PEO (or with PMMA, also seen in Chapter II) does not. It has not been fully investigated, but PAn and PAAm appear compatible, as well. All of these polymers (PEO, PVP, PAAm, PVA, and PMMA) are capable of hydrogen bonding with PAn, but of these five, only PVP and PAAm contain a nitrogen atom in their structure (in addition to a hydrogen-bonding oxygen). This nitrogen is also capable of forming hydrogen bonds with hydrogens in PAn, and may be the added interaction strength that leads to this compatibility. It has been observed that the nitrogen atoms in PAn chains can act as proton acceptors, forming interchain NH - N hydrogen bonds in pure PAn [85]. These two nitrogen containing polymers, PVP and PAAm, thus can similarly form such additional interactions.

III.E. Properties of Multilayer Films

Once grown, the PAn multilayer films generally appear as green (doped) or blue (dedoped) uniform coatings, which can be mostly transparent, depending on the thickness. They all adhere tenaciously to the glass, particularly if the glass has been treated. Film adhesion is monitored in two manners, one way by simply rubbing, and the other by the "Scotch tape test." In this test, a piece of adhesive tape is pressed firmly on the sample, then peeled off. For *all* films deposited on treated glass (silanized), no material comes off in the Scotch tape test. The films are also resistant to light rubbing with one's fingers, but will come off with more aggressive rubbing. Adhesion does vary with substrates, and is best with silanized surfaces.

Some of the properties of these multilayer films are outlined in Table III.1. All values are listed as ranges measured for multiple series of samples. Listed are the polymers displayed in Figure I.4 and their molecular weights (all are polydisperse). All solution concentrations were 0.01 M, as defined in the experimental section, with no pH adjustment. The unperturbed radius of gyration of each polymer, Rg, was calculated using characteristic ratios tabulated in the Polymer Handbook, and assuming theta conditions. The Rg for PAn is estimated at about 80 Å, based on a mw of 25,000 and an estimated characteristic ratio of 12. Using these Rg values, it was determined that 0.01 M

concentration is well below the calculated critical overlap concentration in all cases. Thus, adsorption is from non-overlapping chains in solution. For the case of high mw PAAm, it has been shown that aqueous solutions of concentration less than about 0.015 M contain no aggregates [86].

It is possible, however, that there is some extent of nano-aggregation in the PAn solution, since it is in water, a non-solvent. Lower concentration PAn (10^{-4} M) delivers smoother (as determined by AFM) yet thinner films, with higher dichroic ratios (see Section III.N). This indicates a preferred in-plane chain orientation, more so than in films adsorbed from the higher concentrations (10^{-2} M). This results from the more favorable conditions for chain elongation on the surface due to decreased competition for surface sites.

Included in the table is the average thickness per bilayer for films ranging from 8 to 16 bilayers (column 2), as measured by profilometry. Conductivities (σ, column 3) are measured for fully doped films (doped with MeSA) by the usual van der Pauw technique. The absorbance (at 630 nm) per bilayer is listed for dedoped films (column 4). An approximate vol% PAn is listed in column 5, and is calculated by using an absorbance per thickness calibration curve. This curve was generated by measuring the thickness and absorbance (at 630 nm) for a series of known concentration spin-coated thin films of PAn/PVP. The absorbance per unit thickness is 7.155×10^{-4} abs. units/Å. This calibration gives an extinction coefficient, ε, at 630 nm of about 1.3×10^4 $(M\text{-cm})^{-1}$ for dedoped PAn (where a mole is defined for two aniline structural units). This compares quite favorably to the value of ε reported by Cheung, 1.4×10^4 $(M\text{-cm})^{-1}$, calculated by calibrating with a series of PAn solutions of known concentration [79]. Using this calibration value and the absorbance per bilayer value (column 4), the contribution of PAn per bilayer is estimated. The volume% PAn (column 6) is simply this PAn contribution divided by the thickness per bilayer.

The dichroic ratio listed in column 6 (S-polarized/P-polarized absorbance ratio) gives relative information about the actual chain configuration of PAn. The higher values have preferential in-plane orientation, lower values indicate a more random 3D configuration. Under several assumptions regarding these films (see Section III.N), a dichroic ratio that corresponds to no preferred orientation is 1.13. Thus any ratio greater than 1.13 should have preferred in-plane orientation. If all PAn chains laid in the plane of the surface, then the ratio would be 1.535. Dichroic ratios less than 1.13 indicate

that the chains are preferentially oriented normal to the surface. Values greater than 1.535 are theoretically impossible for the given assumptions. There are some difficulties in determining the absolute dichroic ratio (such as problems with baseline interpretation, and variability of the ratio with wavelength), as well as assumptions about the film's refractive index, but the values do give relative comparisons.

Table III.1. Selected properties of PAn multilayer films ranging from 8 to 16 bilayers (solutions with no pH adjustment.).

Polymer System w/ PAn	Å/ bilayer	σ (S/cm)	Absorbance (630 nm) /bilayer	Est. vol% PAn	Dichroic Ratio
PAAm (5,500,000)	90 - 125	1.9 - 4.0	0.042 - 0.054	53 - 76	1.11 - 1.12
PVP (1,000,000)	65 - 85	2.3 - 3.7	0.032 - 0.045	64 - 74	1.21 - 1.25
PEO (5,000,000)	50 - 70	0.4 - 2.2	0.021 - 0.028	49 - 60	1.21 - 1.26
PVA (86,000)	55 - 65	1.1 - 3.6	0.020 - 0.031	52 - 72	1.22 - 1.24
SPS-low (70,000)	28 - 41	0.1 - 0.5	0.007 - 0.013	26 - 62	1.19 - 1.21
SPS-hi (500,000)	27 - 42	0.1 - 0.4	0.011 - 0.013	43 - 65	1.20

PAAm - poly(acrylamide)   PVP - poly(vinyl pyrrolidone)
PEO - poly(ethylene oxide)   PVA - poly(vinyl alcohol)
SPS - sulfonated polystyrene

It is evident that although each bilayer is approximately the same thickness for a given PAn system, there is a wide range of thicknesses depending on the particular system. In fact, the ionic system, SPS, delivers the thinnest film, while the non-ionic polymers show up to six times the absorbance for the same number of bilayers. In comparing two similar mw

systems at the same concentration, SPS (ionic, Mw=70K) to PVA (non-ionic, Mw=86K), the non-ionic polymer still shows over double the absorbance per bilayer. PVP, at Mw=1M, shows almost three times the absorbance as SPS-990K (seen in Table III.3b).

These thickness differences are related to the strong interactions between polyaniline and water soluble polymers capable of hydrogen bonding. Every repeat unit of PAn is capable of hydrogen bonding with every repeat unit of PVP, PAAm, PEO, and PVA. For the electrostatic interactions, PAn has a very low charge density at pH = 2.5. Only about one in every 20-30 aniline repeat units is protonated, thus there are fewer ionic interaction sites per chain than there are hydrogen bonding sites. This discrepancy is even larger for the case of the nitrogen-containing polymers, PVP and PAAm, which can form additional hydrogen bonds. Apparently, thicker films (more deposited PAn) are obtained in the systems that have the most "binding" interactions.

There are other factors affecting the deposition and resulting properties, however, such as molecular weight, solution pH, and concentration. For example, PAAm delivered a much thicker bilayer than PEO, of comparable molecular weight. It is likely that the increased interactions between PAAm and PAn relative to PEO and PAn act to deposit more PAn. Also noted in Table III.1 is the fact that the dichroic ratio of PAAm system is lower than for PEO. This means less in-plane orientation of the PAn chains (more coiled), which suggests a thicker film. Each system behaves slightly differently, as also evident by the large disparity in molecular weight between PVA and PEO, yet both deliver comparable thicknesses and conductivities. Although there is a significant molecular weight effect on film deposition (to be discussed in the next section), there are also competing effects based on interaction strength. Here it is evident that PAn interacts more strongly with PVA than PEO. In the next two sections, the effects of pH and molecular weight are discussed in more detail.

III.F. Effects of pH on Deposition.

Cheung has mapped out concentration, pH, and adsorption time dependence for PAn/SPS self-assembled systems, showing strong dependence on all three [79]. She has shown that the thickness of the deposited film

increases with lowering the pH, while the dichroic ratio goes through a maximum near pH=3. The thicker films at low pH result from the increased positive charge density on PAn, which increases interaction sites with SPS. For the non-ionic systems of this study, the solution pH plays a different role since the charge density on PAn is a less significant factor. As will be seen, there are indeed pH and thus charge effects, but not to the extent seen in polyelectrolyte systems. For example, non-ionic polymers such a PVP can be deposited onto PAn over a wide pH range, from fully doped (positively charged) to fully dedoped (electrostatically neutral). Multilayer build-up can thus be readily obtained, whereas for polyelectrolytes, adsorption (and particularly multilayer build-up) can be sigificantly hindered if the charge densities are not sufficient. The only reason to keep the PAn slightly doped in the case of non-ionic self-assembly is to keep the PAn aqueous solution stable.

The pH of the non-ionic polymer solution can affect a polymer's ability to hydrogen bond. It has been observed that high pH values can hinder hydrogen bonding, since OH$^-$ groups act to dissociate hydrogen bonds [87, 88]. Table III.2 summarizes results from a series of multilayer films built up from different pH values for the non-ionic polymer. In all cases, the PAn solution remained at pH=2.5 for bath stability reasons. The films were all 8 bilayers thick built up on treated glass substrates. The following observations can be made:

With PEO, low pH hinders adsorption, as evident by the thinner bilayers, while the dichroic ratio remains about the same for all pH values. Since high pH values are known to hinder hydrogen bonding, it might be expected to see the reverse trend. There must be stronger interactions between PEO and PAn in its electrically neutral state (high pH) than with doped PAn (low pH). Of the four polymers considered in this table, PEO appears to have the weakest interaction strength with PAn, as it has a high molecular weight, but forms thinner films. This might be expected in light of the ether linkage likely being the weakest at form hydrogen bonds.

With PVA, as pH increases, the thickness decreases, while the % PAn and the dichroic ratio remain about the same. PVA has a partially anionic nature, which can enhance adsorption at low pH (onto charged PAn). Thus less PVA adsorbs at higher pH, as there is no charge on PAn. This is a similar effect seen with SPS, which is anionic.

Table III.2. Selected properties of PAn multilayer films (8 bilayers) as a function of pH conditions.

System (pH)	Ave. thick. (Å)	Å/bilayer	Absorb./ bilayer	Est.vol% PAn	Dichroic Ratio
PEO - 3.0	269	34	0.0124	52	1.23
PEO - 6.0	413	52	0.0210	57	1.19
PEO - 9.0	396	50	0.0222	63	1.22
PVA - 3.0	537	67	0.0263	55	1.20
PVA - 5.0	438	55	0.0204	52	1.23
PVA - 7.0	369	46	0.0174	53	1.24
PAAm - 3.0	1171	146	0.0688	66	1.09
PAAm - 5.0	728	91	0.0494	76	1.12
PAAm - 7.0	599	75	0.0430	80	1.29
PVP - 4.0	673	84	0.0446	74	1.19
PVP - 5.0	592	74	0.0430	81	1.20
PVP - 6.0	571	71	0.0412	81	1.20

With PAAm, as pH increases, the thickness decreases, while the % PAn and the dichroic ratio increase. At lower pH, there is some positive charge on PAAm, thus charge repulsion allows less elongation of the chains, giving rise to a lower dichroic ratio. These coiled chains result in thicker films, but with a lower percentage of PAn. Evidently, this charge density is not enough to prevent considerable adsorption. There also must be considerable interpenetration of the PAn and PAAm at the lower pH. This is the only case of these four systems that shows significant dichroic ratio dependence on the pH.

With PVP, as pH increases, the thickness decreases slightly, while the % PAn and the dichroic ratio remain about the same. Amides and lactams are known as good solvents for PAn (PVP monomer is a lactam), thus there are strong interactions, and little effect, regardless of pH conditions. Although only

a small pH range is presented in the PVP series, results from earlier experiments at low pH values confirm the relative pH-independent behavior.

From looking at the results tabulated in Table III.2, it is evident that pH effects can be significant in altering the way PAn interacts with other polymers. Again, the primary effects are related to the strength of these interactions, both ionic and otherwise, as determined by the solution pH.

III.G. Effects of Molecular Weight on Deposition.

Reference was mentioned above to molecular weight differences resulting in film thickness differences. A more systematic approach addressing the effects is presented here. Tables III.3a and III.3b outline the results from two molecular weight studies, one for a non-ionic polymer (PVP) and the other for an ionic polymer (SPS). The SPS used is narrow molecular weight distribution, $M_w/M_n = 1.10$, obtained from Polysciences, except for SPS-hi (500K) and SPS-low (70K), which are polydisperse. The PVP is also a "narrow" distribution (obtained from American Polymer Standards), but is much more polydisperse, $M_w/M_n \approx 3$. Again, two samples (PVP-1M and PVP-10K) are not of this narrow distribution, thus are even more polydisperse. It is generally known that in polymer adsorption, low molecular weight chains adsorb more quickly due to diffusion kinetics. High molecular weight chains can replace the low ones with time since they have lower desorption rates due to having more interaction sites per chain. The implication is that in polydisperse systems, the low molecular weight chains will likely adsorb first, and then depending on their interaction strength, might be replaced by higher molecular weight chains. For this reason, monodisperse fractions were used.

The two polymer types have quite different behavior, as evident in these two tables. The deposition of a PAn/PVP film is quite dependent on the molecular weight of the PVP. There appears to be a minimum MW below which no deposition occurs. This MW is about 25K, as the two MWs below this did not build multilayer films. Apparently, the low mw PVP does not have enough exposed bonding sites to adhere an additional layer of PAn. Presumably, many interaction sites are needed for the weaker hydrogen bond, compared to ionic bonding, to adhere a polymer chain. There also appears to be

a maximum molecular weight, above which there is little MW dependence, since both the 350K and 1M PVP show similar film properties.

Table III.3a. Selected properties of PAn/PVP multilayer films (10 bilayers) as a function of PVP molecular weight.

Sample (M_w)	Ave. Thick. (Å)	Å/ bilayer	Absorb./ bilayer	Dichroic Ratio	Est. vol% PAn	σ (S/cm)
PVP 1M *	774	77	0.0403	1.14	73	1.21
PVP 350K	796	80	0.0370	1.17	65	1.65
PVP 125K	562	56	0.0272	1.26	68	1.17
PVP 35K	170	17	0.0072	1.38	59	0.075
PVP 25K	110	11	0.0040	1.47	51	0.10
PVP 10K *	--	--		1.49†		-
PVP 9K	--	--		1.45†		-

* indicates very polydisperse PVP (branched as well), all others are relatively narrow MW distribution, ($M_w/M_n \approx 3$).

† effectively a PAn monolayer.

Table III.3b. Selected properties of PAn/SPS multilayer films (10 bilayers) as a function of SPS molecular weight.

Sample (M_w)	Ave. Thick. (Å)	Å/ bilayer	Absorb./ bilayer	Dichroic Ratio	Est. vol% PAn	σ (S/cm)
SPS 990K	419	42	0.0143	1.19	48	0.11
SPS 500K *	415	42	0.0127	1.20	43	0.11
SPS 350K	407	41	0.0138	1.20	47	0.11
SPS 77K	402	40	0.0128	1.17	45	0.09
SPS 70K *	405	41	0.0125	1.19	43	0.11
SPS 35K	412	41	0.0122	1.18	41	0.06
SPS 5K	406	41	0.0131	1.14	45	0.06

* indicates polydisperse SPS, all others are monodisperse ($M_w/M_n = 1.10$)

The thickness per bilayer decreases with decreasing MW, where the vol% PAn seems constant until a lower MW regime, at which point both the % PAn and

the conductivity drop off. The dichroic ratio increases during this decrease in MW. These two effects, the decreasing thickness and increasing dichroic ratio, with decreasing mw, suggest that the PVP chain is acting as a template for PAn adsorption. Higher mw PVP has more loops extending from the surface, which act to form thicker films with less in-plane PAn orientation. The PAn strongly interacts with the PVP chains, interpenetrating into the PVP loops.

For the ionic system of SPS, there appears to be little molecular weight dependence on most all film characteristics. PAn builds up nicely with SPS for all molecular weights used, ranging from 5K to 990K. Systems that form ionic bonds therefore require much fewer interaction sites in order to form multilayer films. This is evident from the demonstrated multilayer films consisting of poly(thiophene acetic acid) as the polyanion, a short chain polymer consisting of only eight to ten thiophene repeat units [59]. In fact, Yoo has demonstrated multilayer build-up with small ionic molecules containing only two or three charges per molecule [70]. There is little change in the dichroic ratio with molecular weight, indicative of the reduced interactions between PAn-SPS compared to PAn-PVP. The SPS does not act as a template that controls the thickness with extensive interpenetration, like PVP does. The SPS films have a lower vol% PAn than with PVP (due to fewer interaction sites), with about an order of magnitude lower conductivity.

III.H. Interactions of Non-Ionic Polymers with Ionic Polymers.

Investigations have been made into the ability of charged polymers to adhere to non-ionic polymers, and vice versa. We have seen that PEO, PAAm, PVA, and PVP will all build multilayer systems with PAn over a wide range of pH values, discussed in the previous sections. Thus build up is possible on both doped (low pH) and dedoped (high pH) PAn. Here, doped PAn is only partially doped, but has a net positive charge, while the dedoped PAn is electrostatically neutral. Systems of non-ionic polymers with ionc plymers other than PAn have also been considered.

Attempts were made to adsorb PEO and PVP onto charged layers, monitoring the deposition by IR absorbance. It turns out that neither PEO nor PVP will build up multilayers with SPS, a polyanion, in the pH range tested (2.5-6.5). Neither will build up with poly(allyl amine), a polycation at low pH

(2-3). The implication is that there are very strong specific interactions with PAn not related to ionic charges, since these water soluble polymers (PVP and PEO in this case) will not interact with other charged polymers, either positive or negative, in a manner that allows multilayer self-assembly. The interactions with PAn, however, are strong enough to drive the adsorption from water, a good solvent.

Since these interactions are primarily hydrogen bonding, as seen above in Section III.D, it might be expected that multilayer build-up would be possible with most any hydrogen bonding pairs, such as PVP with PVA, or PAAm with PVP, PVA, or PEO. Preliminary results show, however, that none of these four systems forms multilayer films, as determined by IR spectroscopy. This suggests that there are additional specific interactions between PAn and these water-soluble polymers (such as hydrophobic interactions), or that the hydrogen bonding is not of as strong of a nature between PAAm and PVA, for example, as it is between PAn and PVA or PAAm. Certainly one driving force for the deposition of polyaniline is the fact that it is in an unstable solution, thus favors adsorbing onto a surface for thermodynamic reasons. Water is a non-solvent for PAn, thus the PAn chains remain tightly coiled, eager to come out of the metastable solution. This is evident in the wide variety of surfaces that PAn will adsorb onto from the standard 90% water/10% DMAc solution. This driving force is much weaker for the other water soluble polymers, thus the argument that additional interactions with PAn must exist. Certainly there are some hydrophobic interactions related to the fact that these are all polymers with hydrocarbon backbones, despite being water-soluble.

The surface roughness of a polyaniline layer can make subsequent layer adsorption more appealing as well. PAn deposits as a much rougher layer than all of the other polymers of this study, due to its nano-aggregated nature in the unstable solution. This roughness allows an adsorbing chain more interaction sites without the entropic penalty of spreading onto a smooth surface (described in Section I.C.1).

III.I. Conductivity vs. Number of Bilayers

Up to this point, film properties have been described primarily for multilayer films. It was seen in Section III.C that the first bilayer possibly has

73

incomplete coverage, likely due to variable surface conditions on the substrate. To address how properties change as the number of layers increases, single layer properties, at least conductivity and thickness, were measued for two PAn/PVP systems. Conductivity and film thickness as a function of number of bilayers are plotted in Figure III.6. Both films are built up from the same solution concentrations (0.01 M for both PAn and PVP) and pH conditions (pH=2.6 for PAn, pH=4.5 for PVP). The only difference is that one PAn solution was made from dimethyl acetamide (DMAc) in water, while the other from N-methyl pyrrolidone (NMP) in water. This comparison of solvents was done to determine the extent of residual solvent effects of these two PAn solvents. Thicknesses were calculated based on a calibration of the absorbance at 630 nm, conductivities were measured after each bilayer for fully doped (with MeSA) films.

It can be seen in Figure III.6 that after only two bilayers, the films are already within an order of magnitude of their ultimate conductivities. This corresponds to a film thickness of about 75Å. The first bilayer is so thin (< 30Å) likely due to both incomplete coverage and the fact that it is effectively a bilayer of PAn/SPS rather than PAn/PVP. The incomplete coverage is suggested by the lack of any conductivity. The second layer fills in more, with total coverage coming by the third bilayer. After three bilayers, the films are approximately 150Å thick, and have almost reached their eventual conductivity. Each successive bilayer delivers about 80Å (the average bilayer thickness). Beyond three bilayers, there is little subsequent increase in conductivity. These values indicate the connectivity of the first three bilayers.

The film assembled from DMAc is about five times as conductive as that assembled from NMP, even though both films are about the same thickness. This implies that there is residual NMP, which acts to hinder doping by loosely binding or complexing the dopant protons. There is likely less residual DMAc, since PAn retains NMP more tightly than DMAc. Similar results were seen for PAn/PVP blends [57], as described in Chapter II.
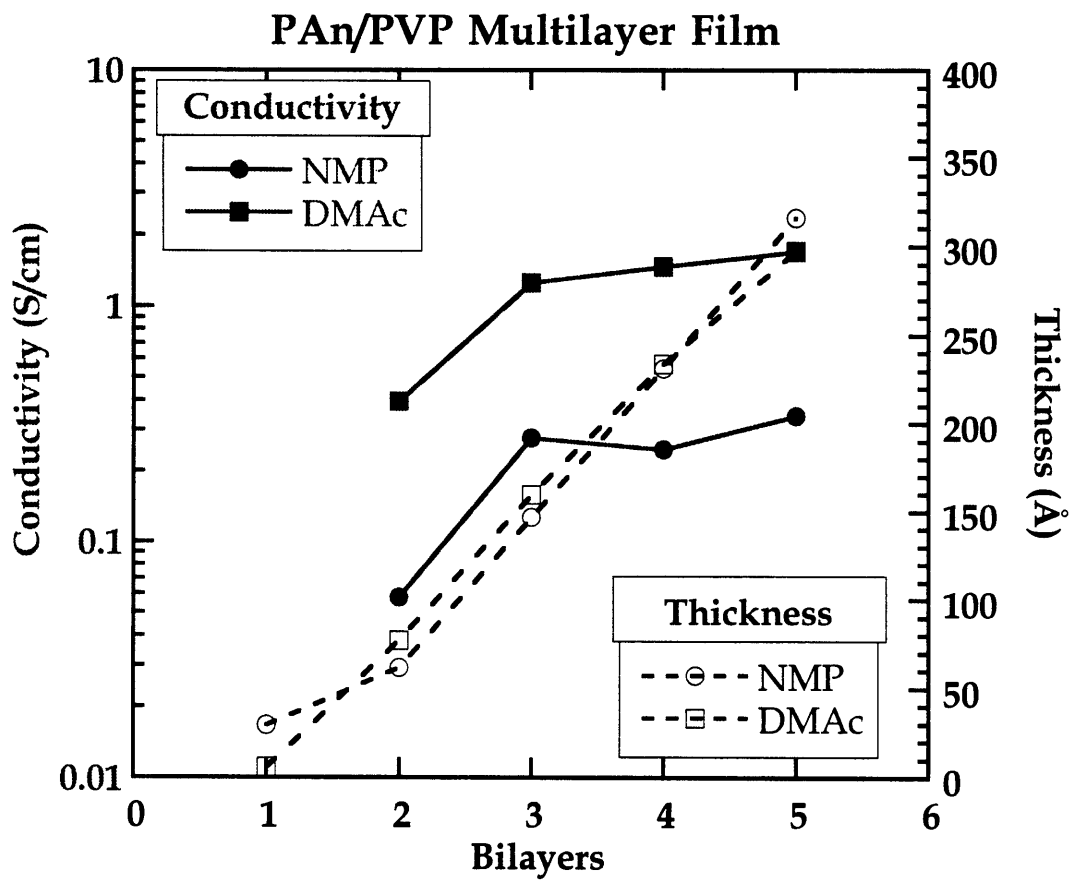
Figure III.6. Conductivity and film thickness of PAn/PVP multilayer films as a function of number of bilayers. (Two PAn dipping solns. compared, one with DMAC, one NMP).

III.J. Layer by Layer Surface Energy as Determined by Contact Angle.

In an effort to gain insight into the nature of each deposited layer, the contact angle of a sessile drop of water on the film's surface has been measured. The information garnered reveals relative surface energies, which is significant in light of the extreme thinness of the films involved.

III.J.1. Contact Angle Background

The technique used requires the placement of a small drop ($\sim$ 5 μl) of deionized water onto the film (on a flat level surface), then measuring the angle between the drop and the surface at the air-liquid-surface interface, as depicted in Figure III.7.
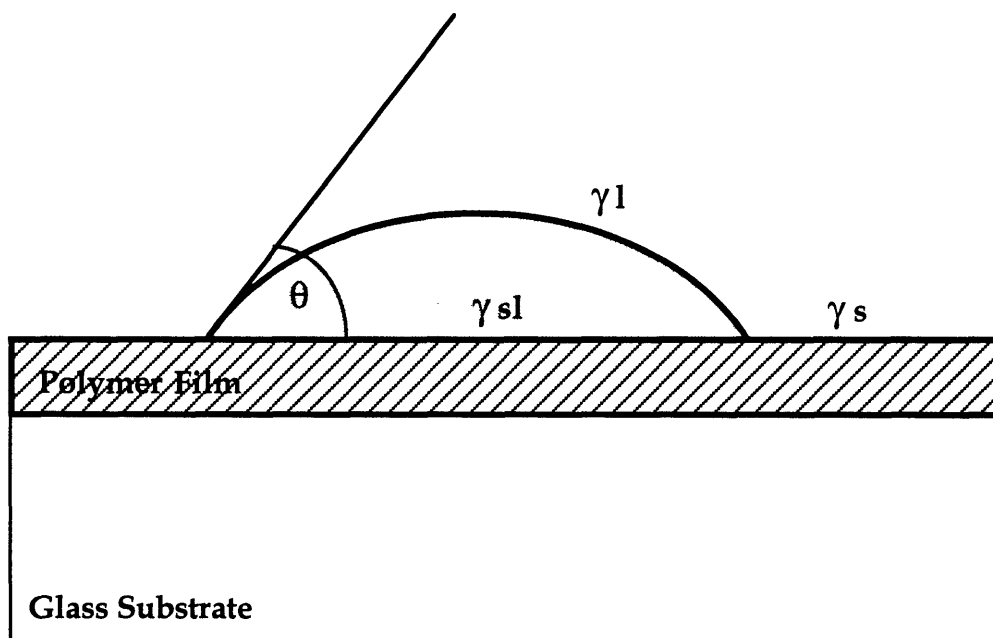
Figure III.7. Schematic of a sessile water drop on a flat surface indicating the contact angle, θ, and the interfacial tensions of the air-solid (γ_s), solid-liquid (γ_{sl}), and air-liquid (γ_l) interfaces.

What is actually measured is the "recently advanced" contact angle, corresponding to a drop consisting of two or more added drops. The contact angle θ is related to the surface or interfacial tensions of the air-solid (γ_s), solid-liquid (γ_{sl}), and air-liquid (γ_l) interfaces by the Young relation:

$$\gamma_s = \gamma_{sl} + \gamma_l \cos\theta \qquad \{1\}$$

For a given liquid, γ_l is constant, thus $\cos\theta$ is proportional to $\gamma_s - \gamma_{sl}$. Small contact angles (better wetting) occur when $\gamma_s - \gamma_{sl}$ is maximum; extremely poor wetting occurs when $\gamma_s < \gamma_{sl}$. Qualitatively, the contact angle increases as γ_s decreases and/or γ_{sl} increases. It has been shown, however, that these two surface energies (γ_s and γ_{sl}) are related [89], thus changes in contact angles can be attributed to changes in γ_s, the surface tension, all geometrical parameters the same. Good has outlined the relation between γ_s and γ_{sl} [89], described here briefly.

He starts with the assumption that the free energy of adhesion between two phases (a solid and a liquid), ΔG^a_{sl}, is equal the geometric mean of the two free energies of cohesion of the two separate phases, ΔG^c_i.

$$\Delta G^a_{sl} = -\sqrt{\Delta G^c_s \Delta G^c_l} \qquad \{2\}$$

The negative sign is for consistency. The free energy of adhesion of bringing two unlike phases together (forming interface sl at the expense of surfaces s and l) is given by

$$\Delta G^a_{sl} = \gamma_{sl} - \gamma_s - \gamma_l \qquad \{3\}$$

Similarly, the free energy of cohesion of bringing two like phases together (thus no interface formed) is given by

$$\Delta G^c_l = -2\gamma_l \text{ and } \Delta G^c_s = -2\gamma_s \qquad \{4\}$$

Thus, combining equations $\{2\}$, $\{3\}$, and $\{4\}$, gives

$$\gamma_{sl} - \gamma_s - \gamma_l = -\sqrt{4\gamma_s\gamma_l} \qquad \{5\}$$

Equation $\{5\}$ now relates γ_{sl} to γ_s and γ_l, and thus can be eliminated from the Young equation $\{1\}$. Combining these two equations, $\{1\}$ and $\{5\}$, gives

$$\gamma_l \cos\theta = \gamma_s - (\gamma_s + \gamma_l - \sqrt{4\gamma_s\gamma_l}) \qquad \{6\}$$

which can be rearranged to give

$$\gamma_s = \gamma_l (1 + \cos \theta)^2/4 \qquad \{7\}$$

This relation assumes apolar liquids and solids, and has been further modified by Good to account for polar interactions. He starts by assuming that the surface tension of a polar phase i can be broken into contributions falling under two classes, Lewis acid-base interactions (AB) and Lifshitz-van der Waals interactions (LW), as such;

$$\gamma_i = \gamma_i^{AB} + \gamma_i^{LW} \qquad \{8\}$$

AB interactions refer to electron sharing interactions such as hydrogen bonding. LW interactions are all other apolar interactions including dispersion forces and dipole interactions. γ_i^{AB} can be further broken down to its acid and base contributions, γ_i^{A} and γ_i^{B}. By accounting for both $\gamma_s^{A} \gamma_l^{B}$ and $\gamma_s^{B} \gamma_l^{A}$ adhesion interactions between a solid and a liquid, it can be shown that rewriting equations {3} and {4} combine to give

$$\gamma_i^{AB} = 2\sqrt{\gamma_i^{A} \gamma_i^{B}} \qquad \{9\}$$

Substituting this result into equation {8}, then rewriting equation {7} gives

$$\gamma_l (1 + \cos \theta) = 2[\sqrt{(\gamma_s^{LW} \gamma_l^{LW})} + \sqrt{(\gamma_s^{A} \gamma_l^{B})} + \sqrt{(\gamma_s^{B} \gamma_l^{A})}] \qquad \{10\}$$

Thus, equation {10} or its simpler form {7} allow for direct relation between the measured contact angle and the solid surface tension. The following conclusions can be drawn regarding this. In equation {7}, as θ increases, **cos** θ decreases (for $0 \leq \theta \leq 180°$), and since all γ_l terms can be considered constant, this means that γ_s must necessarily decrease. Similarly for equation {10}, which is better suited for this study which uses water (a polar liquid) on both polar and apolar surfaces. As θ increases, **cos** θ decreases, and the entire right hand side must decrease. This means that γ_s^{LW}, γ_s^{A}, and/or γ_s^{B} must decrease. Since $\gamma_s = \gamma_s^{LW} + 2\sqrt{\gamma_s^{A} \gamma_s^{B}}$, then γ_s necessarily decreases.

Therefore, the contact angle is a fair measure of a solid surface energy, and not just a measure of the difference between surface tension and interfacial tension, $\gamma_s - \gamma_{sl}$, as obtained from Young's equation. It can be concluded that for the sessile water drop contact angle measurements in this study, an increase in contact angle θ corresponds to a decrease in γ_s, the solid surface energy.

As mentioned, these interfacial energies depend on many factors, such as polar effects, van der Waals interactions, and other specific interactions between the liquid (in this case, water) and the solid. There are also non-intrinsic features that can affect the contact angle, such as surface roughness and film porosity. Young's equation assumes a smooth, homogeneous, rigid, and insoluble surface, thus deviations can be expected for rough surfaces. Wenzel has attempted to quantify this effect by incorporating a roughness factor, r, into Young's equation [90]. The equation takes the form

$$\cos \theta_m = r \cos \theta \qquad\qquad \{11\}$$

where θ_m is the measured contact angle and θ is the Young equation, or smooth surface, contact angle. The roughness factor r is defined as the ratio of the actual surface area to the smooth projection onto a plane. Thus, r is always ≥ 1, which implies that $\theta_m < \theta$ for $\theta_m < 90°$ and $\theta_m > \theta$ for $\theta_m > 90°$. Since measured contact angles of this study were all $< 90°$, the Wenzel relation suggests that $\theta_m < \theta$, or that surface roughness acts to lower the contact angle. The Wenzel relation, however, does not account for relative scales nor lateral degrees of roughness, simply the overall surface area. It is likely that the Wenzel roughness factor applies to roughness on a larger scale than the 40-70 Å measured for the thin films of this study. The issue of surface roughness will be further addressed in the next section.

III.J.2. Contact Angle Study for PAn/PVP Multilayer Films

In the case of the multilayer films of this study, contact angle measurements were used to monitor surface energies as a function of deposited layer. Effects of the underlying layers as well as changes with time were also considered. The drop size used was about 3 mm in diameter, thus averages over

79

about a 7 mm^2 area. Reported values represent averages of three or four drops with the angle measured on both sides of each drop.

The contact angle as a function of deposited layer was measured for a PAn/PVP multilayer system grown on glass coated with a PEI/SPS bilayer. In order to measure surface properties of each individual layer under different conditions, thirteen different films were made, ranging from zero to twelve layers. The individual films did show the expected linear growth, as seen by a linear increase in absorbance vs. layer number, shown in Figure III.8. This implies that the each film can be considered as equivalent to its previous film plus one more layer. Since PVP does not absorb light near 630 nm, the films with PVP as the outer layer have the same absorbance as those with PAn as the outer layer.

Shown in Figure III.9 are three series of contact angle measurements made on the same films under different conditions. Several observations can be made. First, for the "zero layer" which means no PAn, but just the initial adhesion enhancement bilayer of PEI/SPS, the contact angle is initially very low, about 8°. This is due to the relatively high surface energy and strong interaction between SPS and water. Drying this bilayer slightly raises the contact angle, but annealing at 175°C tremendously raises the contact angle. This suggests that the thermally enhanced chain mobility allowed the bilayer to reconfigure to its lowest surface energy configuration, possibly increasing the number of ionic interactions between PEI and SPS, leaving fewer charged sites on the surface. Since the PEI was only physisorbed to the glass surface to begin with, heating to 175°C eased chain mobility as well as possibly thermally breaking any hydrogen bonding that my have been in place.

For the freshly made films, there is an oscillating behavior in the measured contact angle as the surface alternates between PAn and PVP. As expected, the PVP outer surface has the lower contact angle, being a more hygroscopic polymer. This oscillating behavior is indicative of how each added layer acts to completely cover the surface, and in a reproducible fashion. The indication is that the deposited layers are stacking to some extent in discrete layers. Although there is certainly some extent of interpenetration between every layer, the outer surface remains extremely rich in the most recently deposited polymer. Also noted is that the contact angle returns to approximately the same value for each type of layer regardless of the number of layers (except for the first PAn layer, which likely has incomplete coverage).

12 PAn/PVP-1M Films
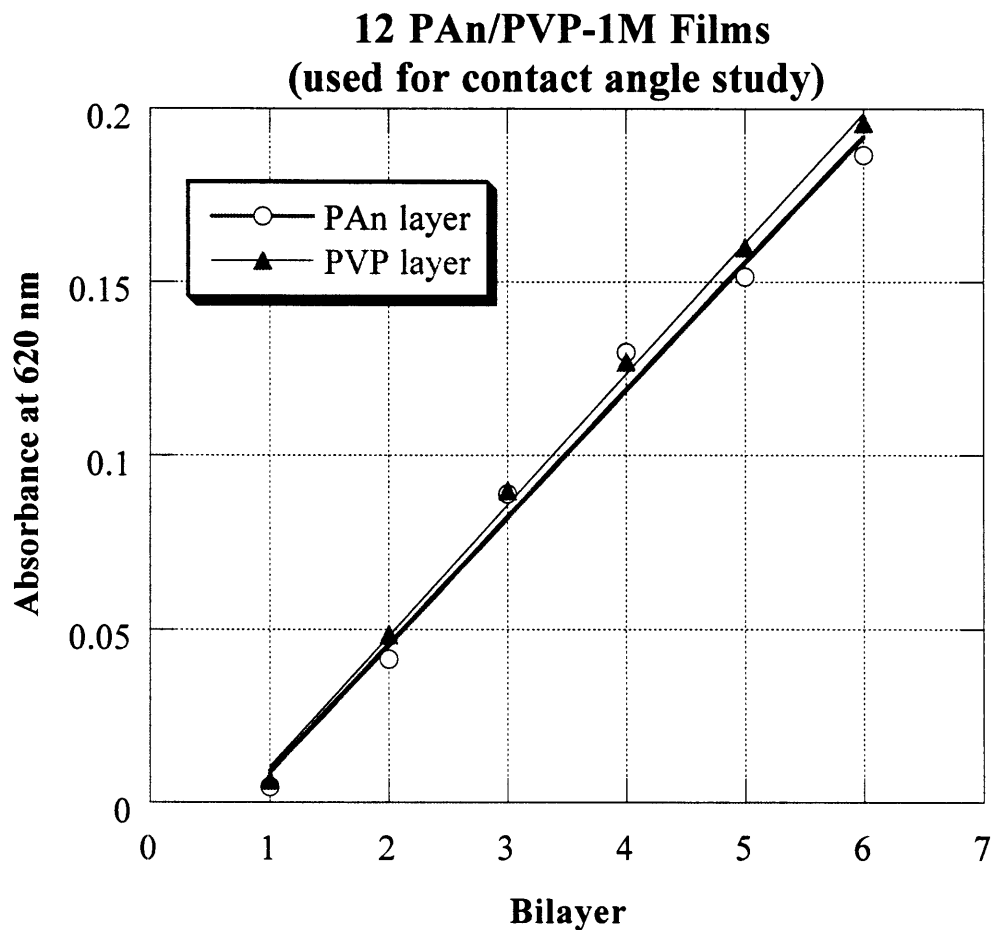**(used for contact angle study)**

Figure III.8. Absorbance at 620 nm vs. number of layers for 12 alternating PAn/PVP layers. Note PVP layer shows no absorbance.
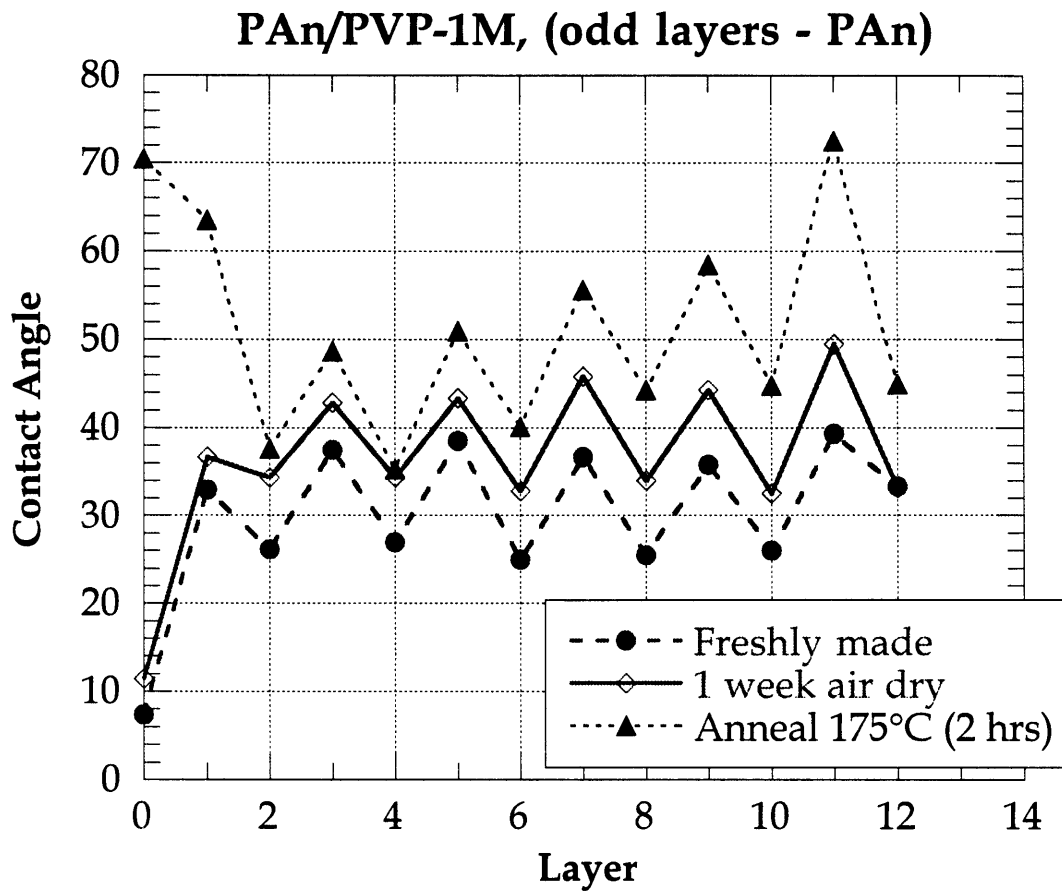
Figure III.9. Contact angle vs. layer number for 12 layers
(6-PAn, 6-PVP, alternating), for three different conditions, as noted.

This implies that the coverage from each layer is complete (after the first layer), as each successive layer erases the effects of underlying layers. These layers are on the order of 70Å thick, 50Å of PAn and 20Å of PVP, as outlined in Section III.F. Yoo has shown thinner layered films to respond differently depending on the underlying substrate [70]. Thus there can be an effect "felt" through the film depending on both film thickness and polymer type.

The stability of this stacked configuration was evaluated by remeasuring the contact angle after extensive drying and annealing. There are aging effects, as seen in Figure III.9 by remeasuring the contact angle one week later. The contact angles have increased by about 6-10°, due to both the increased dryness of the films, and to the film's tendency to reduce its surface energy. This surface rearrangement involves configurational changes that can, for example, bury higher surface energy side groups, as observed in polyelectrolyte systems [91]. The result is to increase the contact angle (poorer wetting for lower surface energy). The oscillating nature remains, however, suggesting that there is not any bulk chain diffusion. Further annealing at an elevated temperature (175°C) for two hours, that is likely above the film's Tg, led to slightly increased contact angles, but the oscillations persisted. Again, there was no bulk diffusion of chains to the surface suggesting no (or little) additional phase mixing between the layers, beyond the first PAn layer. The first PAn layer did show a large increase in contact angle, however, due to the extreme thinness of this layer (and possible incomplete coverage), thus behaves more like the 'zero' layer.

There does appear to be an effect of the number of layers in the annealed samples. The contact angle increases with layer number, whereas this was not the case for the freshly made films. This increase has been attributed to an increase in surface roughness with increasing layers, enhanced during the annealing. These results are seen in Figure III.10 which shows the RMS roughness as measured by atomic force microscopy (AFM) for 10x10 micron areas. Starting with the third layer (second PAn layer), the roughness increases from about 60Å to greater than 70Å by the eleventh layer (sixth PAn layer). Even though the first PAn layer has the lowest RMS roughness (45Å), it still has a very high contact angle. This is related to the incomplete coverage of the first bilayer, mentioned above. It should be noted that the AFM images were taken one month after the films had been annealed at 175°C. Therefore, their contact angles were remeasured immediately after imaging. These results are shown in Figure III.11. The contact angles have dropped by about 6-12°, suggesting either

Roughness of PAn Layer in a PAn/PVP Film
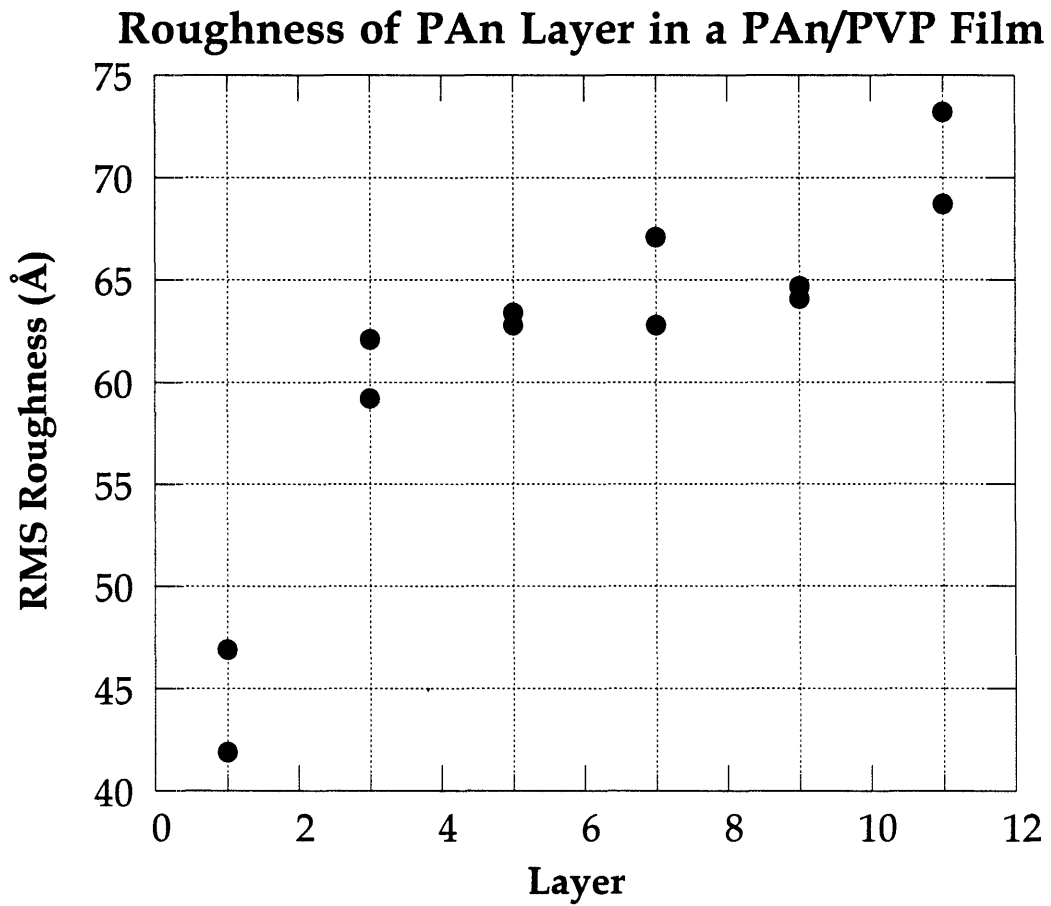
Figure III.10 RMS roughness (as measured by AFM for a 10 x 10 μm area) vs. layer number for PAn layers only (alternating with PVP).
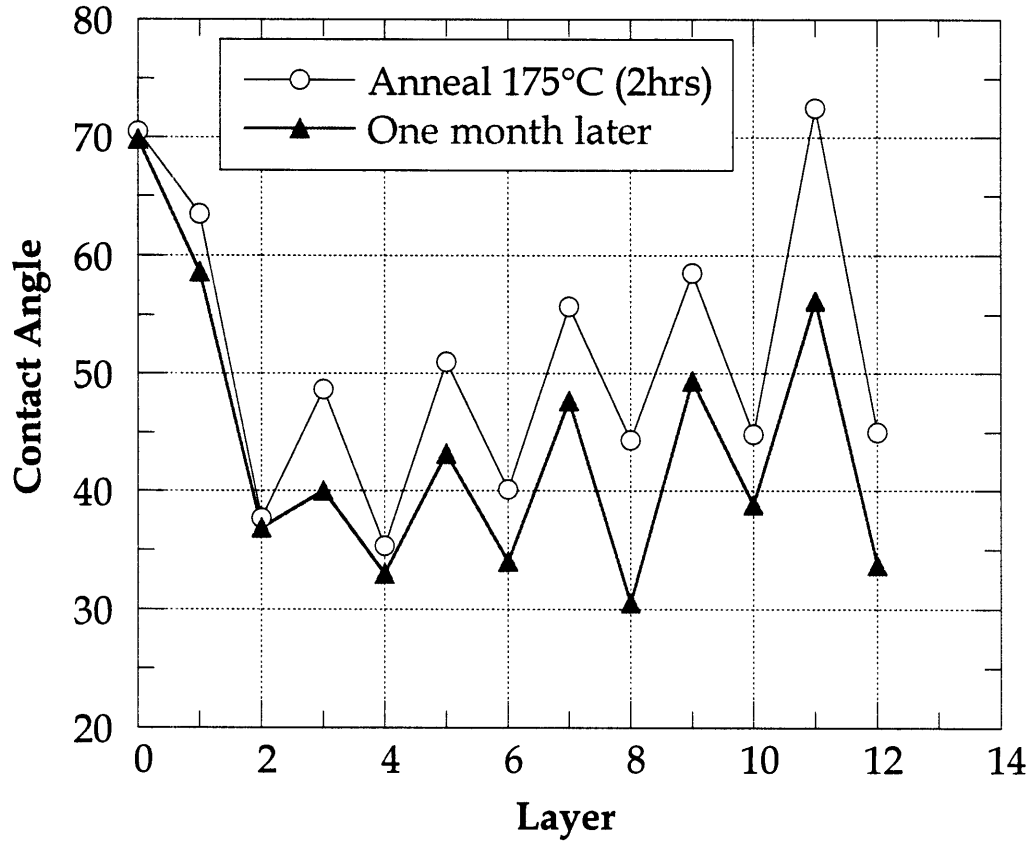
Figure III.11. Contact angle vs. layer number for 12 layers (6-PAn, 6-PVP, alternating), for two different conditions, as noted.

a slight reduction in roughness since the anneal, and/or effects of adsorbed moisture over the month storage in air. The trend of oscillating contact angle with alternating layers and the increase in contact angle with number of PAn layers persists.

The RMS roughness for PAn layers ranges from 60-70Å, while PVP layers have a slightly lower RMS roughness of about 50-55Å. PVP is a flexible polymer that deposits in non-aggregated layers, acting to smooth the surface. AFM surface plots shown in Figures III.12, III.13, and III.14 show 1x1 micron areas of two different PAn layers (Figures III.12 and III.13) and a PVP layer (Figure III.14). The aggregated features are apparent, typical of adsorbed films of PAn. PAn is deposited as both individual chains and nano-aggregates, as described earlier. A more detailed comparison of AFM images is described in Section III.L.

III.K. Monolayer and Multilayer Deposition From Mixed Solutions

In contrast to ionic polymers, the favorable interactions between PAn and these non-ionic hydrogen bonding polymers also makes it possible to form mixed solutions of the two without sacrificing solution stability. In fact, it may be that the presence of one of these polymers acts to increase the stability of an aqueous PAn solution. Two such systems have been investigated, PAn with PVP and PAn with PAAm.

III.K.1. Monolayer Deposition From Mixed Solutions of PAn with PVP and PAAm

Self-assembly-type deposition using these mixed solutions has been demonstrated with the deposition of mixed monolayers of both PAn/PVP and PAn/PAAm. The dipping solutions were prepared by mixing equal volume portions of 0.01 M PAn (pH=2.6) and either 0.01 M PAAm (pH=2.6) or 0.01 M PVP (pH=2.6) to form a 50/50 mixture 0.005 M in both polymers. The solutions appeared miscible and completely soluble in both cases, as no particulates formed upon mixing. Adsorption was onto an SPS treated glass slide, and was monitored as a function of time, showing rapid deposition of a monolayer. Measuring the absorbance as a function of time has revealed these solutions to

μM

0.8

0.6

0.4

0.2

X   0.200 μM/div
Z   60.000 nM/div
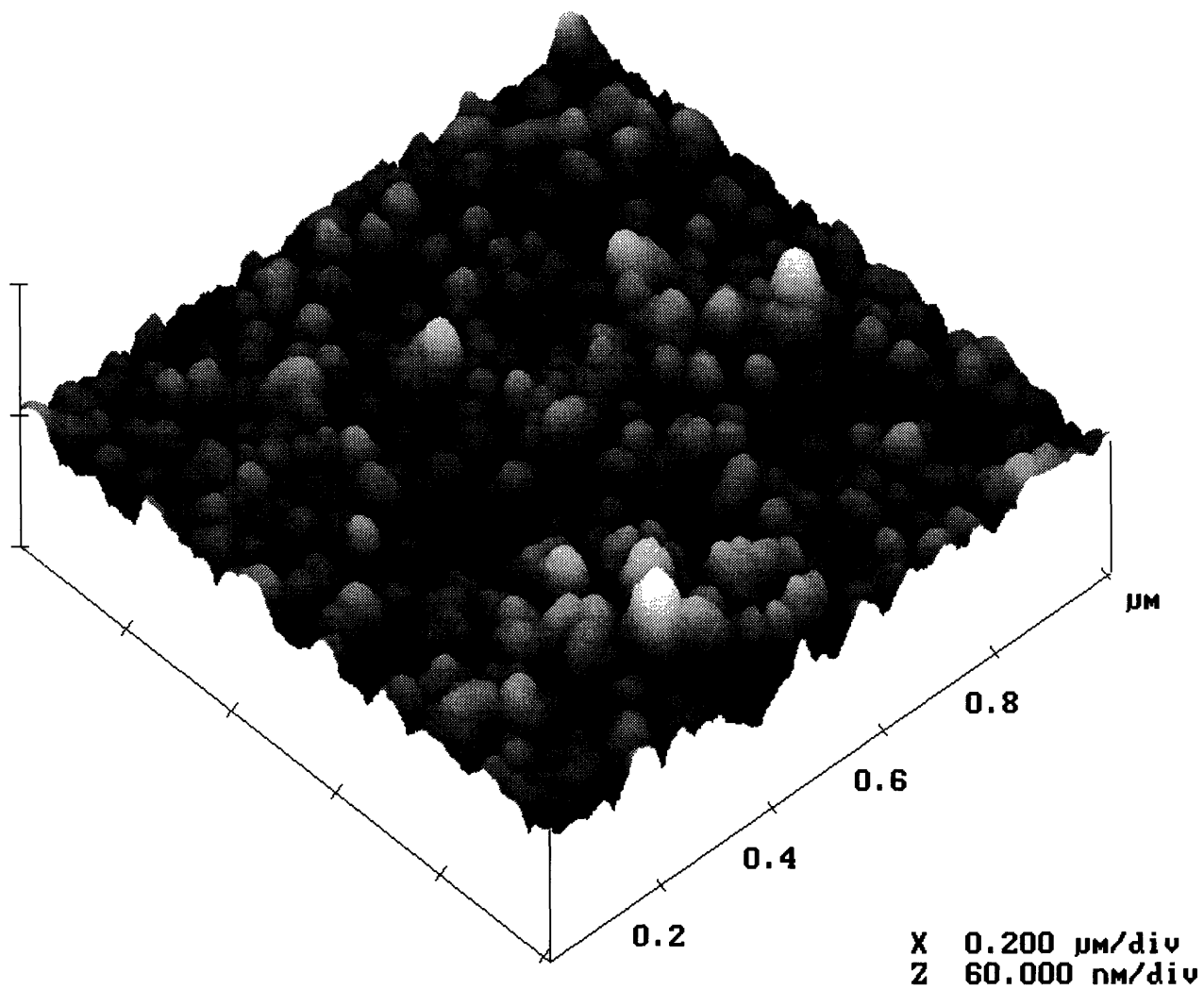
Figure III.12. AFM surface plot of a 1 x 1 μm area of layer 9 (PAn) in the
12 layer PAn/PVP film.

μM

0.8

0.6

0.4

0.2

X 0.200 μM/div
Z 50.000 nM/div
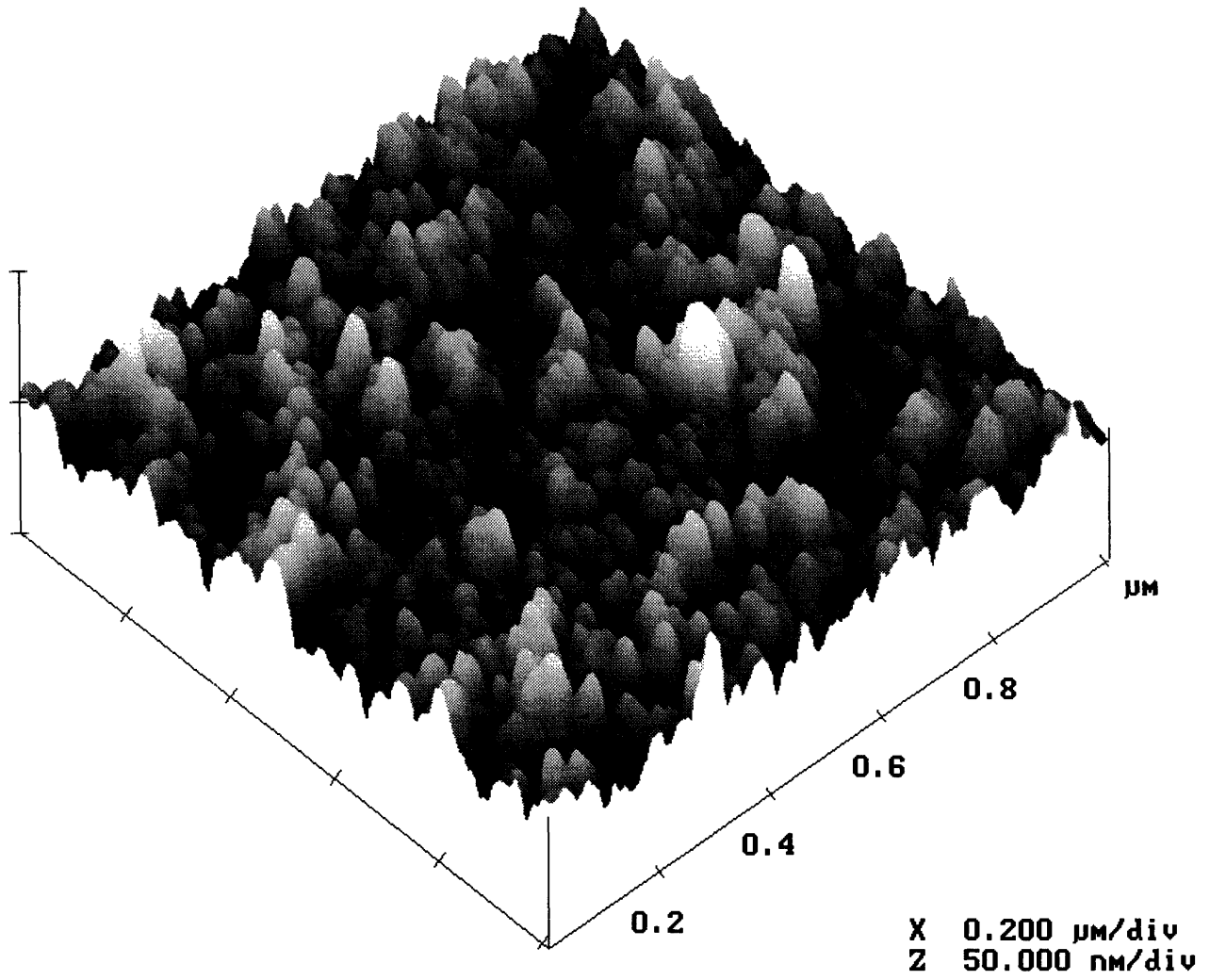
Figure III.13. AFM surface plot of a 1 x 1 μm area of layer 11 (PAn) in the 12 layer PAn/PVP film.
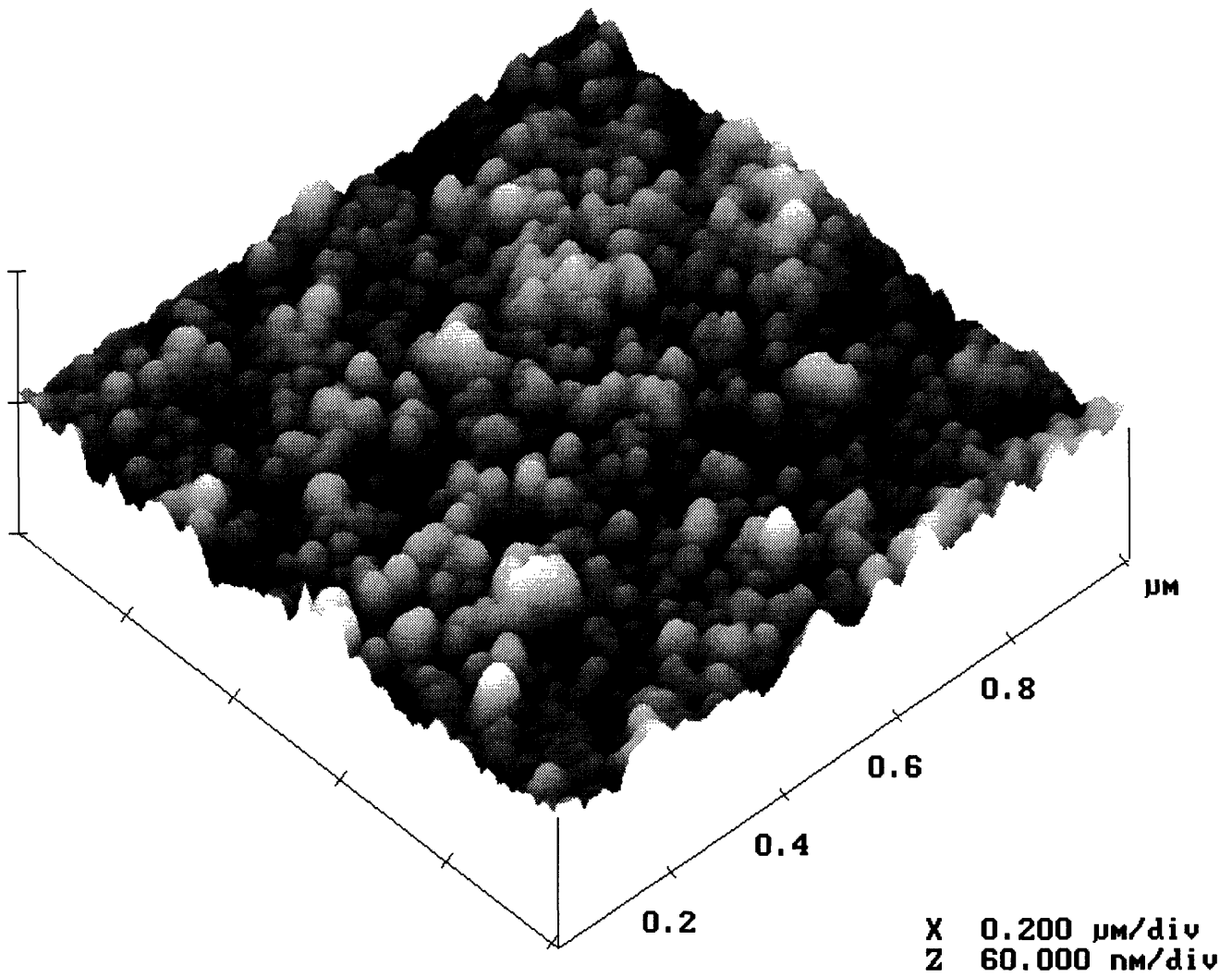
Figure III.14. AFM surface plot of a 1 x 1 μm area of layer 12 (PVP) in
the 12 layer PAn/PVP film.

be self-limiting in deposition, meaning that only a single layer is deposited (over 90% of the eventual thickness in the first 30 minutes). This is seen in the absorbance vs. time plot shown in Figure III.15. Deposition tapered off, virtually stopping after about 45 minutes. Two different dipping solutions are compared in Figure III.15, one made using NMP as the PAn solvent, the other using the usual DMAc. Deposition is virtually identical in both cases, however, films cast from DMAc have higher conductivities, as was seen in Section III.I. Again, this is attributed to higher residual solvent retention with NMP.

No direct thickness measurements have been made; values of 60 Å for the PAn/PVP film and 47 Å for PAn/PAAm are estimated based on assuming the same absorbance as seen in the respective multilayer films. Similarly, they are estimated to have 50-60 vol% PAn. The single layer conductivity (0.1 S/cm for both films) is only about an order of magnitude lower than the eventual conductivity for multilayer films. The significance is that a conducting layer is deposited with a single "dip." The first bilayer in a multilayer system formed by alternative dipping is the thinnest since the first layer of PAn is usually deposited on SPS, leaving a thin, incomplete-covering layer. By using a mixed solution, a thicker first layer can be deposited, as seen with PVP and PAAm. Since these films are about 50-60Å thick, they are highly transparent, and advantageous in the fact that only a single step is required for deposition.

III.K.2. Effect of Substrate on Monolayer Deposition From Mixed Solutions

Since the exact film thicknesses and corresponding vol% PAn deposited have not been determined, it is uncertain exactly what structure is being deposited. Certainly, there is sufficient connectivity of PAn to create a conductive layer. The questions to be addressed concern the manner of deposition from the mixed solution. Do the two polymers co-deposit as a interpenetrated blend, do they deposit sequentially, or does only PAn deposit?

In addressing these questions, attempts were made to deposit PAn and PVP on top of a PAn/PVP mixed layer. Also, mixed layers were deposited onto both PAn and PVP surfaces (as opposed to the polyanionic SPS surface). The results are graphically shown in Figure III.16 for a series of six films, summarized as follows:
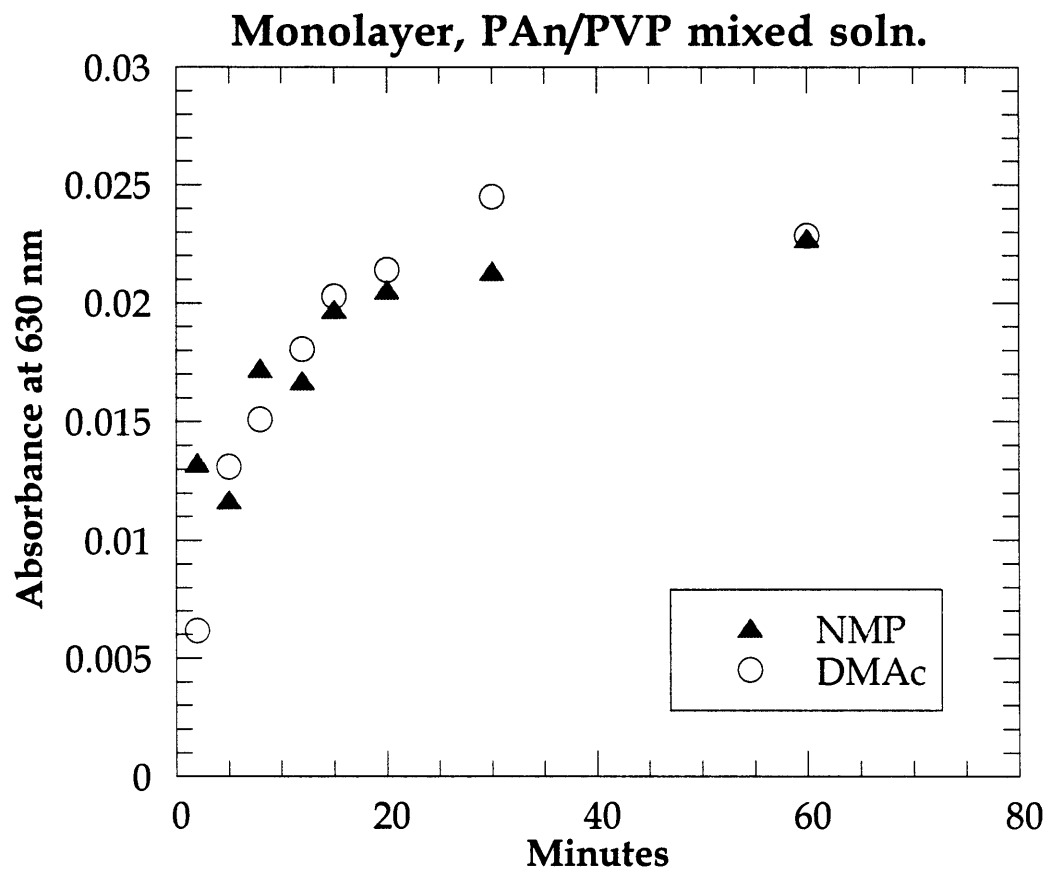
Figure III.15. Absorbance vs. adsorption time for a 50/50 mixed solution PAn/PVP, using either NMP or DMAc as the PAn solvent.

PAn will deposit onto the PAn/PVP mixed layer, but only about half as much as onto pure PVP, as determined by light absorbance (film 1 compared to film 5). Similarly, PAn will adsorb onto a layer of PVP that has first been adsorbed onto a mixed layer, but again shows only about half the usual absorbance (film 2). Since only half as much PAn is being deposited, this indicates that the mixed layer presents a surface that must be a mixture of its two components, PVP and PAn, since PAn will not deposit onto itself. The fact that still only about half as much PAn adsorbs even if a layer of PVP is first adsorbed onto the mixed layer suggests that very little PVP is being deposited. These two results imply that the surface of the mixed layer is heterogeneous, but likely PVP-rich.

For the deposition of the mixed layer on top of PAn and PVP, very little was deposited in both cases (films 4, 5, and 6). Apparently the strong interactions between PAn and PVP in the mixed solution prevent the mixture from forming sufficient interactions with either the PAn or the PVP surface to strongly adhere. The mixed layer deposits nicely onto a negatively charged surface (SPS), suggesting that the positive charge sites along the PAn backbone are what enable the mixed layer deposition. No attempt was made to build up further with PAn on top of this weakly adsorbed mixed layer. This might show that the underlying PAn layer preferentially adsorbed PVP from the mixed solution, had a subsequent full layer of PAn been deposited. This preferential adsorption would not be expected, since the PVP layer did not preferentially adsorb PAn from the mixed solution (film 4).

Contact angle measurements were made on all six films with the results plotted in Figure III.17. The contact angle of the freshly made films for all cases lies between 28-32°, regardless of whether the surface layer was PAn, PVP, or a mixed layer. This range lies between the contact angles measured for freshly deposited PVP (~26°) and PAn (~38°), seen in Figure III.9 for a multilayer film. With the exception of film 1, the PAn surface, this intermediate value of contact value again suggests that the mixed layer consists of a well interpenetrated mixture of PAn and PVP. Since the contact angle lies slightly closer to that of pure PVP, it supports a PVP rich surface. The fact that the PAn surface of film 1 has a low contact angle can be attributed to its relative thinness - this layer consisting of only about half of a usual PAn layer.

Allowing the films to dry in air for two days increased their contact angle up to about 36-38° (including the PEI/SPS "zero" bilayer), seen in Figure

PAn/PVP (50/50) Mixed Soln. Deposition
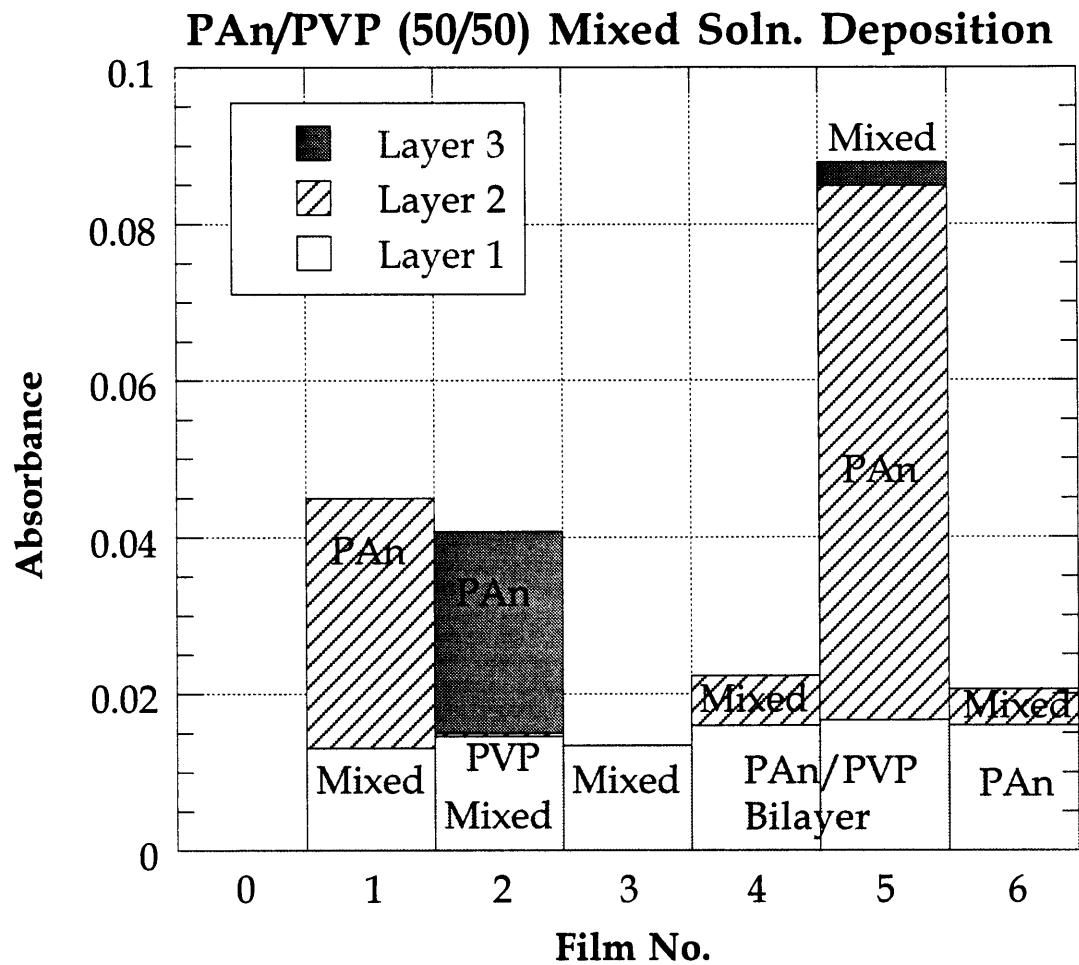
Figure III.16. Histogram of cumulative absorbance for layers of PAn, PVP, and PAn/PVP mixed solution; six different films.
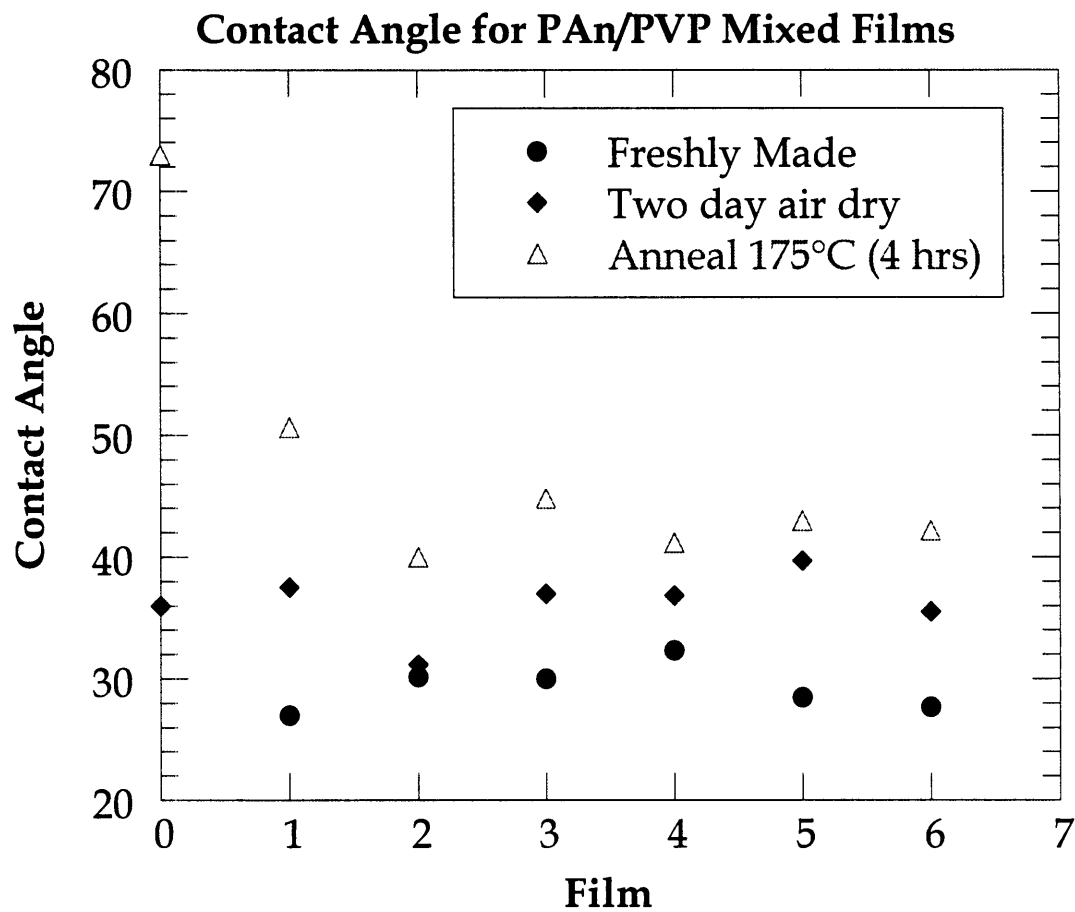
Figure III.17. Contact angle at three different conditions for the six films from Figure III.16.

III.17. One exception was film 2, which was measured after the PVP layer (before the PAn layer), whose contact angle was near 30°. This lower value reflects a PVP-rich surface.

Subsequent annealing at 175°C for four hours led to higher contact angles in all cases, particularly for the PAn surface in film 1. The lowest contact angle is for the PVP surface of film 2, with all the contact angle of the other films (with mixed-layer surfaces) lying in between these two. The implication is that the PAn/PVP mixed solution deposits a well interpenetrated layer with the two polymers strongly interacting with each other.

III.K.3. Varying the PAn/PVP Ratio and Concentration in the Mixed Solution

All of the above mentioned mixed solution work was done using a 50/50 mol ratio at 0.01 M overall concentration (0.005 M of both polymers). The concentration parameter space has also been explored, varying both the PAn/PVP ratio as well as the overall concentration.

First, a series of samples were deposited from a mixed solution at constant overall polymer concentration, 0.01 M, varying the PAn/PVP ratio from 10/90 to 90/10. A single mixed layer was deposited onto two PAn/SPS bilayers on clean glass, using a 30 minute dip time. A two bilayer base was used to ensure a uniform SPS surface covering on which to deposit the mixed layer. The absorbance at 870 nm (corresponding to the absorption maximum for PAn at pH=2.5) is plotted for this series in Figure III.18, showing how the addition of PVP increased the amount of adsorbed PAn. The absorbance due only to the mixed layer is tabulated for the series in Table III.4. Included is the absorbance for the second PAn/SPS layer, which corresponds to the 100% PAn case. All mixed solutions deposit more PAn than the 100% case, even though the concentration of PAn has decreased. The absorbance appears to go through maximum near 75% PAn, which reflects the competing events for adsorption in this system. Adding PVP acts to enhance the adsorption onto SPS, but decreasing the PAn concentration diminishes the amount adsorbed.

The next section addresses the case of constant PAn concentration (0.01 M), with added PVP.

PAn/PVP Mixed Monolayer on 2 Bilayers PAn/SPS

Legend:
- 90% PAn
- 75%
- 50%
- 25%
- 10%
- PAn/SPS

Y-axis: Absorbance at 870 nm (0 to 0.1)

X-axis: Bilayer (0 to 4)
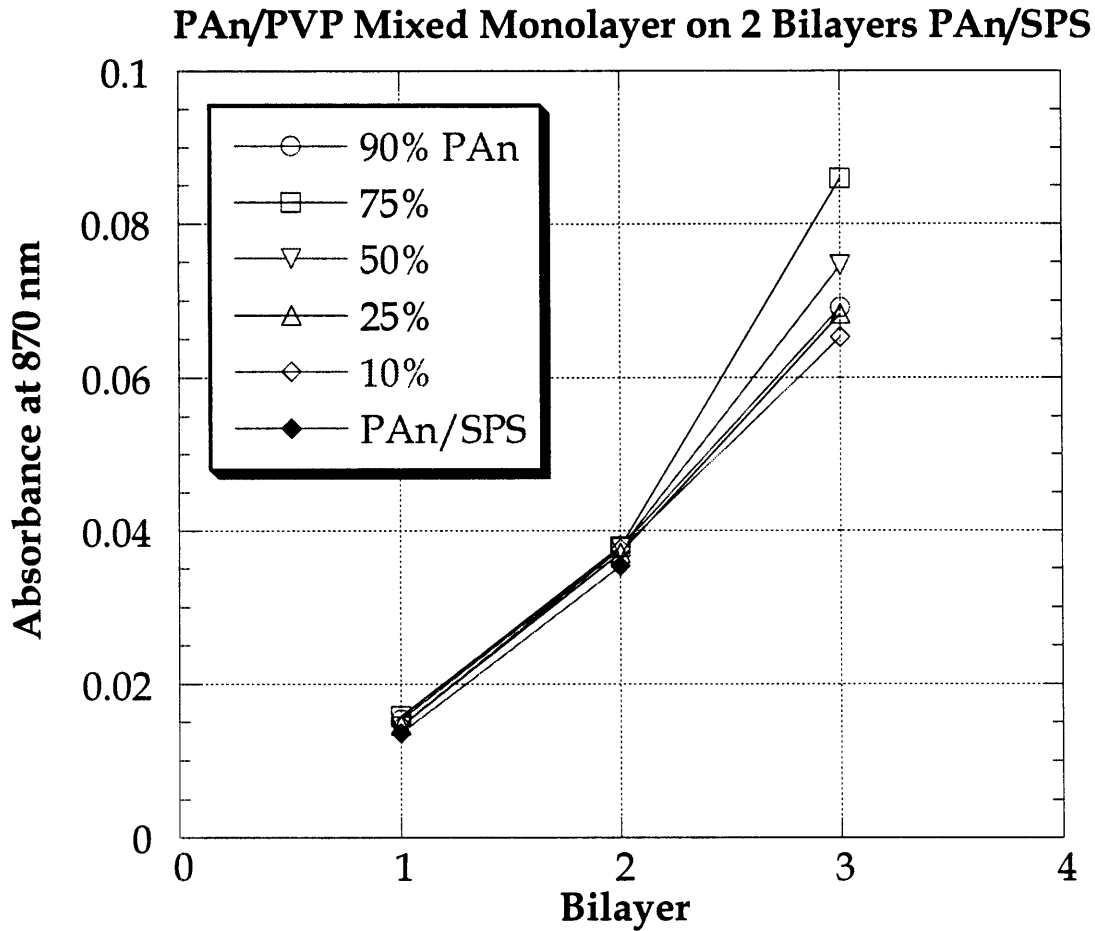
Figure III.18. Absorbance at 870 nm vs. bilayer number for a series of PAn/PVP mixed solution monolayers, varying the PAn/PVP ratio. (Deposited onto two bilayers of PAn/SPS).

Table III.4. Absorbance at 870 nm for PAn/PVP mixed solution layers as a function of solution concentration.

mol% PAn (conc.)	Corrected Absorbance for mixed layer (870 nm)
100 (0.01 M)	0.0112
90 (0.009 M)	0.0157
75 (0.0075 M)	0.0241
50 (0.005 M)	0.0185
25 (0.0025 M)	0.0157
10 (0.001M)	0.0139

Contact angle measurements on this series are plotted in Figure III.19. The freshly made films all have a low contact angle, about 22-25°, with no apparent trend. The low value suggests that in all cases, a significant amount of PVP is being codeposited, and is initially forming a PVP-rich surface. Vacuum drying the films overnight raises the contact angle significantly (to 48-59°), a result of the reduced moisture content as well as the aforementioned tendency of the surface to lower its surface energy through molecular rearrangements. The contact angle appears to increase with %PAn (in solution) as well, from 48° to 59°, suggesting that the films also have increasing % of PAn. PAn segments are present at the surface, causing the increase in the contact angle. Annealing the films at 175°C for three hours further increased the contact angle, as increased chain mobility allowed additional PAn segments to the surface. Again, the higher %PAn films showed higher contact angles.

III.K.4. Multilayer Films of Mixed PAn/PVP with SPS

It has been shown in the previous section that the mixed PAn/PVP layer deposits best onto a negatively charged surface, such as a SPS coated substrate. Very little deposition occurs onto either PAn or PVP, suggesting that the electrostatic attraction between SPS and the lightly doped PAn drives the adsorption. This fact enables multilayer build-up of mixed layer systems by alternating between a mixed PAn/PVP layer and a polyanion layer such as SPS. It should be noted that PVP by itself does not adsorb onto SPS, as was discussed
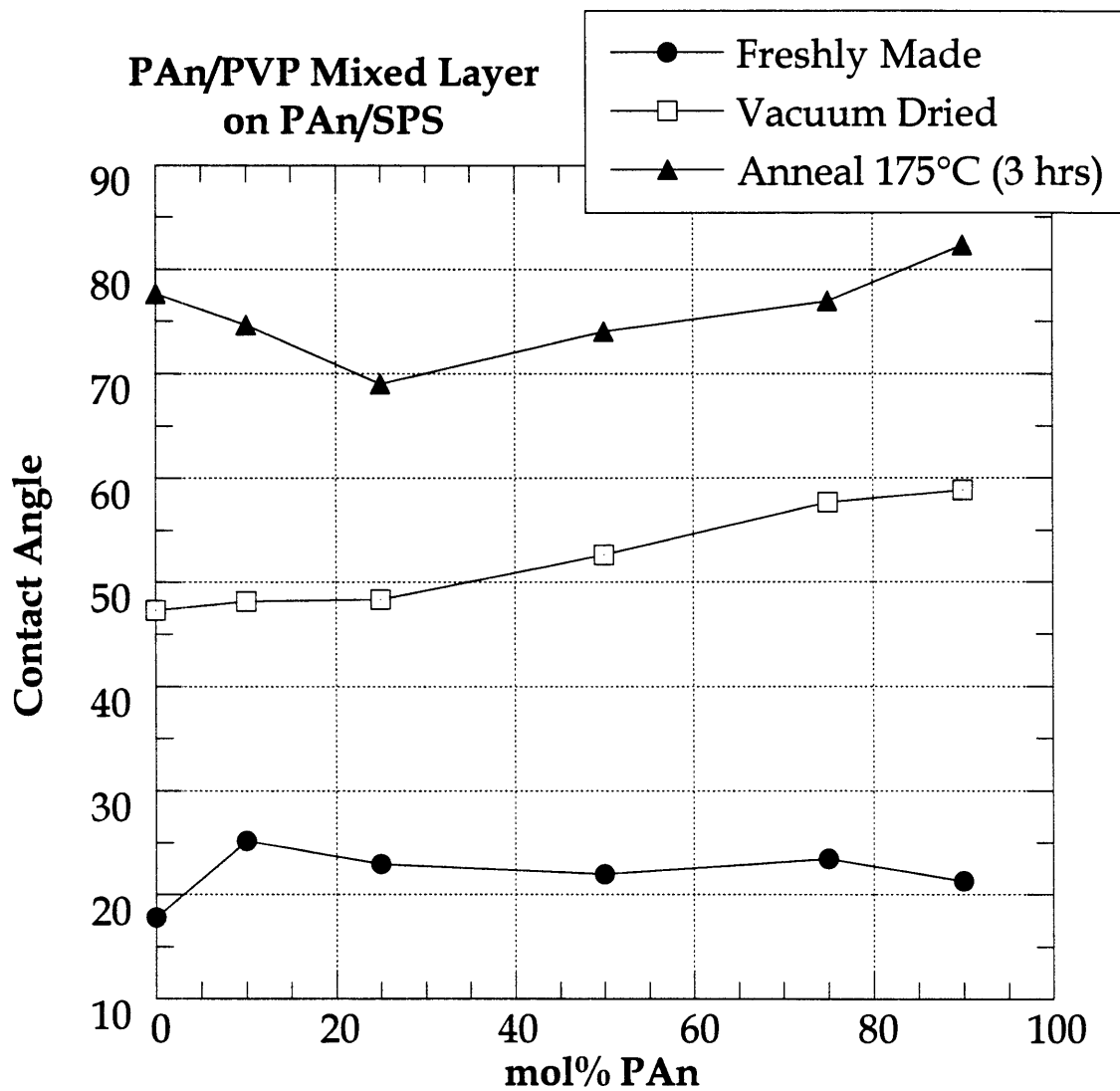
Figure III.19. Contact angle for PAn/PVP mixed solution series (from Figure III.18) for three different conditions.

in Section III.E. Thus, the mixed solution approach enables deposition of multilayers of a heterogeneous conducting layer alternating with a polyanion.

Two series of multilayer films were grown, as described below. The first was deposited from a PAn/PVP solution of constant overall concentration (0.01 M, total of both polymers), varying the PAn/PVP ratio from 25/75 to 75/25. The second series held the PAn concentration constant at 0.01 M while adding PVP to again vary the ratio from 25/75 to 75/25, designated the F-series. In both cases, all solutions were adjusted to pH≈2.5 with MeSA. As before, 30 minute dip times were used for the mixed layers, 15 minutes for the SPS. Layer-by-layer build-up was monitored by UV-vis absorbance.

For the first series, six bilayers were deposited onto SPS-treated glass slides, measuring the UV-vis absorbance after every bilayer. Again, these are partially doped films, thus the absorbance maximum (for PAn) is near 860 nm. Figure III.20 shows the linear growth for these six bilayers for three PAn/PVP solution ratios, 75 mol%, 50%, and 25% PAn. For the first bilayer, all three concentrations deliver about the same amount of PAn, somewhat lower than that seen in the previous section for the 10%-90% PAn series. The absorbance is about 0.008-0.011 here, before it was 0.016-0.024 (Table III.4). The difference is due primarily to the condition of the underlying SPS layer. For the previous case, the base layer consisted of two PAn/SPS bilayers, presenting a more uniform and complete SPS layer. In this case, the substrate is SPS-treated glass, which has a thinner, "spottier" covering. The subsequent layers contain more PAn, comparable to those seen in the previous section. A comparison will be seen shortly, in Table III.5.

As evident in Figure III.20, the most PAn is deposited from the 50% solution. This again reflects the competing nature for adsorption. PVP acts to enhance the deposition, but lowering the PAn concentration decreases the amount available to adsorb.

If the amount of PAn is held constant, at 0.01 M (the F-series), a slightly different trend is seen. Again, linear build-up is observed, plotted in Figure III.21. By eliminating the PAn concentration variable, the effect of PVP can be observed. All three concentrations (75, 50, and 25 mol%) deliver about the same amount of PAn, with the highest concentration of PVP having a slightly higher amount. This corresponds to the effect of PAn-enhanced deposition onto SPS by means of added PVP.
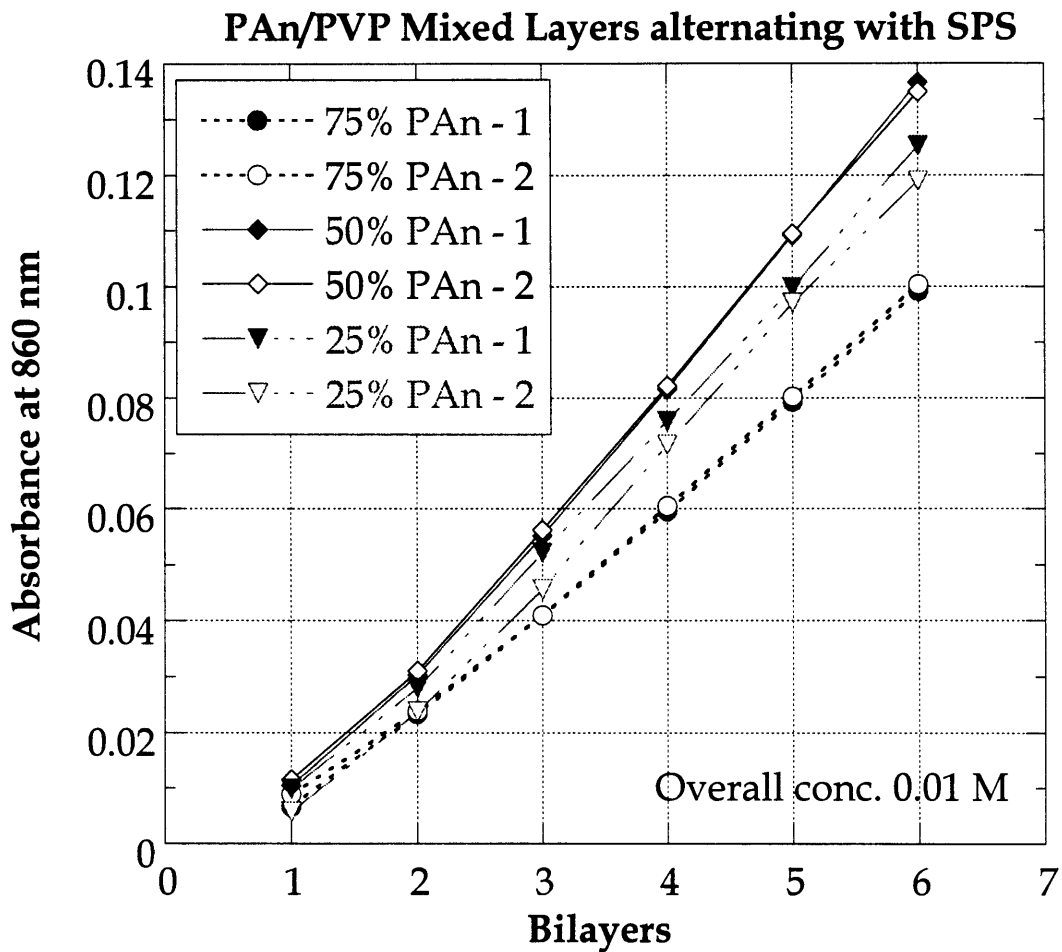
Figure III.20. Absorbance at 860 nm vs. bilayer number for PAn/PVP mixed solution multilayer films built up with SPS. (Three PAn/PVP ratios, overall polymer concentration = 0.01 M).

PAn (0.01 M)/PVP Mixed Layers Alternating with SPS
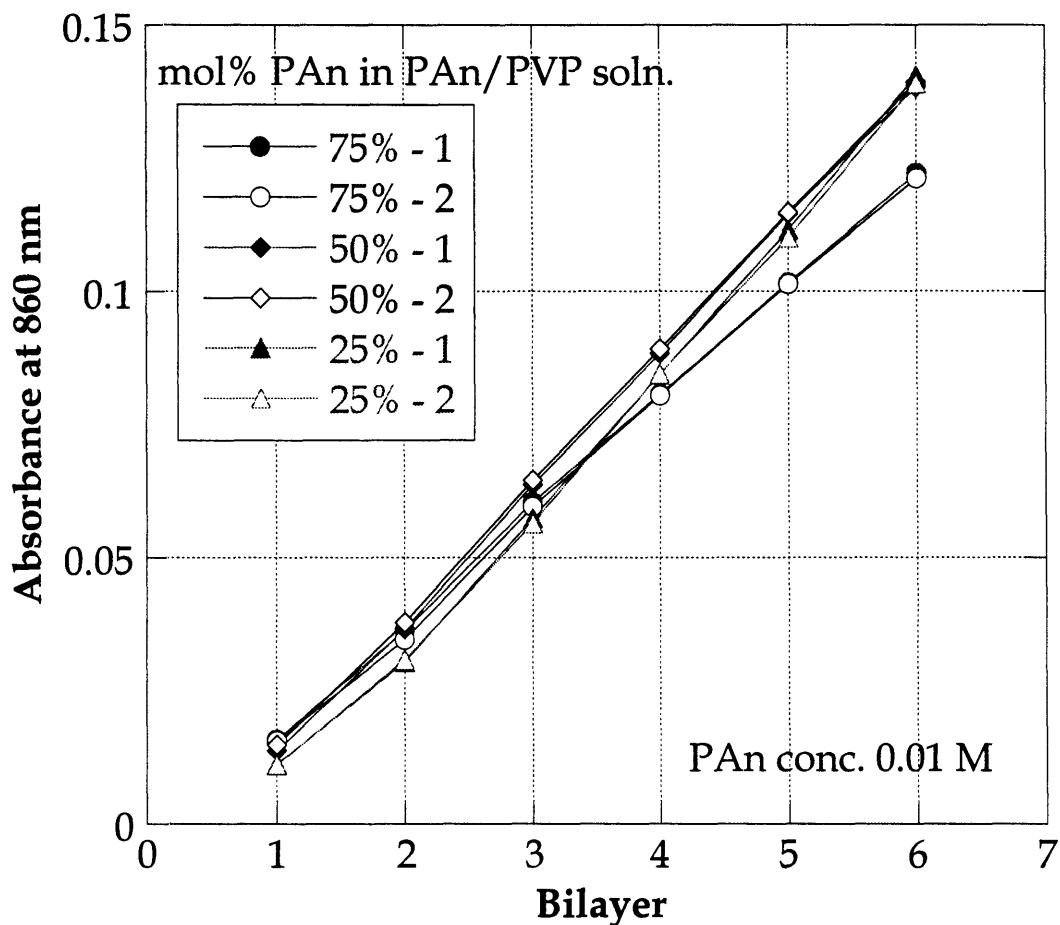
Figure III.21. Absorbance at 860 nm vs. bilayer number for PAn/PVP mixed solution multilayer films built up with SPS. (three PAn/PVP ratios, PAn concentration = 0.01 M).

Film thicknesses were measured by profilometry, revealing the bilayers to measure about 60Å thick and consist of approximately 40 vol% PAn. This includes both the SPS layer and the mixed PAn/PVP layer. Since SPS generally delivers 10-15Å per layer, thus about 20% of the total thickness, this implies that the amount of PVP being deposited never exceeds the amount of PAn. It appears that the amounts of PAn and PVP are about the same, suggesting that the two polymers are highly interacting, and deposit as though they are complexed. These values are tabulated in Table III.5.

Table III.5. Selected properties for six bilayer films of SPS with PAn/PVP mixed solution for varying concentrations of PAn and PVP in the mixed solution, average values for each concentration. F-series has a constant PAn concentration of 0.01 M, the other series has an overall PAn/PVP concentration of 0.01 M.

% PAn in PAn/PVP	Ave. thick. (Å)	Å /bilayer	Abs. at 630 nm	Abs. /bilayer	Est. vol% PAn	Dichroic Ratio	σ S/cm
100 *	245	41	0.0748	0.01246	43	1.19	0.110
75%	284	48	0.0850	0.01416	39	1.26	0.010
50%	342	57	0.1127	0.01878	44	1.29	0.025
25%	378	63	0.1012	0.01687	35	1.29	0.016
F-75%	232	39	0.1143	0.01905	64	1.26	0.094
F-50%	321	54	0.1286	0.02143	52	1.25	0.092
F-25%	323	54	0.1253	0.02088	51	1.27	0.029

* PAn/SPS multilayer film, no PVP.

Dichroic ratios (S-polarized/P-polarized) were also measured, and are tabulated in Table III.5 as well. This ratio gives a relative indication as to the average preferred chain orientation of the PAn chains. The ratio lies between 1.25-1.30 for all concentrations, indicative of an in-plane orientation preference, but little or no difference for changing concentrations.

Conductivity measurements show the films to be about one order of magnitude lower than PAn/SPS systems for the lower concentration PAn series, and about the same for the 0.01 M PAn series (F-series). There is little or

no increase in conductivity from a single mixed layer, seen in Section III.K.1, to the multilayers here. In all cases, the conductivity is lower by at least an order of magnitude to the PAn/PVP multilayer films. This is due to several factors, primarily that the PAn/PVP mixture acts to dilute the PAn chains, reducing effective interchain charge transfer, as was seen in blended films in Section II.F. Also, as was seen in section III.H, the PAn/SPS multilayer films generally have a lower conductivity than the PAn/PVP systems, by about an order of magnitude. The cause of this is uncertain, and might be simply due to the PAn thickness per bilayer, which is less in PAn/SPS than in PAn/PVP (see Table III.1)

III.L. Surface Topography by Atomic Force Microscopy

An important issue in understanding the structure of the films is the relative smoothness of the deposited films, and how the various parameters such as molecular weight and number of bilayers affects the surface roughness. To elucidate these effects, samples consisting of self-assembled polymer films on both glass slides and silicon wafers were imaged by atomic force microscopy. Clean glass and clean silicon were imaged first as references. The reported root mean square (RMS) roughness values show the range measured for at least five different scans per sample. For the RMS roughness measurements, the scan area was generally 10 μm x 10 μm.

Table III.6 summarizes results from a series of films on both glass and silicon. As expected, silicon is the smoothest, with an average RMS roughness (R_q) of 3-6 Å. Glass has a roughness of only 5-9 Å. Silanizing the glass with a trifunctional silane slightly increases the roughness (R_q = 7-12 Å), and coverage appears complete. The behavior is similar with silanized silicon. One layer of low mw SPS (70K) on the trifunctional silane does not significantly change the appearance or roughness, still around R_q = 10-16 Å. Coating glass with a layer of PEI rather than silanizing gives slightly smoother films, R_q = 7-9 Å. PEI will not deposit onto silicon, however.

A monolayer of PAn on glass has R_q = 39-47 Å. The PAn film appears aggregated; Table III.6 gives a rough estimate of the diameter of the aggregates. A monolayer of PAn on silicon has R_q = 50-70 Å. The PAn deposited a rough, aggregated layer, similar to the film on glass. The coverage was not quite

complete, and adhesion was not as good as with glass. A layer of PAn on SPS-silanized glass has only slightly increased roughness, R_q = 45-53 Å, as does a layer of PAn on SPS-PEI-glass, R_q = 45-55 Å. This is despite the increased roughness of a layer of SPS-hi on PEI on cleaned glass, R_q = 20-29 Å, vs. SPS-low on silanized glass, R_q = 10-16 Å.

The increased roughness in going from SPS on silane to SPS on PEI may be due entirely to the increased mw of the SPS (70K to 500K), since the PEI monolayer (7-9 Å) is slightly smoother than the trifunctional silane (7-12 Å).

Table III.6. RMS roughness of various films as measured by AFM.

Sample	RMS Roughness (Å)	Appearance
1. clean glass	5-9	smooth
2. clean silicon	3-6	smooth
3. silanized glass (trifunctional)	7-12	uniform, 15 nm aggregates.
4. silanized silicon (trifunctional)	9-18	uniform, 16 nm aggregates.
5. PEI on clean glass	7-9	uniform
6. PAn on clean glass	39-47	30-38 nm aggregates
7. PAn on clean silicon	50-70	38 nm aggregates
8. SPS-low on silanized silicon	10-16	15 nm aggregates
9. SPS-low on silanized glass	8-9	16 nm aggregates
10. PAn on SPS-low silanized glass	45-53	32-38 nm aggregates
11. SPS-hi on PEI on clean glass	20-29	25-38 nm aggregates
12. PAn on SPS-hi on PEI-glass	45-55	30-38 nm aggregates
13. 5 bilayers PAn/PVP	63-70	On SPS treated glass
14. 20 bilayers PAn/PVP	56-91	On SPS treated glass
15. 5 bilayers PAn/SPS	29-43	Low conc. PAn (10^{-4} M)

Two PAn/PVP multilayer samples were imaged, numbers 13 and 14 in Table III.6, showing slightly increased roughness with increasing number of bilayers. Apparently, the addition of bilayers does not act to planarize the films, but rather continues to slightly roughen. Even one layer of SPS increases the roughness of a glass slide, and subsequent layers act to roughen the surface even more. The low concentration PAn solutions (10^{-4} vs. 10^{-2} M) deposit the smoothest films, indicating the more favorable conditions for chain elongation

on the surface due to decreased competition for surface sites. It is also possible that there are fewer or smaller aggregates in the lower concentration PAn solution, thus delivering a smoother layer.

III.M. Neutron Reflectivity Study

In collaborative work with Mayes and Kellogg [92], neutron reflectivity experiments have been performed to address questions about the nature of the bilayer interfaces and surface roughness. The technique is sensitive to gradients in the neutron scattering length density normal to the film surface, thus is well suited to characterizing internal layer organization as well as surface roughness. The particular system under study was SPAn/PAH (sulfonated polyaniline/ poly(allylamine hydrochloride)). This is an ionic system with relatively thin bilayers (about 15Å). Films of 40 bilayers were prepared, selectively labeling certain blocks of bilayers with deuterated SPAn.

In short, the multilayer structure was found to have broad interfaces, on the order of 45Å. Considering that each bilayer is only 15Å, this implies that there is considerable interfacial diffusion and/or a highly corrugated interface, that appears to become rougher as more layers are deposited. The surface roughness was estimated to be about 95Å, supporting the idea of irregular (wavy or corrugated) interfaces. Parallel AFM measurements on films with 32 bilayers revealed an RMS roughness of about 80Å, consistent with the neutron reflectivity data fits. The deposition was uniform in terms of average bilayer thickness, however, as all films had about the same overall thickness, and linear growth was always seen in monitoring the deposition.

Preliminary results on PAn/PEO systems have revealed, again, very rough surfaces, and irregular or diffuse interfaces.

III.N. Chain Orientation by Dichroism Studies

One method for determining chain orientation of molecules on surfaces is that of polarized light spectroscopy. By measuring the absorption of light polarized parallel (P) compared to that perpendicular (S) to the plane of incidence, the average orientation of a chromophore transition moment can be

determined. This approach has been applied to Langmuir-Blodgett films [93-96], which are quite similar to self-assembled films in that they are both thin films usually deposited on both sides of the substrate (glass, in this case). The absorption maximum is measured for the two polarizations at off-normal incidence. For S polarized light, the electric field component lies entirely in the plane of the substrate. For P polarization, the electric field vector has components both in the plane of, and perpendicular to, the plane of the substrate. The average orientation of the transition moment is thus dependent on the dichroic ratio, or the ratio of S absorbance to P absorbance. For polyaniline, this transition moment lies effectively along the chain axis, thus the average chain orientation can be determined from the dichroic ratio. None of the other polymers of this study absorbs visible light, thus do not interfere with interpretation of the PAn chain orientation. A similar experiment can be done with infrared spectroscopy to probe the orientation of these other polymers. Several example spectra are shown in Figure III.22.

Using the relations outlined in references [93-95], the ratio of P absorption to S absorption is given in equation {12},

$$\frac{A_P}{A_S} = \frac{n_1 \cos i + n_3 \cos r}{n_1 \cos r + n_3 \cos i} \left(\cos i \cos r + \frac{n_1^3 \, n_3 \sin^2 i}{n_2^4 \tan^2 \phi} \right) \qquad \{12\}$$

where n_j is the refractive index of phase j (1 = air, 2 = polymer film, 3 = glass substrate), and i is the angle of incidence at the air-film interface, and r is the angle of refraction at the film-glass interface. The angle ϕ is the angle of the transition moment from the surface normal, assuming uniaxial orientation. This angle can be thought of as the average angle of the PAn chains from the surface normal.

Relative chain orientation for PAn multilayer films were determined for several sets of films. The dichroic ratio (S/P) was measured at three different angles of incidence, 30°, 45°, and 60°. Using equation {12}, the average chain axis angle, ϕ, was calculated, using the following values: $n_1 = 1.0$, $n_2 = 1.6$, $n_3 = 1.5$, and r was determined by Snell's law, $n_3 \sin r = n_1 \sin i$. There is some uncertainty in the index of refraction for the thin PAn multilayer films, n_2. A refractive index of n = 1.6 has been reported for thin polyaniline films grown electrochemically, at a wavelength of 600 nm [97, 98]. The index, n, increases
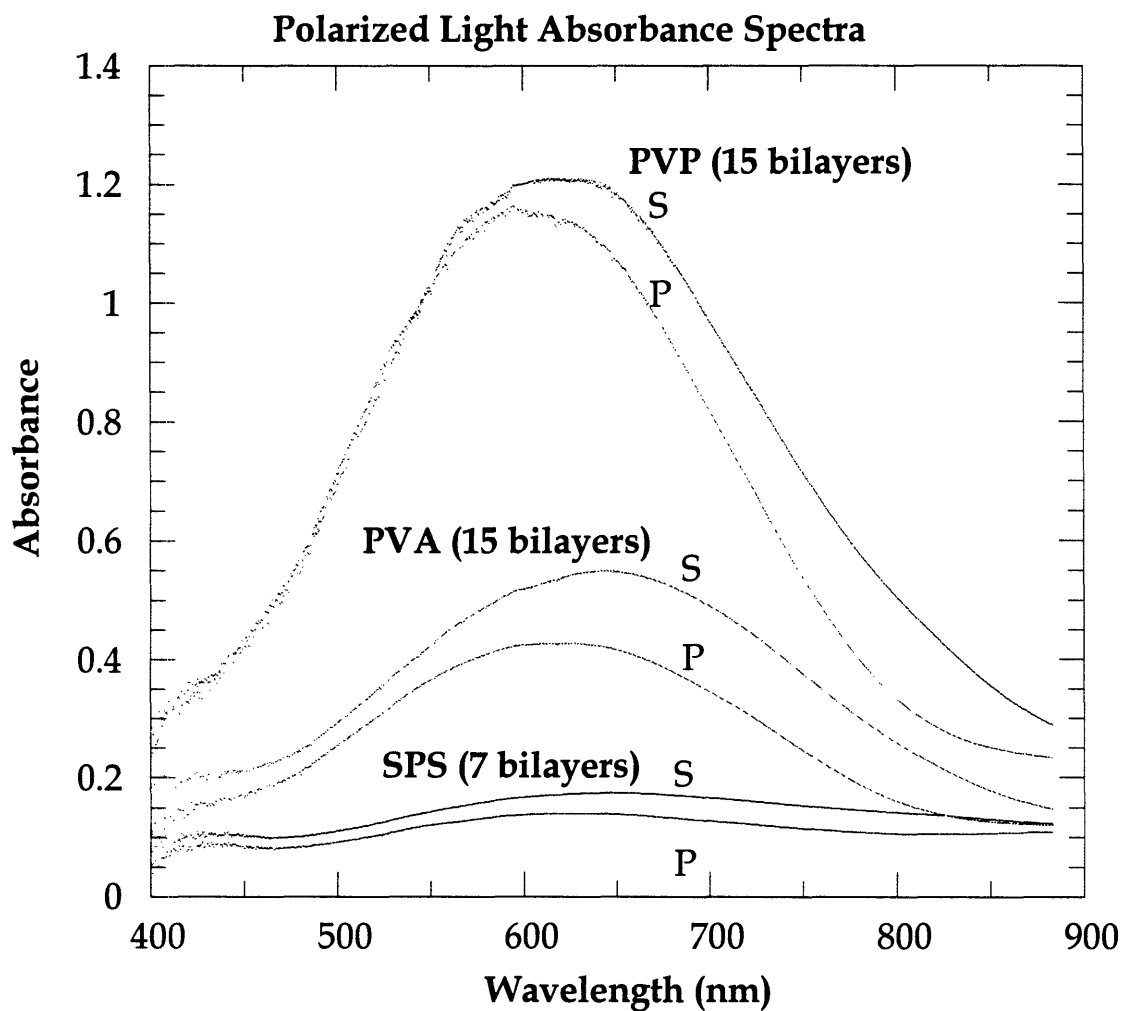
106

Figure III.22. Polarized UV-visible absorption spectra for three PAn multilayers, PAn/PVP, PAn/PVA, and PAn/SPS, with S and P polarization. (Angle of incidence is 45°)

with decreasing wavelength. Values as low as 1.17 were measured for doped films [97]. Ellipsometry measurements in our lab at three wavelengths, 488, 633 and 830 nm, show the value to range from 1.7-2.1, quite a large range. Since there is a fourth power relation for n_2 in equation {12}, it is important to accurately know this value. Thus current calculated values for ϕ remain uncertain. Qualitatively, however, this technique is quite useful for making relative comparisons between various film-forming conditions.

For dichroic measurements made on several samples of varying PAn concentration, the following observations can be made. The lower concentration PAn solutions (low = 10^{-4} M) had the highest dichroic ratios, indicating that these films have the most "flattened" chain orientation, or the most preferential in-plane orientation. This behavior is expected since the more dilute environment allows chains to reconfigure to a more extended state on the surface, thus increasing their adsorption interactions. Solutions made from DMAc rather than NMP generally delivered higher ratios, as well. Again, stronger interactions with NMP reduces available adhesion sites along the PAn chain, decreasing its ability to extend along the surface. Most all of the multilayer thin films had a dichroic ratio of about 1.18-1.26, indicating a slight preferential in-plane orientation of the PAn chains, with the exception of multilayer flms made with PAAm. As discussed in Section III.F, the configuration of PAAm is more strongly dependent on pH than the other systems, most likely due to the fact that it can be positively charged at low pH values, thus experiences some charge repulsion from the positively charged PAn layer.

CHAPTER IV. CONCLUSIONS, SUMMARY, AND FUTURE WORK

The controlled manipulation of conducting polymers will prove to be extremely useful in quite a variety of applications ranging from thin film conducting coatings to large scale bulk materials. It is the goal of this thesis to address some of the issues concerning structure and the nature of interactions within conjugated polymer assemblies, focusing on one particularly promising conducting polymer, namely polyaniline.

IV.A. Summary - PAn/PVP Blends

It has been shown in this work that relatively stable, electrically conducting compatible blends of PAn with PVP can be cast from both NMP and DMAc. The two polymers were miscible to the extent probed by thermal analysis, light microscopy, and SAXS. The formation of a single-phase blend is solvent-dependent, however, depending on the blend ratio and molecular weights. NMP is the preferred solvent (over DMAc), even though both are good solvents for the individual homopolymers. Compatible blends with a conductivity on the order of pure PAn (~1 S/cm) require ≥ ~25 wt% PAn, but conductivities two orders of magnitude lower (~0.01 S/cm) can be obtained with less than 5 wt% PAn. Although a relatively low apparent percolation threshold (about 3-5% PAn) is obtainable, it is not clear that miscibility is best to lower the percolation threshold. Completely dissolved (and dilute) PAn, if uniformly distributed in an insulating matrix, would have significant barriers for interchain charge transport. TGA results revealed high solvent retention, particularly NMP, up to as high as 33% for pure PAn solvent-cast films, even after considerable drying. The strong interactions between PAn and NMP act to retain NMP in the films, which leads to reduced conductivity.

109

The above reported conductivity values are for blends cast in the undoped form, then subsequently doped. Conducting blends of *fully doped* PAn with PVP can also be cast directly from solution, again with NMP a better solvent than DMAc. There is, however, a significant conductivity drop for these systems compared to the post-doped system (about two orders of magnitude). The blend films with high wt% PAn show evidence of crystallites, seen under crossed polarizers in a light microscope. There is still considerable compatibility between the two components, however, as evident by the films' uniform appearance under the microscope. In all cases, the presence of residual NMP remains problematic.

IV.B. Summary - Self-Assembly of PAn Multilayer Films

Building up multilayer thin films can be readily achieved with a wide variety of combinations, as demonstrated in this paper with polyaniline. Conductivities on the order of 2-4 S/cm are readily obtained with thicker multilayers, with a minimum thickness of about 200Å. These thin film assemblies are controllably grown by means of adjusting solution chemistry and composition, most importantly pH, concentration, and molecular weight. In the case of films with PAn, it has been shown that multilayer films can be built up by means of both electrostatic forces as well as secondary forces like hydrogen bonding. Solution pH and molecular weight effects (of the counter-polymer) have been described. There has been no investigations yet into the effect of the molecular weight of the PAn, but this is certainly a very important issue.

It is apparent in the case of the non-ionic polymers that there are additional interactions other than hydrogen bonding that lead to this build-up. Certainly, hydrophobic interactions are important in the deposition of PAn (as water is a non-solvent), but it is not clear what other interactions are driving the deposition of the non-ionic polymers. Investigations have been made into the ability of charged polymers to adhere to non-ionic polymers, and vice versa. PEO and PVP will build multilayer systems with PAn at both low pH (2.6), thus positively charged, and "neutral" pH (4.5-6.5). PEO and PVP will not build up multilayers with SPS, a polyanion, nor PAH, a polycation, at any pH. The implication is that either there are very strong specific interactions with PAn, or

that these water soluble polymers (PVP, PEO, etc.) will not interact with charged polymers in a manner that allows multilayer self-assembly.

Investigations into the ability of hydrogen-bonding pairs other than PAn to form multilayer films have also shown no build-up. All possible hydrogen acceptor/hydrogen donor combinations were tried with PVP, PAAm, PEO, and PVA, with no build-up. Again, there are strong interactions such as additional H-bonding or specific interactions with PAn that enable this multilayer growth using non-electrostatic polymer adsorption.

A variety of techniques has been used to assess the structure of these multilayer films. It appears that the deposited films are relatively rough and wavy, but by all indications, they are continuous with uniform growth. They have diffuse interfaces, but the surface is completely changed (covered) upon addition of each subsequent polymer layer. AFM results indicate some extent of nano-aggregation of the PAn chains, thus the relatively rough surfaces. Polarized light spectroscopy confirms that for these films cast from higher concentrations (10^{-2} M PAn) the PAn chains have only slight preferred in-plane orientation.

It has yet to be determined, but the strong interactions of PAn with certain water-soluble polymers such as PVP or PAAm may act to stabilize aqueous solutions of a mixture of the two. Deposition is possible from a mixed solution of PAn with PVP or PAAm. This is advantageous from a processing perspective, as well as in forming thicker films in one dip. A conductive film can be deposited in a single step in the case of these mixed solutions (conductivities on the order of 0.1 S/cm). Although these mixed solutions are self-limiting (they only form monolayers, just like a homopolymer solution), it is possible to form multilayers by alternating the mixed layer with a layer of SPS. The mixed layer deposits as a compatible blend, as evident by intermediate contact angles between that of PAn and PVP. Since the mixed layer will not deposit onto a PAn nor a PVP layer, but does deposit onto a negatively charged layer (like SPS), this implies that the presence of charged PAn drives the deposition, but significant amounts of PVP are co-deposited.

There are strong interactions between PAn and DMAc, and even stronger with NMP. It has been shown that these residual solvent interactions can lead to reduced conductivity, and slightly less in-plane orientation of PAn chains in self-assembled films.

Contact angle measurements have shown the layering structure to have some discreteness. Even though there is strong evidence for interpenetrated

layers, each deposited layer remains rich in its own self, effectively covering the surface. This layering persists through many bilayers, as well as after long anneals at relatively high temperatures. Despite the compatibility of a system like PAn/PVP, the bilayers maintain their original layered structure, at least to the extent of having surfaces rich in one polymer.

IV.C. Future Work

There are some logical extensions of this work that would address in more detail the questions about multilayer film structure, mechanisms of adsorption, and the nature of the specific interactions between PAn and other polymers. Further work concerning the electrical properties would also be of interest. Some possibilities are:

1. Depth profiling of self-assembled films.

Shimidzu and coworkers [99, 100] have done depth profiling on electrochemically grown multilayered structures of conducting polymers by means of secondary-ion mass spectrometry (SIMS). They used relatively thicker films, on the order of 1000-5000Å, than those grown by self-assembly, 100-1000Å. More distinctively, their layers were on the order of 250-500Å thick, while self-assembled bilayers range from 20-80Å per bilayer. These thinner films may pose a resolution problem, but are certainly well suited for SIMS due to the lack of charging in the films, a problem normally associated with polymer films. Preliminary attempts to profile by x-ray photoelectron spectroscopy (XPS) were not successful due to resolution limitations of the instrument.

2. Polymer adsorption - effects of PAn molecular weight and of ionic strength.

There are many adsorption parameters left unexplored that are of significant importance in understanding and fully characterizing the adsorption of PAn. For example, a single molecular weight (distribution) PAn was used throughout this thesis, due to the synthesis route used. Higher (and lower) molecular weights are obtainable by adjusting the synthesis conditions [40], although there is no simple way to obtain a narrow molecular weight

distribution. It has been shown that molecular weight can play an important role for the adsorption of non-ionic polymers; this parameter should be explored for PAn as well.

It is well known in polyelectrolyte adsorption that the solution ionic strength plays a very important role, as it controls chain configurations. It can be expected that the presence of ions would also affect non-ionic polymer adsorption, but it is not clear as to what type of effects to expect. It would also be interesting to explore the adsorption of sulfonated polyaniline (SPAn), which is an unusual polymer in that it can have both positive and negative charges at the same time along its chain, it is water soluble, and it is electrically conducting (although an order of magnitude lower than PAn). Certainly, there would be interesting effects of pH, ionic strength, etc. with SPAn.

3. Enhancing conductivity with surfactant-type dopants.

Many groups, as mentioned in the introduction, have shown enhanced conductivity for PAn by using larger, surfactant-type dopants like DBSA and CSA. These dopants, due to their large size, may act to enhance ordering by means of forming "stratified" organization of the PAn chains. All of the films of this work were doped by either MeSA or HCl. Although MeSA forms one of the most stable conducting films, preliminary results indicate that the potentially enhanced conductivity with DBSA or CSA will have enhanced stability. "Secondary doping," or solvent-induced ordering of PAn has been demonstrated with m-cresol. Preliminary results show no conductivity enhancement in these thin, multilayer films (MeSA-doped). It is possible that the effect is most significant only with larger dopants like CSA and DBSA.

4. Annealing and/or orienting.

It is well known that thermal annealing of polymers can enhance order, and may prove to do so with these films. Preliminary results indicate that there is no improvement in conductivity after several hours of annealing at 90°C, even upon re-doping. This is below the T_g of PAn, however, and future annealing should be at higher temperatures. The actual T_g of PAn is not known, since it does not display a T_g in calorimetry, and DMA on pure PAn has not been done. It has been estimated around 150-180°C, and was addressed in Section II.C.

Heating can act to dedope PAn, thus doping will be necessary after annealing for long times or elevated temperatures.

It is also well known that axially orienting conjugated polymers acts to enhance conductivity by increasing the conjugation length, and by easing interchain charge transport by means of increased order. Several possible approaches to ordering self-assembled films are as follows. One simple means is by depositing the films onto a plastic substrate, then stretching. Another approach is to adsorb the films onto grooved surfaces such that the chains are driven to align in an "epitaxial" fashion. One last alignment method is by applying an extremely strong magnetic field. We have tested this approach, and results show that polyaniline chains will align at field strengths on the order of 10 Tesla, and there is some remnance of alignment after the field is turned off.

5. Structure by neutron reflectivity and x-ray reflectivity.

X-ray reflectivity measurements could be useful in determining the extent of order of the layers in a multilayer film. Well defined, regular layers will show strong Bragg scattering peaks, where diffuse, corrugated layering will show little scattering. Similarly, neutron reflectivity can be used as a probe to assess the extent of layering in appropriately labeled multilayer structures.

6. Additional investigations addressing the miscibility of PAn blends.

Transmission electron microscopy (TEM) would allow the direct observation of phase separation on the nanometer scale, if it exists. A good staining agent for PVP is RuO_4, thus contrast should be assured.

Polymer-polymer miscibility can also be probed by NMR, by observing the extent of like-chain interactions vs. unlike-chain interactions. This technique is only useful for domain sizes smaller than about 1000Å. Also, a comparison of thermal behavior (Tg and ΔCp) for phase separated blends such as PAn/PMMA may provide more insight into the thermal behavior of PAn/PVP blends.

There are many other techniques useful in the determination of polymer miscibility, as well as a logical area of parameter space that could be explored. For example, polymer miscibility is usually temperature dependent. In the case of the hydrogen bonding interactions between PAn and PVP, heating the blend would dissociate the hydrogen bonds, likely driving phase separation. Although

it has not been determined, a PAn/PVP blend likely has LCST (lower critical solution temperature) phase behavior. The kinetics of phase separation are also critical to the final morphology, as polymer mobility can determine the extent of phase separation. High molecular weights and/or temperatures well below T_g are two hindrances to polymer mobility, which can leave a blend in a non-equilibrium morphological state.

These are but a few of the many possible directions that this work can lead.

REFERENCES

1. J.H. Burroughes and R.H. Friend in Conjugated Polymers, edited by J.L. Brédas and R. Silbey, (Kluwer Academic Publishers, The Netherlands 1991), pp. 555-662.

2. J.R. Ellis in Handbook of Conducting Polymers, Vol. 1, edited by T.A. Skotheim, (Marcel Dekker, Inc., New York 1986), pp. 489-505.

3. F. Kajzar and J. Messier in Conjugated Polymers, edited by J.L. Brédas and R. Silbey, (Kluwer Academic Publishers, The Netherlands 1991), pp. 509-554.

4. R.H. Baughman, L.W. Shacklette, R.L. Elsenbaumer, E. Plichta, and C. Becht in Conjugated Polymer Materials: Opportunities in Electronics, Optoelectronics, and Molecular Electronics, edited by J.L. Brédas and R.R. Chance, (Kluwer Academic Publishers, The Netherlands 1990), pp. 559-582.

5. M.G. Kanatzidis, *Chem. and Eng. News*, **68 (49)**, 36 (1990).

6. N. Oyama, T. Tatsuma, T. Sato, T. Sotomura, *Nature*, **373**, 598 (1995).

7. T. Nakajima and T. Kawagoe, *Synth. Met.*, **28**, C629 (1989).

8. K.T. Tzou and R.V. Gregory, *ACS Polymer Preprints*, **35 (1)**, 245 (1994).

9. C.-H. Hsu, J.D. Cohen, and R.F. Tietz, *Synth. Met.*, **59**, 37 (1993).

10. D.C. Trivedi and S.K. Dhawan, *Synth. Met.*, **59**, 267 (1993).

11. Y. Yang and A.J. Heeger, *Appl. Phys. Lett.*, **64 (10)**, 1245 (1994).

12. Y. Cao, G.M. Treacy, P. Smith, and A.J. Heeger, *Appl. Phys. Lett.*, **60 (22)**, 2711 (1992).

13. G. Gustafsson, Y. Cao, G.M. Treacy, F. Klavetter, N. Colaneri, and A.J. Heeger, *Nature*, **357**, 477 (1992).

14. M.-N. Collomb-Dunand-Sauthier, S. Langlois, and E. Genies, *J. Appl. Electrochem.*, **24**, 72 (1994).

15. B.P. Jelle and G. Hagen, *J. Electrochem. Soc.*, **140 (12)**, 3560 (1993).

16. Daimler-Benz HighTechReport, 3, 44 (1994).

17. T. Kobayashi, H. Yoneyama, and H. Tamura, *J. Electroanal. Chem.*, **161**, 419 (1984).

18. Y. Cao, N. Colaneri, P. Smith, and A.J. Heeger, *ACS Polymer Preprints*, **35 (1)**, 253 (1994).

19. V.G. Kulkarni, W.R. Matthew, J.C. Campbell, C.J. Dinkins, and P.J. Durbin, *Proc. Soc. Plast. Eng.*, 665 (1991).

20. M. Angelopoulos and N. Patel, *ACS PMSE Proc.*, **71**, 222 (1994).

21. M. Angelopoulos, N. Patel, J.M. Shaw, N.C. Labianca, and S.A. Rishton, *J. Vac. Sci. Technol. B*, **11 (6)**, 2794 (1993).

22. J.A. Conklin, S.C. Huang, and R.B. Kaner, *ACS Polymer Preprints*, **35 (1)**, 251 (1994).

23. D.A. Wrobleski, B.C. Benicewicz, K.G. Thompson, and C.J. Bryan, *ACS Polymer Preprints*, **35 (1)**, 265 (1994).

24. H. Stubb, E. Punkka, and J. Paloheimo, *Materials Science and Eng. Reports*, **10 (3)**, (1993).

25. H. Naarman and N. Theophilou, *Synth. Met.*, **22**, 1 (1987).

26. H. Shirakawa, E.J. Louis, A.G. MacDiarmid, C.K. Chiang, and A.J. Heeger, *J. Chem. Soc. Chem. Commun.*, 578 (1977).

27. W.J. Feast and R.H. Friend, *J. Materials Sci.*, **25**, 3796 (1990).

28. M.F. Rubner in <u>Molecular Electronics</u>, edited by G.J. Ashwell, (Research Studies Press Ltd., England 1992), pp. 65-116.

29. W.-Y. Zheng and K. Levon, submitted for publication (1995).

30. A.G. MacDiarmid, J.-C. Chiang, M. Halpern, W.S. Huang, S.L. Mu, N.L.D. Somasiri, W. Wu, and S.I. Yaniger, *Mol. Cryst. Liq. Cryst.*, **121**, 173 (1985).

31. Y. Wei, G.-W. Jang, K. Hsueh, E.M. Scherr, A.G. MacDiarmid, and A.J. Epstein, *Polymer*, **33 (2)**, 314 (1992).

32. P.M. McManus, R.J. Cushman, S.C. Yang, *J. Phys. Chem.*, **91**, 744 (1987).

33. A.G. MacDiarmid and A.J. Epstein, *Faraday Discuss. Chem. Soc.*, **88**, 317 (1989).

34. Y. Wang, Ph.D. Thesis, Massachusetts Institute of Technology, 1991.

35. K. Amano, H. Ishikawa, A Kobayashi, M. Satoh, and E. Hasegawa, *Synth. Met.*, **62**, 229 (1994).

36. J. Yue, A.J. Epstein, and A.G. MacDiarmid, *Mol. Cryst. Liq. Cryst.*, **189**, 255 (1990).

37. J. Yue and A.J. Epstein, *J. Amer. Chem. Soc.*, **112**, 2800 (1990).

38. J. Yue, H.W. Zhao, K.R. Cromack, and A.J. Epstein, *J. Amer. Chem. Soc.*, **113**, 2665 (1991).

39. D.W. Van Krevelen, <u>Properties of Polymers</u>, 2nd Ed., (Elsevier Scientific, The Netherlands 1976), p. 339.

40. E.J. Oh, Y. Min, J.M. Wiesinger, S.K. Manohar, E.M. Scherr, P.J. Prest, A.G. MacDiarmid, and A.J. Epstein, *Synthetic Metals*, **55-57**, 977 (1993).

41. C.Y. Yang, Y. Cao, P. Smith, and A.J. Heeger, *ACS Polymer Preprints*, **34 (1)**, 790 (1993).

42. Y. Cao and A.J. Heeger, *Synth. Met.*, **52**, 193 (1992).

43. Y. Cao, P. Smith, and A.J. Heeger, *Synth. Met.*, **48**, 91 (1992).

44. A. Andreatta and P. Smith, *Synth. Met.*, **55**, 1017 (1993).

45. Y. Min, A.G. MacDiarmid, and A.J. Epstein, *ACS Polymer Preprints*, **35 (1)**, 231 (1994).

46. Y.-G. Min, Y. Xia, A.G. MacDiarmid, and A.J. Epstein, *Synthetic Metals*, in press (1994).

47. S.Y. Yang and E. Ruckenstein, *Synth. Met.*, **59**, 1 (1993).

48. E. Ruckenstein and S.Y. Yang, *Synth. Met.*, **53**, 283 (1993).

49. R.L. Elsenbaumer, U.S. Patent No. 4,983,322 (1991).

50. C.C. Han, R.L. Elsenbaumer, L.W. Shacklette, and G.G. Miller, International Patent Application, No. WO 92/11644 (1992).

51. D.C. Trivedi and S.K. Dhawan, *Synth. Met.*, **58**, 309 (1993).

52. Y.-H. Liao and K. Levon, *ACS PMSE Proc.*, **69**, 327 (1993).

53. B.D. Malhotra, S. Ghosh, and R. Chandra, *J. Appl. Polym. Sci.*, **40**, 1049 (1990).

54. Y. Kang, M.-H. Lee, and S.B. Rhee, *Synth. Met.*, **52**, 319 (1992).

55. L. Sun, S.C. Yang, and J.-M. Liu, *ACS Polymer Preprints*, **33 (2)**, 379 (1992).

56. K. Shannon and J.E. Fernandez, *J. Chem. Soc., Chem. Commun.*, **5**, 643 (1994).

57. W.B. Stockton and M.F. Rubner, *Mat. Res. Soc. Symp. Proc.*, **328**, 257 (1994).

58. W.B. Stockton and M.F. Rubner, *ACS Polymer Preprints*, **35 (1)**, 319 (1994).

59. M. Ferreira, J.H. Cheung, and M.F. Rubner, *Thin Solid Films*, **244**, 806 (1994).

60. J.H. Cheung, A.C. Fou, M.F. Rubner, *Thin Solid Films*, **244**, 985 (1994).

61. A.C. Fou, O. Onitsuka, M. Ferreira, and M.F. Rubner, submitted to *Mat. Res. Soc. Symp. Proc.*, Fall MRS Meeting (1994).

62. A.C. Fou, O. Onitsuka, M. Ferreira, D. Howie, and M.F. Rubner, *ACS PMSE Proc.*, **72**, 160 (1995).

63. M. Ferreira, M.F. Rubner, and B.R. Hsieh, *Mat. Res. Soc. Symp. Proc.*, **328**, 119 (1994).

64. A.C. Fou, D.L. Ellis, and M.F. Rubner, *Mat. Res. Soc. Symp. Proc.*, **328**, 113 (1994).

65. W.B. Stockton and M.F. Rubner, submitted to *Mat. Res. Soc. Symp. Proc.*, Fall MRS Meeting (1994).

66. P.W. Atkins, Physical Chemistry, 2nd Ed., (W.H. Freeman and Co., San Francisco 1982), pp. 1014-1017.

67. T.A. Vilgis and G. Heinrich, *Macromolecules*, **27 (26)**, 7846 (1994).

68. G. Decher, J.D. Hong, and J. Schmitt, *Thin Solid Films*, **210/211**, 831 (1992).

69. Y. Lvov, G. Decher, and H. Möhwald, *Langmuir*, **9**, 481 (1993).

70. D.S. Yoo, unpublished results, MIT 1994.

71. Y. Lvov, G. Decher, and G. Sukhorukov, *Macromolecules*, **26 (20)**, 5396 (1993).

72. M. Li and J.B. Schlenoff, *Anal. Chem.*, **66**, 824 (1994).

73. E.R. Kleinfeld and G.S. Ferguson, *Science*, **265**, 370 (1994).

74. J.-C. Chiang and A.G. MacDiarmid, *Synth. Met.*, **13**, 193 (1986).

75. C.-H. Hsu, P.M. Peacock, R.B. Flippen, S.K. Manohar, and A.G. MacDiarmid, *Synthetic Metals*, **60**, 233 (1993).

76. L.J. van der Pauw, *Philips Res. Repts.*, **13**, 1 (1958).

77. A. Alix, V. Lemoine, M. Nechtschein, J.P. Travers, and C. Menardo, *Synth. Met.*, **29**, E457 (1989).

78. S.-A. Chen and H.-T. Lee, *Synth. Met.*, **57**, 1040 (1993).

79. J.H. Cheung, Ph.D. Thesis, Massachusetts Institute of Technology, 1993.

80. M.M. Coleman, K.H. Lee, D.J. Skrovanek, and P.C. Painter, *Macromolecules*, **19**, 2149 (1986).

81. M.M. Coleman, Y. Xu, and P.C. Painter, *Macromolecules*, **27**, 127 (1994).

82. C. Le Menestrel, D.E. Bhagwagar, P.C. Painter, M.M. Coleman, and J.F. Graf, *Macromolecules*, **25**, 7101 (1992).

83. L. Jong, E.M. Pearce, T.K. Kwei, W.A. Hamilton, G.S. Smith, and G.H. Kwei, *Macromolecules*, **25**, 6770 (1992).

84. L. Jong, E.M. Pearce, T.K. Kwei, L.C. Dickinson, *Macromolecules*, **23**, 5071 (1990).

85. Ph. Colomban, A. Gruger, A. Novak, and A. Régis, *J. Molecular Structure*, **317**, 261 (1994).

86. P. Gramain and P. Myard, *J. Colloid and Interface Sci.*, **84 (1)**, 114 (1981).

87. M.A. Cohen Stuart and H. Tamai, *Macromolecules*, **21**, 1863 (1988).

88. M.A. Cohen Stuart and H. Tamai, *Langmuir*, **4**, 1184 (1988).

89. R.J. Good in <u>Contact Angle, Wettability, and Adhesion,</u> edited by K.L. Mittal (VSP, The Netherlands, 1993), pp.3-36.

90. R.D. Hazlett in <u>Contact Angle, Wettability, and Adhesion,</u> edited by K.L. Mittal (VSP, The Netherlands, 1993), pp.173-181.

91. D.S. Yoo and M.F. Rubner, *Proc. ANTEC-Boston*, 1995.

92. G.J. Kellogg, A.M. Mayes, W.B. Stockton, M. Ferreira, M.F. Rubner, and S.K. Satija, *Mat. Res. Soc. Symp. Proc.*, **351**, 325 (1994).

93. T. Kawai, J. Umemura, and T. Takenaka, *Langmuir*, **5**, 1378 (1989).

94. M. Vandevyver, A. Barraud, R.-Teixier, P. Maillard, and C. Gianotti, *J. Colloid and Interface Sci.*, **85 (2)**, 571 (1982).

95. P.-A. Chollet, *Thin Solid Films*, **52**, 343 (1978).

96. D. den Engelsen, *J. Phys. Chem.*, **76 (23)**, 3390 (1972).

97. A. Redondo, E.A. Ticianelli, and S. Gottesfeld, *Mol. Cryst. Liq. Cryst.*, **160**, 185 (1988).

98. C. Barbero and R. Kötz, *J. Electrochem. Soc.*, **141(4)**, 859 (1994).

99. T. Iyoda, H. Toyoda, M. Fujitsuka, R. Nakahara, K. Honda, T. Shimidzu, S. Tomita, Y. Hatano, F. Soeda, A. Ishitani, and H. Tsuchiya, *Thin Solid Films*, **205**, 258 (1991).

100. M. Fujitsuka, R. Nakahara, T. Iyoda, T. Shimidzu, S. Tomita, Y. Hatano, F. Soeda, A. Ishitani, H. Tsuchiya, and A. Ohtani, *Synthetic Metals*, **53**, 1 (1992).